Metallogeny of the Lesser Caucasus: From arc construction to post-collision evolution

Robert Moritz[1,a], Rafael Melkonyan[2], David Selby[3], Nino Popkhadze[4], Vlademir Gugushvili[4], Rodrig Tayan[2,*] and Vagif Ramazanov[5,]**

[1] Department of Earth Sciences, University of Geneva, Rue des Maraîchers 13, 1205 Geneva, Switzerland

[2] Institute of Geological Sciences, National Academy of the Republic of Armenia, Baghramyan Avenue 24, 0019 Yerevan, Armenia

[3] Department of Earth Sciences, University of Durham, DH1 3LE United Kingdom

[4] A. Djanelidze Institute of Geology of I. Javakhishvili Tbilisi State University, Politkovskaia St. 5, 0186 Tbilisi, Georgia

[5] Geological Department, Baku State University, Z. Khalilov St. 23, Az1145, Baku, Azerbaijan

* deceased March 25th 2016
** deceased May 7th 2014

[a] corresponding author: Robert MORITZ, University of Geneva, Rue des Maraîchers 13, 1205 Geneva, Switzerland; e-mail: robert.moritz@unige.ch

Abstract

This contribution reviews the metallogenic setting of the Lesser Caucasus within the framework of the complex geodynamic evolution of the Central Tethys belt during convergence and collision of Arabia, Eurasia and Gondwana-derived microplates. New rhenium-osmium molybdenite ages are also presented for several major deposits and prospects, allowing us to constrain the metallogenic evolution of the Lesser Caucasus. The host rock lithologies, magmatic associations, deposit styles, ore controls and metal endowment vary greatly along the Lesser Caucasus as a function of the age and tectono-magmatic distribution of the ore districts and deposits. The ore deposits and ore districts can be essentially assigned to two different evolution stages: (1) Mesozoic arc construction and evolution along the Eurasian margin, and (2) Cenozoic magmatism and tectonic evolution following late Cretaceous accretion of Gondwana-derived microplates with the Eurasian margin.

The available data suggest that during Jurassic arc construction along the Eurasian margin, i.e. the Somkheto-Karabagh belt and the Kapan zone, the metallogenic evolution was dominated by subaqueous magmatic-hydrothermal systems, VMS-style mineralization in a fore-arc environment or along the margins of a back-arc ocean located between the Eurasin margin and Gondwana-derived terranes. This metallogenic event coincided broadly with a rearrangement of tectonic plates, resulting in steepening of the subducting plate during the middle to late Jurassic transition.

Typical porphyry Cu and high-sulfidation epithermal systems were emplaced in the Somkheto-Karabagh belt during the late Jurassic and the early Cretaceous, once the arc reached a more mature stage with a thicker crust, and fertile magmas were generated by magma storage and MASH processes. During the late Cretaceous, low-sulfidation type epithermal deposits and transitional VMS-porphyry-epithermal systems were formed in the northern Lesser Caucasus during compression, uplift and hinterland migration of the magmatic arc, coinciding with flattening of the subduction geometry.

Late Cretaceous collision of Gondwana-derived terranes with Eurasia resulted in a rearrangement of subduction zones. Cenozoic magmatism and ore deposits stitched the collision and accretion zones. Eocene porphyry Cu-Mo deposits and associated precious metal epithermal systems were formed during subduction-related magmatism in the southernmost Lesser Caucasus. Subsequently, late Eocene-Oligocene accretion of Arabia with Eurasia and final closure of the southern branch of the Neotethys resulted in the emplacement of Neogene collision to post-collision porphyry Cu-Mo deposits along major translithospheric faults in the southernmost Lesser Caucasus.

The Cretaceous and Cenozoic magmatic and metallogenic evolutions of the northern Lesser Caucasus and the Turkish Eastern Pontides are intimately linked to each other. The Cenozoic magmatism and metallogenic setting of the southernmost Lesser Caucasus can also be traced southwards into the Cenozoic Iranian Urumieh-Dokhtar and Alborz belts. However, contrasting tectonic, magmatic and

sedimentary records during the Mesozoic are consistent with the absence of any metallogenic connection between the Alborz in Iran and the southernmost Lesser Caucasus.

Introduction

The Lesser Caucasus is a major segment of the Tethyan belt, which extends from the Black Sea to the Caspian Sea, across Georgia, Armenia and Azerbaijan (Figs 1 and 2). This mountain belt links the Western and Central metallogenic Tethys belts with their extensions into Asia (Jankovic, 1977, 1997; Richards, 2015). The Lesser Caucasus was formed as a consequence of convergence and collision of Eurasia, Gondwana-derived terranes and Arabia, and it evolved from a Jurassic nascent subduction-related magmatic arc environment to a Neogene post-collisional setting (Fig. 3). This geodynamic evolution resulted in episodic ore formation in response to particular tectonic and magmatic events across the entire belt (Figs 1, 2 and 3).

In this contribution, we focus on ore deposit belts and districts from the Lesser Caucasus only (Figs 1 and 2), and discuss their genetic link with adjoining metallogenic provinces in eastern Turkey and northern Iran. While the metallogenic aspects of the Tethyan segments along Turkey and Iran have been relatively well addressed in recent contributions (e.g. Yigit, 2009; Kusçu et al., 2013; Aghazadeh et al., 2015), there is only fragmentary information available about the Lesser Caucasus in reviews about Tethyan metallogeny and Tethyan porphyry belts (e.g. Tvalchrelidze, 1980, 1984; Cooke et al., 2005; Richards, 2015). We deliberately restrict this review to the Lesser Caucasus, because of its particular position as a link between the Turkish and Iranian mountain belts, and to keep this report to a reasonable length. We are aware that the metallogenic evolution of this part of the Tethys belt goes beyond the geographic limits of the Lesser Caucasus, such as the Greater Caucasus for example (Tvalchrelidze, 1980, 1984), which includes orogenic gold-style mineralization (Kekelia et al., 2008), intrusion-related gold and polymetallic style mineralization (Okrostsvaridze et al., 2015), and black shale-hosted gold and polymetallic deposits, such as the famous Filizçay and Kızıldere deposits (Markus, 2002; Kekelia et al., 2004).

The main host rock, alteration, ore characteristics, and ages of the ore districts and deposits described in this review are presented in Figures 1 and 2, summarized in Table 1, and set in a geodynamic scheme in Figure 3. New Re-Os molybdenite ages obtained for several ore deposits and occurrences are summarized in Table 2. The host rock lithologies, magmatic associations, deposit styles, ore controls and metal endowment vary greatly along the Lesser Caucasus as a function of the age and tectono-magmatic distribution of the ore districts and deposits. The mineral districts of the Lesser Caucasus can be grouped and discussed according to their distribution among the major tectonic and magmatic zones of this mountain belt (Fig. 2). The first group includes mineral districts associated with the Mesozoic subduction-related, magmatic evolution of the Eurasian margin, which are hosted by the Kapan zone, the Somkheto-Karabagh belt and its northern Georgian extension, named the Artvin-Bolnisi zone (Fig. 2). The second group includes ore deposits of Cenozoic age that can be correlated with tectonic and suture zones outlining the boundaries between the Eurasian margin and terranes or microplates of Gondwana origin.

Geodynamic evolution of the Caucasus

The Caucasus orogenic belt extends from Crimea along the Black Sea to the Southern Caspian Sea, and is subdivided into the Greater Caucasus in the north, the intermontane Transcaucasian Massif, and the Lesser Caucasus to the south, sitting astride on the Eurasian plate and Gondwana-derived plates (Khain, 1975; Adamia et al., 1981, 2011). The Greater Caucasus is a fold-and-thrust mountain belt consisting of Proterozoic and Paleozoic metamorphic and magmatic basement rocks, covered by Mesozoic and Cenozoic sedimentary rocks. It developed during late Proterozoic and Paleozoic subduction of the Prototethys and Paleotethys along the Paleozoic Eurasian margin, named the Scythian platform. The Greater Caucasus was affected by the Variscan, Triassic-Jurassic Cimmerian and Alpine orogenies (Adamia et al., 1981, 2011; Kazmin, 2006; Saintot et al., 2006).

The Transcaucasus massif consists of Neoproterozoic to Paleozoic metamorphic, ophiolitic and granitic basement rocks (Bagdasaryan et al., 1978; Gamkrelidze and Shengelia, 1999; Shengelia et al., 2006; Zakariadze et al., 2007; Mayringer et al., 2011), covered by late Triassic to Cenozoic volcano-sedimentary rocks. Neoproterozoic and early Cambrian rocks of the Transcaucasus massif share affinities with island arcs of the Arabian-Nubian shield. The Transcaucasus massif was accreted to Eurasia during the early Carboniferous, followed by Paleoetethys subduction-related Permo-Carboniferous magmatism (Zakariadze et al., 2007). To the west, the Transcaucasus massif extends into the Sakarya and Pontide zones (Okay and Sahintürk, 1997; Yilmaz et al., 2000; Mayringer et al., 2011). The extension to the east into Iran is still open to question (Kalvoda and Bábek, 2010).

The Lesser Caucasus constitutes the southernmost part of the Caucasus, and its geometry was shaped by indentation tectonics (Philip et al., 1989). It was formed during north- to northeast-verging Jurassic-Cretaceous subduction of a northern branch of the Neotethys beneath the Eurasian margin (Figs 3a-b; Kazmin et al., 1986; Zonenshain and Le Pichon, 1986; Rolland et al., 2011), and closed during the late Cretaceous, when the Gondwana-derived South Armenian block was accreted to Eurasia (Fig. 3c; Rolland et al., 2009 a, b). As a consequence of the blocked subduction setting along the Eurasian margin, the active late Cretaceous-Cenozoic Neotethys subduction zone jumped to the southwest of the Turkish Bitlis-Pütürge massif (Fig. 3c; Kazmin et al., 1986; Zonenshain and Le Pichon, 1986; Rolland et al., 2012). Interpretations about the final Arabia-Eurasia collision range between the late Cretaceous (Mohajjel and Ferguson, 2000) and the Miocene (McQuarrie et al., 2003; Guest et al., 2006; Okay et al., 2010). However, a collision between the late Eocene and the early

Oligocene (40-25 Ma) is favored by a majority of studies for the Caucasian-Zagros region (Vincent et al., 2005; Allen and Armstrong, 2008; Agard et al. 2011; Ballato et al., 2011; Verdel et al., 2011; McQuarrie and van Hinsberger, 2013).

Geological setting and evolution of the Lesser Caucasus

The Lesser Caucasus consists of three tectonic zones (Fig. 2): (1) the magmatic and sedimentary Somkheto-Karabagh belt and Kapan zone, (2) the Sevan-Akera suture zone, and (3) the South Armenian block (Sosson et al., 2010; Adamia et al., 2011). The ~350 km-long Somkheto-Karabagh belt and the ~70 km-long Kapan zone or block (Gevorkyan and Aslanyan, 1997; Mederer et al., 2013) belong to the Eurasian margin (Figs 1 and 2) and were developed along the southern margin of the Transcaucasian massif. Both belts have similar geologic and tectonic characteristics and are interpreted as a discontinuous Jurassic to Cretaceous tholeiitic to calc-alkaline island-arc formed during Neotethyan subduction (Sosson et al., 2010; Adamia et al., 2011), segmented by sub-latitudinal strike-slip faults (Kazmin et al., 1986; Gabriyelyan et al. 1989; see SSF? in Fig. 2). The Somkheto-Karabagh and Kapan belts are subdivided in five broad series separated by unconformities, recording uplift and erosion events, including: (1) a thick sequence of Bajocian and Bathonian volcanic, volcanoclastic and sedimentary rocks, and a subsidiary Callovian sequence, (2) late Jurassic-early Cretaceous magmatic and sedimentary rocks, (3) mid- to late Cretaceous volcanic, volcanoclastic and sedimentary rocks, (4) Paleogene rocks, and (5) Quaternary rocks (Achikgiozyan et al., 1987; Sosson et al., 2010; Adamia et al., 2011; Mederer et al., 2013). The Mesozoic sequences are underlain by Proterozoic and Palaeozoic basement rocks in the Loki, Khrami, and Akhum-Asrikchai massifs of the northern Somkheto-Karabagh belt (Gamkrelidze and Shengelia, 1999; Shengelia et al., 2006; Zakariadze et al., 2007). The late Cretaceous extremity of the northern Somkheto-Karabagh belt in Georgia is known as the Artvin-Bolnisi zone (Figs 1 and 2; Gamkrelidze, 1986; Yilmaz et al., 2000).

The ophiolite sequences of the Sevan-Akera zone represent the suture zone between the Eurasian Somkheto-Karabagh belt and the Gondwana-derived South Armenian block (Figs 1 and 2). The suture zone is the relict of two contemporaneous and parallel east- to northeast-verging subduction zones, one being located along the Somkheto-Karabagh belt, and a second intra-oceanic subduction zone, located to the west, between the Eurasian margin and the South Armenian block, explaining the formation of a back-arc oceanic basin between the two subduction zones (Fig. 3a; Galoyan et al., 2009; Rolland et al., 2009b, 2010, 2011; Hässig et al., 2013a, b). The ophiolites were obducted on the South Armenian block between 88 and 83 Ma (Galoyan et al., 2007; Rolland et al., 2010), and final collision between the Eurasian margin and the South Armenian block took place at 73-71 Ma (Rolland et al., 2009 a, b). According to recent paleomagnetic data, it remains open to question whether the ocean between the South Armenian block and the Eurasian margin was already closed or still open during the Santonian (~83.5-86 Ma), with geological data speaking in favor of the second interpretation (Meijers et al., 2015). The Sevan-Akera ophiolite is correlated with the Izmir-Ankara-Erzincan suture zone of northern Anatolia (IAES in Fig. 1; Yilmaz et al., 2000; Hässig et al., 2013b). In the southernmost Lesser Caucasus, the tectonic boundary between the Eurasian Kapan block and the Gondwana-derived South Armenian block is outlined by the northwest-trending, dextral strike-slip Khustup-Giratakh fault (Fig. 2), where ultramafic rock, gabbro, spilite, andesite and radiolarite of the Zangezur tectonic mélange are interpreted as ophiolite remains (Knipper and Khain, 1980; Burtman, 1994), and are imbricated with late Precambrian to early Cambrian metamorphic rocks and Devonian and Permian sedimentary rocks (Belov, 1969; Khain, 1975). Hässig et al. (2013a) correlate the Zangezur tectonic mélange zone with the Sevan-Akera ophiolite, although relationships are hidden by Cenozoic molasse and volcanic rocks (Fig. 2; Khain, 1975; Burtman, 1994). Melkonyan et al. (2000) and Hässig et al. (2015) suggest the presence of an additional Jurassic-Cretaceous west-verging subduction zone of the Neotethys along the Gondwana-derived South Armenian block (Fig. 3a).

The Gondwana-derived South Armenian block is located to the southwest of the Sevan-Akera suture zone, and is mainly exposed in southwestern Armenia, Nakhitchevan and the Tsaghkuniats massif, north of Yerevan (Fig. 2; Shengelia et al., 2006; Hässig et al., 2015). The terminology of the South Armenian block can be traced back to Kazmin et al. (1986), and it is also named Iran-Afghanian terrane (Gamkrelidze, 1997; Gamkrelidze and Shengelia, 2007) and Nakhitchevan-South Armenia (Adamia et al., 2011). It includes the Miskhan/Tsaghqunk-Zangezur, Yerevan-Ordubad, Araks and the Paleozoic-Triassic Daralagez subterranes described in earlier contributions (e.g. Khain, 1975; Gamkrelidze, 1986; Zonenshain and Le Pichon, 1986; Melkonyan et al., 2000; Saintot et al., 2006). It consists of Proterozoic metamorphic basement rocks (Belov and Sokolov, 1973; Meijers et al., 2015), and an incomplete succession of Devonian to Jurassic sedimentary and volcanogenic rocks, intruded by late Jurassic granodiorite and leucogranite (Hässig et al., 2015; Meijers et al., 2015), unconformably covered by late Cretaceous sedimentary rocks (Belov, 1968; Sosson et al., 2010), Albian-early Turonian volcanic rocks (Kazmin et al., 1986), and Paleocene sedimentary rocks (Djrbashyan et al., 1977). Paleozoic stratigraphic and lithological characteristics of the South Armenian block differ from the ones of the Eurasian margin and correlate with the Malatya-Keban platform of the Tauride block (Robertson et al., 2013), therefore supporting its Gondwanian origin (Sosson et al., 2010). Paleolatitude interpretations based on magnetic data indicate that the South Armenian block was located farther to the south during the early-middle Jurassic, and was separated by a 2700 ± 600 km wide ocean from the Eurasian continent (Bazhenov et al., 1996; Gamkrelidze and Shengelia, 2007). Barrier and Vrielynck (2008), Sosson et al. (2010), Hässig et al. (2013a, b, 2015) and Meijers et al. (2015) group the South Armenian block together with the Eastern Anatolian platform or Anatolide-Tauride block (e.g., Figs 3a-c), and interpret it as the northeastern part of the Tauride microcontinent since the Jurassic. By contrast, Adamia et al. (1981; 2011) group the South

Armenia terrane together with the Sanandaj-Sirjan zone into the Central Iranian platform since the Jurassic, a paleoreconstruction shared by Golonka (2004) and Alavi (2007).

Abundant Cenozoic magmatic activity is recognized throughout the Lesser Caucasus (Kazmin et al., 1986; Lordkipnadze et al., 1989; Sosson et al., 2010). Paleocene to Eocene magmatism stitches the collisional structures (Rolland et al., 2011), and is generally interpreted as being related to final subduction of the Neotethys along the Eurasian margin (Kazmin et al., 1986; Lordkipnadze et al., 1989; Vincent et al., 2005; Moritz et al., in press), coeval with the voluminous, subduction-related Eocene magmatism in Iran (e.g., Allen and Armstrong, 2008; Agard et al., 2011; Ballato et al., 2011; Verdel et al., 2011). Other authors suggested a post-collisional geodynamic setting for the Eocene magmatism of the Lesser Caucasus (Dilek et al., 2010; Sosson et al., 2010). Subsequent Neogene and Quaternary magmatism is syn- to post-collisional (Kazmin et al., 1986; Lordkipnadze et al., 1989; Karapetian et al., 2001; Adamia et al., 2010; Sosson et al., 2010; Neill et al., 2015; Moritz et al., in press). The Dalidag pluton along the Sevan-Akera zone, the Pambak nepheline-bearing syenite pluton north of Yerevan, and the composite Meghri-Ordubad and Bargushat plutons in the southernmost Lesser Caucasus, at the contact between the South Armenian block and the Kapan zone, are major intrusions emplaced during the Cenozoic (Fig. 2; Khain, 1975; Moritz et al., in press).

The EW-oriented Adjara-Trialeti belt in western Georgia consisting of a Cretaceous volcanic arc and Paleogene flysch and volcanic rocks, and the Talysh mountains along the Azerbaijan side of the Caspian Sea (Fig. 1), consisting of Senonian to Paleocene flysch and Eocene-Oligocene volcanic rocks display similar geological characteristics and evolution. They are interpreted to have formed in back-arc settings during the Paleogene evolution of the Lesser Caucasus, which subsequently experienced basin inversion, uplift and transpression during the late Eocene to early Oligocene, attributed to the initiation of Arabian-Eurasian collision (Khain, 1975; Lordkipnadze et al., 1979, 1989; Zonenshain and Le Pichon, 1986; Brunet et al., 2003; Vincent et al., 2005; Adamia et al., 2010; Asiabanha and Foden, 2012).

Re-Os molybdenite geochronology

Molybdenite-bearing samples were collected from outcrops and drill cores. Sample descriptions, locations and Re-Os results are reported in Table 2. The molybdenite grain size is typically between 100 to 500 μm. All samples were hand picked from crushed samples under a binocular to remove remaining impurities. An average of 30 mg of pure molybdenite separate was obtained for each sample. The Re and Os abundance and isotope composition determinations for ~10 to 50 mg aliquants of these molybdenite separates were conducted at the University of Durham (U.K.) as described by Selby and Creaser (2001a, b). In brief, weighted aliquots of the molybdenite mineral separates and tracer solution (^{185}Re + isotopically normal Os) were loaded into a Carius tube with 11N HCl (1 ml) and 15.5N HNO_3 (3 ml), sealed, and digested at 220°C for ~24 h. Osmium was purified from the acid medium using solvent extraction ($CHCl_3$) at room temperature and microdistillation methods. The Re fraction was isolated using standard anion column chromatography. The purified Re and Os fractions were loaded onto Ni and Pt wire filaments, respectively, and their isotopic compositions were measured using negative thermal ionization mass spectrometry (Creaser et al., 1991; Völkening et al., 1991). Analyses were conducted on a Thermo Scientific TRITON mass spectrometer, with the Re and Os isotope composition measured using static Faraday collection. During the course of this study Re and Os blanks were <3 and 0.5 pg, respectively, with the $^{187}Os/^{188}Os$ of the blank being 0.25 ± 0.03. Internal uncertainties include uncertainties related to Re and Os mass spectrometer measurements, blank abundances and isotopic compositions, spike calibrations (0.24% on ^{187}Os and 0.30% on Re, 2), and reproducibility of the RM8599 NIST molybdenite standard Re and Os isotope values. Molybdenite of this study was analyzed during the same period as that of Lawley and Selby (2012), which presents an Re-Os age for RM8599 of 27.6 ± 0.1 and 27.6 ± 0.1 Ma, which is in agreement with the proposed age of 27.74 ± 0.11 Ma (n = 18; Markey et al., 2007). The molybenite Re-Os model ages were calculated using the equation $t = \ln (^{187}Os/^{187}Re + 1)/\lambda$, where and λ is the ^{187}Re decay constant ($1.666 \times 10^{-11} \pm 0.017\ a^{-1}$; Smoliar et al., 1996).

Ore formation during Jurassic magmatic arc construction along the Eurasian margin

The middle Jurassic to late Cretaceous geodynamic evolution of the Lesser Caucasus is characterized by long-lasting subduction of the Tethys oceanic lithosphere along the Eurasian margin, with progressive magmatic arc construction along the Somkheto-Karabagh belt and the Kapan zone (Fig. 3; Rolland et al., 2011). Ore formation was diachronous along the arc and resulted in several major mineral districts described below, which include contrasting ore deposit types. The more recent deposits are essentially porphyry-epithermal-type, but the origin of the earliest deposits remains the subject of debate.

The Alaverdi mining district: Jurassic lithologically- and structurally-controlled base metal deposits

The Alaverdi district of northern Armenia includes the Alaverdi, Akhtala, and Shamlugh deposits (Fig. 4; Table 1), of which only the last one is presently in production (since 2003). Copper ore extraction dates back to 4500 years BC and industrial mining began in the 18th century by French companies (Kozlovsky, 1991). This district accounted for 13% of Cu production of the Russian Empire in the beginning of the 20th century. The rock units are subdivided into middle Jurassic and late Jurassic-early Cretaceous complexes (Fig. 4; Sopko, 1961). Older crystalline basement was neither observed in outcrops, nor intercepted by a 1100m-long drill hole. The Alaverdi, Akhtala and Shamlugh ore deposits are hosted by the 3.5 km-thick middle Jurassic complex, defined as Bajocian and Bathonian. They consist of lava, lava breccia, tuff, and pyroclastic rock, with basaltic, andesitic to dacitic and subsidiary rhyolitic compositions, and interlayered sandstone. The late Jurassic-early Cretaceous complex is composed of basaltic andesite, andesite and tuff breccia interlayered with sandstone and limestone (Sopko, 1961; Lebedev and Malkhasyan, 1965; Ghazaryan, 1971). The oldest middle Jurassic unit yielded K-Ar whole-rock ages of 169 ± 1 and 171 ± 2 Ma (Bagdasaryan and Melkonyan, 1968), and the Haghpat plagiogranite (Fig. 4) yielded a K-Ar whole-rock age of 161 ± 3 Ma (Bagdasaryan, 1972).

The majority of the ore bodies are controlled by roughly NS- and EW-oriented faults, and by intersection between steeply dipping NE-oriented dikes and sill-like bodies (Zohrabyan and Melkonyan, 1999). At shallow levels, the ore bodies form stockworks and subhorizontal, stratiform lenses, whereas subvertical veins are the common ore type at deeper levels, especially at Alaverdi and Shamlugh (Fig. 4; Zohrabyan and Melkonyan, 1999; Calder, 2014). A Bajocian unit called keratophyre, consisting of rhyolitic pyroclastic rocks, constitutes a distinct marker and ore-bearing horizon in the district (Fig. 4), extending laterally from the Alaverdi deposit through Shamlugh to the Akhtala deposits (Nalbandyan and Paronikyan, 1966; Nalbandyan, 1968). At Shamlugh (Fig. 4), ore lenses are hosted by the Bajocian keratophyre, immediately below a rhyolite sill, termed "albitophyre" in the district (Sopko, 1961), and dated at 155.0 ± 1.0 Ma by U-Pb zircon geochronology (Calder, 2014). Because the albitophyre was affected by hydrothermal alteration related to ore-formation (Nalbandyan, 1968; Calder, 2014), the 155.0 ± 1.0 Ma age of the sill sets a maximum age of ore formation at Shamlugh. At the Akhtala deposit, ore bodies are also controlled by the contact of a subvolcanic quartz-feldspar porphyry dome with andesite and basalt within the lowermost Bajocian magmatic complex (Zohrabyan and Melkonyan, 1999), stratigraphically below the Shamlugh and Alaverdi deposits (Sopko, 1961; Calder, 2014).

Regional propylitic alteration predates ore formation and affects the lithologies within the Alaverdi district. It consists of prehnite, zeolite, chlorite, carbonate, albite, epidote, actinolite, and hematite. Regional epidote alteration is particulary well developed in the lowermost middle Jurassic sequences (Nalbandyan, 1968). Hydrothermal alteration spatially associated with the ore bodies at Alaverdi, Akhtala and Shamlugh consists of silicification, sericite, chlorite, carbonate and disseminated pyrite. Pyrophyllite and dickite were also described at Akhtala (Nalbandyan, 1968). The main opaque minerals at the Alaverdi and Shamlugh deposits are chalcopyrite, pyrite, sphalerite, bornite, chalcocite, and subsidiary galena, tennantite, stannite, bismuthite, native gold and silver, and electrum in a gangue of quartz, carbonate, sericite, and chlorite (Table 1; Sevunts, 1972; Khachaturyan, 1977). The Akhtala deposit is characterized by a barite, galena and sphalerite association, with subsidiary chalcopyrite, tennantite, tetrahedrite, bornite, cassiterite, electrum, and native gold and silver in a gangue of quartz, carbonate, sericite, chlorite, kaolinite, anhydrite and gypsum (Paronikyan, 1962). Local Fe-oxide-rich siliceous rocks at the Shamlugh deposit were interpreted as exhalative chert (Calder, 2014), but may also be a product of silicification and hematite alteration (e.g. Çağatay, 1993; Karakaya et al., 2012).

Kapan mining district: diversity of ore styles during Jurassic magmatic arc construction

The Kapan district in southern Armenia (Fig. 2), close to the border with Iran, consists of the producing Shahumyan and past-producing Centralni east and west deposits (Fig. 5). Industrial mining in the Kapan district dates back to the mid-19th century. At least 370,000 tons of Cu were mined in the Kapan district since 1953 (Wolfe and Gossage, 2009). Production in the open pit and underground workings of Centralni East ceased in 2005 and the Centralni West underground operation closed in 2008. The underground Shahumyan deposit remains the only active mine of the district.

Like in the Alaverdi district, the geology in Kapan is dominated by a middle Jurassic complex, and an late Jurassic-early Cretaceous complex (Achikgiozyan et al., 1987; Mederer et al., 2013, 2014). There are no older crystalline basement outcrops, and basement was not intercepted by an ~400m-long drill hole. The ore deposits are hosted by a ~1 km-thick Bajocian and Bathonian andesitic to dacitic sequence with subsidiary basaltic and rhyolitic compositions, consisting of lava, lava breccia, tuff, and pyroclastic rock. They were deposited in both subaerial and subaqueous environments, and include hyaloclastite, widespread amygdaloidal and porphyritic textures, and subsidiary pillow lava structures (Cholahyan et al., 1972; Achikgiozyan et al., 1987). District-wide epidote alteration is characteristic for the base of the middle Jurassic section and becomes less intensive towards the upper part of the middle Jurassic magmatic complex (Achikgiozyan et al., 1987). Quartz dacite from the middle Jurassic sequence was dated at 162 ± 5 Ma by K-Ar whole rock geochronology (Sarkisyan, 1970). There are no plagiogranite outcrops in the Kapan district, but a tonalite clast sampled in a polymict pebble dike yielded a U-Pb zircon age of 165.6 ± 1.4 Ma (Mederer et al., 2013), and gabbro-diorite bodies were intersected by drill holes at a depth of 390 m (Tumanyan, 1992). The middle Jurassic magmatic complex was partly eroded and unconformably covered by late Jurassic-early Cretaceous basaltic andesite, andesite and tuff breccia interlayered with sandstone and limestone (Akopyan, 1962; Achikgiozyan et al., 1987). Granodiorite, quartz-monzodiorite, gabbro and monzogabbro from the late Jurassic-early Cretaceous complex yielded U-Pb zircon ages between 131.5 ± 2.1 and 137.7 ± 1.6 Ma (Mederer et al., 2013).

Mineralization styles, metal endowment, paragenesis and hydrothermal alteration vary among the three main deposits of the Kapan district (Table 1). Centralni West is a Cu deposit, Centralni East a Cu-Au deposit, and Shahumyan is a polymetallic Cu-Au-Ag-Zn±Pb deposit, essentially mined for gold at present. East-west-oriented and steeply S-dipping ore veins, with up to 8% Cu, are the dominant mineralization style at the Centralni West deposit, accompanied by local replacement of the host rock matrix, where ore and gangue minerals precipitated around clasts of permeable volcano-sedimentary host rocks. The mineral assemblage consists predominantly of chalcopyrite and pyrite, with minor sphalerite, tennantite-tetrahedrite and galena, and traces of tellurides and sulfide-bismuth minerals in a quartz and carbonate gangue. Host rock alteration consists of chlorite, carbonate, epidote, and sericite (Achikgiozyan et al., 1987; Mederer et al., 2014). Hydrothermal muscovite from Centralni

West yielded an $^{40}Ar/^{39}Ar$ plateau age of 161.8 ± 0.8 Ma (50% of the released gas), which is considered to be the most reliable mineralization age within the Kapan district (Mederer, 2014; Mederer et al., 2014).

Stockwork is the dominant mineralization style at Centralni East, and most of the veins are roughly EW-orientated and dip steeply to the south. Vein-type ore bodies dominate over stockwork-style mineralization with increasing depth (Achikgiozyan et al., 1987). This deposit contains an intermediate- to high-sulfidation state sulfide mineral paragenesis, including mainly pyrite, colusite, tennantite-tetrahedrite, chalcopyrite and specular hematite, subsidiary luzonite, galena, enargite, bornite, sphalerite, covellite, and minor native silver and tellurides (Table 1). Quartz is the dominant gangue mineral with minor barite and gypsum. Silicification, phyllic alteration and residual quartz alteration with sericite, dickite and diaspore affect the andesitic to dacitic host rocks (Mederer, 2014; Mederer et al., 2014). Re-Os isochron dating based on five pyrite samples yielded an age of 144.7 ± 4.2 Ma (Mederer et al., 2014). Mederer (2014) discussed the reliability of the latter age: in the case this age was accepted, it would mean that ore formation at the Centralni East deposit, which is hosted by middle Jurassic magmatic rocks, occurred at the Jurassic-Cretaceous transition.

The presently producing Shahumyan deposit (Table 1) consists of over 100 steeply dipping EW-oriented veins, which can be traced for several hundred meters along strike, and over a vertical extent generally between 100 and 300 m. The veins are cut by the late Jurassic-early Cretaceous magmatic complex, which overlies the middle Jurassic rock complex. Distal propylitic alteration consists of chlorite, epidote, carbonate and pyrite. Phyllic alteration with sericite, quartz and pyrite prevails in proximity to the ore bodies. With decreasing depth, the phyllic alteration grades into an argillic alteration assemblage including dickite, quartz, pyrite and sericite. East-west-oriented and steeply dipping veins consisting of coarse-grained bladed pink alunite, and minor hematite, pyrite and quartz occur on surface in the northeastern part of the Shahumyan deposit, and alunite, associated with kaolinite and dickite, replaces plagioclase phenocrysts of the quartz-dacite host rock (Mederer, 2014). The coarse-grained bladed alunite yielded a slightly disturbed $^{40}Ar/^{39}Ar$ plateau age of 156.1 ± 0.8 Ma for only 40% of the released gas. Such an age is consistent with the local geological setting, but it would imply ore formation during the late Jurassic (Mederer, 2014; Mederer et al., 2014). Pyrite, chalcopyrite, sphalerite, tennantite-tetrahedrite and galena predominate at Shahumyan in a gangue consisting of early quartz and late stage carbonate. Up to 40 µm-sized inclusions of enargite, digenite, bornite and chalcocite occur in pyrite. Most of the gold and silver is associated with tellurides (Matveev et al., 2006; Mederer et al., 2014), but Achikgiozyan et al. (1987) reported the presence of native gold.

Jurassic geodynamic and metallogenic evolution of the Lesser Caucasus

Magmatism along the Eurasian margin evolved from tholeiitic to calc-alkaline from the middle Jurassic to early Cretaceous (Kazmin et al., 1986; Lordkipadnize et al., 1989; Zohrabyan, 2007). Bonitites were reported locally along the Somkheto-Karabagh belt by Kazmin et al. (1986) and Lordkipadnize et al. (1989). Minor and trace element data (Ti, Z) also reveal an evolution from tholeiitic to transitional compositions during the middle Jurassic to an essentially calc-alkaline composition during the late Jurassic-early Cretaceous (Zakariadze et al., 1987; Mederer, 2013; Calder, 2014). These data document progressive magmatic arc construction along a convergent margin, starting in a nascent, immature suprasubduction environment during the Jurassic and evolving to a more mature arc environment during the Cretaceous.

If one accepts the interpretations by Galoyan et al. (2009), Rolland et al. (2009b, 2010, 2011) and Hässig et al. (2013a, b), the Jurassic-Cretaceous ocean immediately adjacent to the west of the Eurasian margin was a back-arc basin (Fig. 3a). Yilmaz et al. (2000) suggest that the Somkheto-Karabagh belt evolved from a middle Jurassic arc setting to a late Jurassic-Cretaceous fore-arc environment. Rolland et al. (2011) recognize a major regional exhumation episode attributed to a subduction geometry steepening at ~166-167 Ma based on $^{40}Ar/^{39}Ar$ cooling ages from the northern Somkheto-Karabagh belt. The latter interpretation is consistent with Nd and Sr isotope data, which reveal a larger mantle input in the source regions of the late Jurassic-early Cretaceous magmatic rocks in comparison to the middle Jurassic rocks, which is attributed to progressive slab roll-back (Mederer et al., 2013; Calder, 2014).

Based on geochronological data, the Centralni West Cu deposit with an age of 161.8 ± 0.8 Ma (Mederer, 2014), and the Shamlugh base metal deposit with an upper 155.0 ± 1.0 Ma age limit (Calder, 2014) are the oldest ore occurrences in, respectively, the Kapan and the Alaverdi districts (Fig. 2). In fact, because of the stratigraphic position of the Akhtala deposit within the lowermost Bajocian magmatic complex (Zohrabyan and Melkonyan, 1999), ore formation may have started prior to 155 Ma in the Alaverdi district. It can be concluded, that the earliest ore deposit formation along the Somkheto-Karabagh belt and the Kapan zone, likely took place along a nascent magmatic arc setting, rimming a back-arc ocean, broadly coinciding with a major rearrangement of the subduction geometry, as the subducting plate was progressively steepening during the middle to late Jurassic transition.

In both the Kapan and the Alaverdi districts, there is ample evidence for a seawater environment during deposition of the middle Jurassic host rocks and during ore formation, including abundant hyaloclastite, and subsidiary pillow lava structures in the volcanic and volcanoclastic rocks interlayered with reef limestone and carbonaceous sandstone in the middle Jurassic sequence at Kapan (Cholahyan et al., 1972; Achikgiozyan et al., 1987; Mederer et al., 2013). At the Shamlugh deposit, the ore-bearing Bajocian keratophyre is overlain by marine sedimentary rocks (Sopko, 1961), and sulfide and pumice clasts within shale immediately overlying the ore horizon indicate that mineralization was reworked during sedimentation, and that the latter was coeval with the waning stages of Jurassic volcanism (Calder, 2014). Strontium and sulfur isotopic compositions of, respectively, carbonates and sulfates support the participation of seawater in the hydrothermal system at Shamlugh (Calder, 2014). The same is the case for the Sr isotopic composition of late stage carbonates in ore deposits of the Kapan district (Mederer, 2013). These features, together with the hydrothermal alteration including chlorite, carbonate, quartz, epidote, pyrite and sericite, and the Cu-dominant metal association, are consistent with an ore-forming system in a submarine environment during the middle to late Jurassic transition, comparable to volcanogenic massive sulfide (VMS) type deposits (Galley et al., 2007).

Middle Jurassic plagiogranite intrusions are recognized along the entire Somkheto-Karabagh belt (Melkonyan, 1965, 1976; Ghazaryan, 1971), including the Jurassic Haghpat plagiogranite of the Alaverdi district (Fig. 4). Together with clasts of tonalite from subvertical polymict pebble dikes dated at 165.6 ± 1.4 Ma and the presence of gabbro-diorite intersected by drill-holes in the Kapan district (Mederer et al., 2013), they provide evidence of intrusive activity at depth during Middle Jurassic nascent arc construction along the Somkheto-Karabagh belt and the Kapan zone. This intrusive association together with the tholeiitic to transitional composition of the middle Jurassic volcanic complex is reminiscent of composite, synvolcanic gabbro-diorite-tonalite clusters underlying eruptive centers, interpreted as heat engines sustaining hydrothermal systems in VMS districts (Galley, 2003; Galley et al., 2007). In addition, the district-wide epidote alteration at the base of the middle Jurassic complex in both the Alaverdi and the Kapan districts (Naldanbyan, 1968; Cholahyan et al., 1972; Achikgiozyan et al., 1987) is comparable to semi-conformable epidote-dominated hydrothermal alteration zones also described at depth in many VMS districts, immediately at the top of synvolcanic gabbro-diorite-tonalite intrusions (Galley, 1993; Galley et al., 2007). In brief, the early mineralization stages at the Centralni West Cu and Shamlugh deposits in or adjacent to a subduction-related, submarine magmatic arc, characterized by a tholeiitic to calc-alkaline evolution at the middle to the late Jurassic is comparable to other typical VMS districts and submarine hydrothermal systems (de Ronde et al., 2005, 2011; Huston et al., 2011; Hannington et al., 2005). The setting could be analogous to a fore-arc environment if we accept the interpretation of Yilmaz et al. (2000) for the Somkheto-Karabagh belt. Similar fore-arc VMS systems have been described in the Dominican Republic (Torró et al., 2016), and in the Uralides, where they are defined as Baimak-type ore deposits (Herrington et al., 2005a,b).

In the Kapan area (Fig. 5), the Centralni East and Shahumyan deposits contain high-sulfidation state opaque mineral and advanced argillic alteration assemblages, including alunite and enargite, which are typically recognized in subaerial epithermal and porphyry settings (e.g., Rye et al., 1992; Einaudi et al., 2003; Rye, 2005; Simmons et al., 2005). However, the same alteration and opaque mineral associations are also reported in submarine hydrothermal systems and VMS deposits, where they are considered as evidence for the involvement of magmatic-hydrothermal sulfur (e.g., de Ronde et al., 2005; 2011; Huston et al., 2011). The questionable ages obtained for the Centralni East (Re-Os pyrite isochron age of 144.7 ± 4.2 Ma) and Shahumyan deposits (disturbed $^{40}Ar/^{39}Ar$ plateau age of 156.1 ± 0.8 Ma for alunite) leave the question open as to whether the two deposits are roughly contemporaneous with the Centralni West deposit or if they represent three, independent pulses of mineralization between 162 and 145 Ma (Mederer, 2014; Mederer et al., 2014). Because of such uncertainties, the deposits from the Kapan district may represent either (1) coeval hybrid VMS-epithermal-porphyry systems, or (2) juxtaposition of different mineralization styles with different ages, due to rapid changes in local tectonic, magmatic, sedimentary and ore-forming conditions, as described in subaqueous metallogenic settings within Pacific magmatic arcs and in Australia (Hannington, 1997, 2011; Large et al., 2001).

Late Jurassic to early Cretaceous mature magmatic arc evolution along the Eurasian margin: Porphyry Cu systems and associated epithermal deposits

The Teghout deposit: porphyry-Cu ore formation in the Alaverdi mining district

The Teghout porphyry-Cu deposit is a distinct and the youngest deposit of the Alaverdi district (Fig. 4). Teghout has been mined since 2015, and it is spatially associated with the polyphase, calc-alkaline Koghb-Shnokh intrusion (Fig. 4), which marks the final stage of the late Jurassic magmatic evolution. Quartz diorite-tonalite yielded a U-Pb zircon age of 152.87 ± 0.72 Ma (Calder, 2014), and leucogranite from the same intrusion yielded a Rb-Sr isochron age of 156 ± 3 Ma (Melkonyan and Ghukasian, 2004), confirming earlier geological interpretations (Aslanyan, 1958; Melkonyan, 1976). Re-Os molybdenite dating yielded an age of 145.85 ± 0.59 Ma (Table 2), which coincides with K-Ar ages of 145.5 ± 0.5 Ma and 149 ± 3 Ma for muscovite separates from quartz-molybdenite veins (Paronikyan and Ghukasian, 1974). The tonalite and quartz-diorite porphyry stock-like bodies and dikes, and the sulfide mineralization of the Teghout deposit are structurally controlled by N- to ~NE-oriented faults or zones of deformed rocks. The Koghb-Shnokh intrusion and its country rocks were affected by initial actinolite-epidote and epidote-chlorite alteration, followed by quartz-sericite alteration and silicification. The mineralization consists of sulfide stockwork, dissemination and veins. Predominant pyrite is accompanied by chalcopyrite and molybdenite, subsidiary sphalerite, galena, chalcocite, covellite, bornite, and magnetite in a gangue of quartz, anhydrite, carbonate and gypsum (Table 1). Rare enargite, luzonite, and native gold have also been reported (Amiryan et al., 1987).

Gedabek and adjoining districts: Early Cretaceous, apical porphyry Cu and epithermal systems

Gedabek ore deposit district: Mining in the Gedabek district started about 2000 years ago, with industrial mining beginning about 1849 at the Gedabek mine (Fig. 6a). About 56,000 tons of copper and 134.16 tons of gold-silver doré were produced from 1864 to 1917, when mining activity ceased with the start of the Russian Revolution. Gedabek is the major porphyry-epithermal district of the Somkheto-Karabagh belt (Fig. 6a; Babazadeh et al., 1990). The district is characterized by a long magmatic evolution starting with Bajocian and Bathonian andesitic to rhyolitic volcanic and pyroclastic rocks, and the emplacement of the ~65 km^2-large Atabek-Slavyan plagiogranite, dated at 152-172 Ma by K-Ar geochronology (Ismet et al., 2003). Late Jurassic-early Cretaceous diorite and granodiorite, and subsidiary aplites of the Gedabek intrusion were dated by whole-rock K-Ar geochronology between 129 and 142 Ma, with one outlier at 150 Ma (Ismet et al., 2003). The Gedabek intrusion is reported as Kimmeridgian on the local maps (Fig. 6a), but an early Cretaceous age for this intrusion is more consistent with the K-Ar ages reported by Ismet et al. (2003). The ore deposits and prospects of the district are spatially related to the emplacement of quartz-diorite and granodioritic porphyritic stocks and dikes post-dating the Gedabek intrusion, and the middle Jurassic Atabek-Slavyan plagiogranite (Fig. 6a; Babazadeh et al., 1990). The porphyry-Cu Garadagh, Kharkhar, and Djaygir prospects are located in the northern part of the district, and are spatially associated with the Atabek-Slavyan massif. This part of the district experienced the most intense uplift of the region (Babazadeh et al., 1990). Epithermal deposits and prospects with variable sulfidation state characteristics are mainly located to the south of the district at Gedabek, Bittibulag, Novogorelovska, etc. (Fig. 6a).

According to Babazadeh et al. (1990), the ore deposits of the Gedabek district are controlled by a deep-seated, ~NS-oriented, orogen-transverse arc-shaped fault. The 700 to 800 m-wide stockwork-type ore bodies of the porphyry Cu deposits are stretched along the same direction over a distance of 1.5 to 2 km. The major part of mineralization in the porphyry systems is associated with the central quartz-sericite-pyrite alteration evolving outwards into a quartz-sericite and argillic alteration, and propylitic alteration in the periphery (Table 1). Potassic alteration is only poorly developed in this mining district (Babazadeh et al., 1990). This suggests that the Garadagh, Kharkhar, and Djaygir prospects represent the apical parts of typical porphyry Cu systems (Sillitoe, 2010). The quartz diorite and granodioritic porphyritic stocks and dikes, associated with the porphyry Cu prospects are also hydrothermally altered and impregnated with sulfides. The highest ore grades are located in the apical parts of a quartz diorite porphyry intrusion at the Garadagh and Kharkhar prospects. At Kharkhar, alteration consists essentially of sericite-quartz, local argillic alteration (kaolinite), surrounded by propylitic alteration. The main opaque minerals are pyrite and chalcopyrite, and subsidiary molybdenite, with one molybdenite sample from Kharkhar yielding a Re-Os age of 133.27 ± 0.53 Ma (Table 2).

Gedabek, Bittibulakh and Novogorelovka are the best described epithermal occurrences (Table 1; Fig. 6a). Bittibulakh is located along a NW-oriented structure at the contact with Bajocian andesite and andesitic tuff and the Atabek-Slavyan plagiogranite. The Cu-As-Au mineralization is a 60 m by 50 m-sized body, including small lenses of enargite and barite surrounded by quartz-pyrite veins and disseminations, and the wall-rock alteration consists of silicification, sericite and kaolinite. Novogorelovka is a Cu-Zn stockwork-type NW-oriented ore body, hosted by early Bajocian andesite and andesitic tuff crosscut by a late Jurassic quartz diorite. The host rocks are silicified, sericitized and kaolinitized. Gedabek is the best-studied deposit and only operating mine in the district. The ore body is a sub-horizontal lens of highly silicified rocks at the contact between middle Jurassic andesitic volcanoclastic rocks and a late Jurassic granodiorite. Hydrothermal alteration is lithologically controlled by a subhorizontally bedded volcaniclastic rock sequence. Early low-sulfidation alteration and mineralization includes pervasive silicification, microcrystalline adularia and disseminated pyrite, and is crosscut by argillic alteration, including kaolinite, and stockwork mineralization, with the later paragenetic assemblages consisting of an intermediate- to high-sulfidation assemblage, including enargite and covellite. Throughout the paragenetic sequence, sphalerite changes in composition from Fe-rich to Fe-poor. Electrum is deposited before the transition towards a late enargite-covellite assemblage (Hemon et al., 2012; Hemon, 2013). According to Hemon (2013), the alteration characteristics and the temporal evolution of the hydrothermal system at Gedabek are comparable with the Round Mountain deposit, U.S.A. (Sander and Einaudi, 1990).

Chovdar and Gosha high-sulfidation epithermal systems, and Dashkesan deposit: The Chovdar deposit is located to the northwest of the major Dashkesan deposit (Fig. 2), and mining started in 2014. The deposit is hosted by middle Jurassic basic to felsic volcanic rocks and tuff (Fig. 6b). Gold mineralization is associated with subvertical barite-polymetallic veins and with highly silicified stratiform horizons, which include occurrences of vuggy silica, and disseminated pyrite and kaolinite. The silicified rock is highly brecciated in some places. Vuggy silica, with vugs filled with pyrite, enargite, tetrahedrite-tennantite and kaolinite was encountered during drilling (Table 1).

The major Dashkesan Fe-Co deposit, in proximity to Chovdar, consists of stratiform magnetite-hematite skarn bodies, crosscut by uneconomic Co-bearing sulfide bodies. The ore bodies are hosted by late Jurassic sedimentary rocks intruded by early Cretaceous (Neocomian) gabbro and granite of the Dashkesan intrusion, which is coeval with the Gedabek intrusion. Late Jurassic volcanic rocks adjacent to the skarn bodies, at a location named Alunite Dag, are pervasively altered to alunite, with associated kaolinite, sericite and silicification, grading laterally into hematite alteration (Kashkai, 1965; Baskov, 2012).

The Gosha prospect, northwest of the Gedabek district (Fig. 2), is mainly hosted by Bajocian andesitic pyroclastic rocks, intruded by small dioritic intrusions. Mineralization is controlled by steeply dipping EW- and NS-oriented faults filled with clay minerals (kaolinite) and disseminations and small clusters of pyrite (Fig. 6c). The host rock is locally brecciated. Gold is associated with pyrite and tellurides along the faults and veins. The host rocks are silicified, and contain kaolinite and disseminated pyrite (Table 1).

The Mehmana mining district of the sourthernmost Somkheto-Kabaragh belt

The Mehmana district is located in the southeasternmost part of the Somkheto-Karabagh belt (Fig. 2), and includes the Drmbon/Gizilbulag Cu-Au deposit, the Mehmana Pb-Zn deposit and several other occurrences are described as porphyry Cu type. The main host rocks are Bajocian and Bathonian volcanic and volcano-sedimentary rocks, covered by late Jurassic volcanic breccia and sedimentary rocks (Vardanyan, 2008; Mederer et al., 2014). Steeply E-dipping andesite and dacite dikes crosscut the middle and late Jurassic volcanic rocks. The major granitic to tonalitic Mehmana intrusion from the western part of the district has been dated at 154-147 Ma by U-Pb zircon geochronology (Galoyan et al., 2013), and 131-152 Ma ages were obtained by K-Ar dating of quartz diorite and granodiorite from the same intrusion (Ismet et al., 2003).

At Drmbon/Gizilbulag, the economic mineralization consists of three lens-shaped lithologically controlled ore bodies, which grade downwards into brecciated host rock with stockwork and disseminated mineralization. The ore bodies are hosted by late Bajocian andesite and dacite, and are capped by a quartz dacite sill, which is interpreted to have been a major fluid barrier during ore-formation by Vardanyan and Zohrabyan (2008). The main opaque minerals are pyrite, chalcopyrite, galena and gold in a quartz matrix, followed by sphalerite and chalcopyrite in a carbonate matrix (Table 1). In proximity to the ore deposit, the host rocks are altered to sericite and abundant hematite, and chlorite and carbonate replace mafic minerals. Pre- to syn- mineralization polymict matrix-supported pebble dikes crosscut late Jurassic agglomerates, and contain blocks of Oxfordian limestone. Therefore, the mineralization is interpreted as syn-to post-Oxfordian in age (Vardanyan, 2008; Mederer et al., 2014).

Porphyry-Cu and epithermal ore deposits: mature stage of the Somkheto-Karabagh magmatic belt

The Teghout deposit is the oldest, typical stockwork-style porphyry Cu system along the Somkheto-Karabagh belt, with an age of 145.85 ± 0.59 Ma (Table 2). This indicates that the switch from a submarine magmatic-hyrothermal or VMS mineralization style to typical porphyry ore-forming systems occurred within 10 m.y. or less in the Alaverdi district (Fig. 4). The next significant porphyry-epithermal event occurred at about 133 Ma in the central Somkheto-Karabagh belt at the Gedabek district (Fig. 6a). These classical epithermal-porphyry centers were clearly formed during the subduction evolution of the Somkheto-Karabagh belt (e.g. Fig. 3a). They document that this belt had evolved towards a mature island-arc stage at the Jurassic-Cretaceous transition and during the early Cretaceous, once the arc was sufficiently thickened, and when sufficient amounts of fertile magmas were generated over time by MASH processes, as is observed for typical porphyry districts (Richards, 2003; Cooke et al., 2005; Sillitoe, 2010; Hou et al., 2011; Chiaradia, 2014).

The porphyry Cu and high-sulfidation epithermal ore deposit association of the Gedabek district, with the adjoining Gosha prospect and Chovdar deposit (Fig. 6), is comparable to the Panagyurishte district in Bulgaria, where several paired porphyry-epithermal systems are present (Moritz et al., 2004; Von Quadt et al., 2005; Chambefort et al., 2007; Kouzmanov et al., 2009). Babazadeh et al. (1990) stated that the Gedabek district experienced intense uplift during the early Cretaceous. This interpretation is shared by Sosson et al. (2010), who describe a major erosion event and unroofing of the plutons of the magmatic arc during the early Cretaceous. Sosson et al. (2010) attributed the uplift to subduction of an oceanic plateau or an intra-oceanic spreading ridge. Given such an uplift and denudation setting, it remains open to question how the epithermal deposits and prospects were preserved in the Gedabek district. Indeed, epithermal ore deposits, which form within the uppermost part of the crust, are particularly vulnerable to rapid erosion (Hedenquist et al., 2000; Simmons et al., 2005). Concealement by basin sedimentation or tectonic processes following shortly ore formation are typically required to preserve old epithermal deposits (e.g., Masterman et al., 2002; Kesler et al., 2004; Chambefort and Moritz, 2006). Further studies are necessary to understand, which processes can explain the preservation of epithermal deposits and prospects in the Gedabek district.

Interpretation of the ore deposits in the Mehmana district (Fig. 2) remains more equivocal, especially to understand whether the deposits were formed in subaqueous or subaerial environments. Because of the poor age constraints, the ore deposits and prospects from the Mehmana district could be coeval with the early mineralization stages of the Kapan and Alaverdi districts (Mederer et al., 2014). On the other hand, younger ages are very likely, based on the reported presence of the Kashen porphyry Cu and epithermal style mineralization in the Mehmana district (Mederer et al., 2014), and therefore ore formation in this district could be roughly contemporaneous with porphyry and epithermal systems at Teghout or Gedabek. Clearly, further comprehensive studies are necessary to verify this.

Local hydrothermal alteration and sulfide veining occur within the late Jurassic-early Cretaceous and Paleogene magmatic complexes of the Kapan block, suggesting the presence of porphyry-type ore-forming systems, but their age remains uncertain. They include polymetallic veins at Bartsravan (Fig. 5) hosted by volcanic and subvolcanic rocks (Zohrabyan et al., 2003), and stockwork-type Cu-Au-Mo mineralization at Shikahogh (Fig. 5), at the outer contact of an early Cretaceous intrusion within late Jurassic and early Cretaceous rocks (Achikgiozyan et al., 1987).

Toukhmanouk precious and base metal prospect – an anomaly?

The Toukhmanouk prospect is located within the Tsaghkuniats massif, belonging to the easternmost part of the Gondwana-derived South Armenian block (Fig. 2; Shengelia et al., 2006; Hässig et al., 2015), in an area with abundant prospects and mines, including the Meghradzor deposit and the Hanqavan prospect (Fig. 7). Eocene to Holocene sedimentary and magmatic rocks outcrop in the eastern downthrown block along the Marmarik fault, and the western uplifted block exposes Jurassic intrusions, and metasedimentary and metamorphic basement rocks. Toukhmanouk consists of ~NE-oriented, subvertical quartz-carbonate-sulfide vein swarms crosscutting Jurassic and Cretaceous volcanic and intrusive rocks (Wheatley and Acheson, 2011), as well as trondhjemite interpreted as Proterozoic in age. The vein corridors are typically 150 to 200 m-wide, and can be traced along strike for more than 1 km. The main sulfides are sphalerite, galena, pyrite and arsenopyrite, and the valuable commodities are gold and silver (Table 1). Molybdenite was dated at 146.14 ± 0.59 Ma by Re-Os geochronology (Table 2). Although the latter Re-Os age ect coincides with the one of the Teghout deposit at 145.85 ± 0.59 Ma (Table 2), it cannot be linked to the long-lasting Jurassic-Cretaceous east-verging subduction underneath the Somkheto-Karabagh arc, because Toukhmanouk lies within the South Armenian block, to the west of the Sevan-Akera suture zone, that is on the opposite side of the active Eurasian margin to which the porphyry deposits at Teghout and Gedabek are related to (Fig. 2). However, Melkonyan et al. (2000) and Hässig et al. (2015) suggested that a S- to SW-verging Jurassic-early Cretaceous subduction zone was active along the eastern margin of the South Armenian block (Fig. 3a). Therefore, the Toukhmanouk ore-forming system maybe a product of subduction beneath the South Armenian block, if we accept such a geodynamic interpretation.

The Bolnisi mining district, Artvin-Bolnisi zone: epithermal and transitional mineralization systems during late Cretaceous arc evolution along the Eurasian margin

The late Cretaceous Bolnisi district (~87-71 Ma) is the last major metallogenic event before the South Armenian block was accreted with the Eurasian margin (Fig. 3b). It documents hinterland migration of the active magmatic arc, which Rolland et al. (2011) attribute to a flatter geometry of the subducting oceanic slab. This resulted in uplift of the arc and a compressional setting during the late Cretaceous (Rolland et al., 2011).

Mining in the Bolnisi district started during the Bronze age according to archaeological investigations (Hauptmann and Klein, 2009), and the Sakdrisi deposit is reported as the world's oldest gold mine (Feresin, 2007; Stöllner et al., 2014). The ore deposits and prospects of the Bolnisi mining district are hosted by late Cretaceous rocks emplaced in a depression between the two uplifted Khrami and Loki basement blocks (Fig. 8), composed of Neoproterozoic to Palaeozoic metamorphic and intrusive rocks, and covered by early Jurassic to early Cretaceous volcanic and sedimentary sequences (Zakariadze et al., 2007; Adamia et al., 2011). The late Cretaceous host rocks are subdivided into six volcanogenic suites, generally interpreted to be Cenomanian to Campanian in age, and overlain by Maastrichtian limestone and marl (Gambashidze, 1984; Apkhazava, 1988; Gugushvili et al., 2014; Popkhadze et al., 2014). The arc-related, calc-alkaline volcanic rocks include abundant pyroclastic rocks, lava, extrusive domes and sub-volcanic intrusions and dikes, with a predominantly rhyolitic, dacitic, and andesitic composition, except one Santonian suite (Tanzia) and one late Campanian suite

(Shorsholeti), which are dominantly basaltic, and partly alkaline in composition (Lordkipnadze et al., 1989; Gugushvili et al., 2014; Popkhadze et al., 2014). The late Cretaceous volcanic rocks were deposited in a shallow water environment (Adamia et al., 2011).

Gugushvili (2004), and Gugushvili et al. (2014) recognized a stratigraphic control on the distribution of ore deposits and prospects in the Bolnisi district. The presently producing Madneuli deposit and the Tsiteli Sopeli, Kvemo Bolnisi and David Gareji prospects from the eastern part of the district (Fig. 8) are hosted by the stratigraphically older volcanic and volcano-sedimentary rocks of the Mashavera suite interpreted as late Turonian to early Santonian in age. A second group of ore occurrences, including the presently producing Sakdrisi deposit, and the Darbazi, Imedi, Beqtakari, Bnelikhevi and Samgreti prospects, in the western district (Fig. 8), are hosted by volcanic and volcano-sedimentary rocks of a stratigraphically younger suite named Gasandami suite, and interpreted as Campanian in age. A granodiorite porphyry to quartz diorite porphyry intrusion crosscut by drilling at a depth of 800-900 m beneath the Madneuli deposit hosted by the Mashavera suite was dated by whole-rock K-Ar geochronology at 88-89 Ma (Rubinstein et al., 1983; Gugushvili and Omiadze, 1988), and rhyolite domes from the same area yielded whole-rock K-Ar ages of 84-85 Ma (Gugushvili, 2004). Moritz et al. (2012) reported U-Pb zircon ages of 86.6 and 87.1 Ma for dikes crosscutting the Mashavera unit. All ages are consistent with Coniacian to Santonian stratigraphic ages of the Mashavera suite. Pyroclastic rocks at Sakdrisi and rhyolite domes from the Sakdrisi and Beqtakari areas (Fig. 8) yielded K-Ar ages of 77.6 Ma and 71-72 Ma, respectively (Gugushvili, 2004), which are consistent with the Campanian stratigraphic age of the Gansandami host rock unit. Nannoplankton determinations by Migineishvili and Gavtadze (2010) of samples from the Mashavera suite suggest a younger Campanian age, which question the above-mentioned Coniacian to Santonian radiometric ages.

The Madneuli polymetallic deposit

The Madneuli open pit exposes different styles of mineralization. One mineralization style consists of a deep, vertical stockwork and breccia composed of, respectively, veins and matrix with a quartz-pyrite-chalcopyrite assemblage with subsidiary enargite, covellite and sphalerite, passing upwards into quartz-barite-sphalerite-galena-pyrite subvertical veins, and into stratiform massive sulfide ore bodies with sphalerite, galena, chalcopyrite, pyrite and tennantite-tetrahedrite, and sandstone lenses cemented by barite in the uppermost levels (Gugushvili et al., 2001; Migineishvili, 2002, 2005; Gialli et al., 2012; Gialli, 2013). The copper ore was mined at the beginning at Madneuli and is now nearly exhausted. The immediate host rocks of the stockwork and vein mineralization are silificied and pass laterally into a quartz-sericite-pyrite zone, followed by a distal quartz-chlorite-sericite envelope. The hanging wall on top of the stratiform sulfide and barite lenses is dominated by chlorite alteration (Gialli et al., 2012; Gialli, 2013). Migineishvili (2002, 2005) reported alunite, kaolinite, pyrophyllite and jarosite in the altered rocks from the shallow part of the deposit. Little et al. (2007) described fossils from the Madneuli deposit interpreted as polychaete worm tubes, which belong to fauna typically found in submarine hydrothermal vents. A second style of mineralization is a steep zone consisting of a quartz-chalcedony vein network containing pyrite, hematite, gold, tellurides, and subsidiary chalcopyrite surrounded by a quartz-chlorite-pyrite alteration zone (Azhgirey and Berman, 1984; Geleishvili, 1989; Gialli et al., 2012; Gialli, 2013). This second mineralization type is presently mined at Madneuli, and includes the economic gold reserves of the deposit (Gugushvili, 2004; Migineishvili, 2005) with an average Au content of 1.3 ppm in 30 Mt of ore. The host-rock volcano-sedimentary successions were deposited under alternating subaqueous and subaerial conditions related to intermittent uplift and subsidence phases (Gugushvili et al., 2001, 2014; Migineishvili, 2002, 2005). Detailed field and petrographic studies by Popkhadze et al. (2014) support the subaqueous origin of the majority of the host rocks, including thick pyroclastic sequences. Although there are divergences about details, the proposed genetic models are consistent with a submarine magmatic-hydrothermal system, similar to a transitional VMS-epithermal setting with a potential porphyry system at depth (Gugushvili et al., 2001, 2014; Migineishvili, 2002, 2005; Gialli et al., 2012; Gialli, 2013). A vertical distribution of mineralization styles similar to the one of Madneuli is recognized in other prospects and deposits of the Bolnisi district, including Sakdrisi, Kvemo Bolnisi and David Gareji (Fig. 8), with copper-rich ore bodies at depth grading into sphalerite, galena, barite and gold-bearing mineralization in the shallower parts of the mineralized systems (Gugushvili et al., 2001, 2014; Gugushvili, 2004).

The Sakdrisi epithermal deposit

The Sakdrisi deposit (Fig. 8) is part of a ~2 km-long, NE-trending range, which includes four other prospects. It is hosted by a subhorizontal sequence of rhyodacitic, dacitic, and andesitic volcanic and volcanoclastic rocks, which have been silicified down to a depth of 100-150 m below surface, locally the wallrock alteration consists of carbonates and clay minerals (illite), and epidote is encountered locally at depth, about 150-200 m below surface (Gugushvili, 2004; Gugushvili et al., 2014). Subvertical gold-bearing quartz-barite zones predominate in the SW-part of the Sakdrisi trend with gold grades ranging between 1.4 and 3 ppm, where open pit mining is currently carried out, and subvertical quartz-chalcedony zones dominate in the NE-part (Gugushvili, 2004; Gugushvili et al., 2014), where gold was mined during the Bronze age (Hauptmann and Klein, 2009; Stöllner et al., 2014).

The Beqtakari epithermal prospect

The Beqtakari gold and base metal prospect (Fig. 8) is hosted by felsic to intermediate volcanic rocks of the Gansadami formation, belonging to the upper stratigraphic sequence of the Bolnisi district. It consists of two distinct ore zones: (1) one silicified zone exposed on surface with local barite and enriched in gold devoid of base metals, and (2) a second zone crosscut by drilling, consisting of a lithologically-controlled, folded breccia sequence mineralized with base and precious metals. The main opaque minerals in the later ore zone are sphalerite, chalcopyrite, pyrite, barite, and subsidiary galena and tennantite-tetrahedrite, cementing the clasts of the breccia. Hydrothermal alteration along the ore bodies consists of interlayered illite/smectite, quartz, calcite and monmorillonite, grading out into distal propylitic alteration (Lavoie, 2015; Lavoie et al., 2015).

Collision and suture zones between Eurasia and Gondwana-derived terranes: Major controls on Cenozoic porphyry and epithermal deposits

Abundant Cenozoic magmatic activity, including the Dalidag, Pambak, Meghri-Ordubad and Bargushat plutons (Fig. 2), can be traced along the collision and suture zones, which outline the accretionary boundary between the Gondwana-derived South Armenian block and the Jurassic-Cretaceous limit of the Eurasian margin (Figs 1, 2 and 3). This major collision zone, which partly coincides with the Miskhan-Zangezur or Tsaghqunk-Zangezur zone (e.g. Khain, 1975; Gamkrelidze, 1986; Melkonyan et al., 2000; Saintot et al., 2006) and the regional dextral active Pambak-Sevan-Sunik fault system (Fig. 2; Philip et al., 2001; Karakhanian et al., 2004), is the location of several significant mining districts, which are products of the complex Cenozoic subduction to collision/post-collision evolution during final convergence of Arabia and Eurasia. Most of this important collision and metallogenic zone is concealed beneath the widespread blanket of Miocene to Pleistocene sedimentary and volcanic rocks (Figs 1 and 2), but certainly constitutes an important exploration target for future discoveries.

The Meghri-Ordubad district: Neotethys subduction to post-collision metallogenic evolution

The Meghri-Ordubad district lies in the Zangezur-Ordubad region, astride the territories of southern Armenia and Nakhitchevan, and extends southwards into Iran (Fig. 5). Its eastern boundary is the NW-oriented, dextral strike-slip Khustup-Giratakh fault, which constitutes the major tectonic boundary between the Kapan block of the Eurasian margin and the Gondwana-derived South Armenian block (Fig. 5). The composite Meghri-Ordubad and Bargushat plutons and the associated porphyry Cu-Mo and epithermal deposits and prospects are mainly located in the central N-trending, uplifted Zangezur block, which is separated from the downthrown western Nakhitchevan block by the NW-oriented dextral strike-slip Ordubad-Salvard fault (Fig. 5; Tayan et al., 1976). The central, NS-oriented 3.5 to 4 km-wide Meghri-Tey graben-synclinal structure is the major ore deposit control (Tayan et al., 1976, 2005; Hovakimyan et al., 2015). With an area of about 1400 km^2, the composite Meghri-Ordubad and Bargushat intrusions form the largest single pluton cluster of the Lesser Caucasus. The Meghri-Ordubad and Bargushat plutons intrude Devonian to Paleocene sedimentary basement and cover rocks of the South Armenian block (Belov, 1968; Djrbashyan et al., 1976; Tayan et al., 1976).

Previous Rb-Sr isochron (Melkonyan et al., 2008, 2010), whole-rock K-Ar dating (Ghukasian et al., 2006), and recent U-Pb zircon ages combined with lithogeochemical data (Moritz et al., in press) have allowed us to subdivide the pluton assembly into two broad stages. Initial normal arc, calc-alkaline to high-K calc-alkaline magmatism, broadly between ~50 and ~40 Ma, resulted in the emplacement of gabbroic and dioritic to granodioritic-granitic intrusions, coeval with extensive, Eocene subduction-related arc volcanism in Iran (e.g., Vincent et al., 2005; Allen and Armstrong, 2008; Ballato et al., 2011; Verdel et al., 2011). The subsequent Oligocene to Mio-Pliocene magmatic evolution coincided with the 40 to 25 Ma-old Arabian-Eurasian collision to post-collision tectonic evolution of the Caucasian-Zagros region (e.g., Vincent et al., 2005; Allen and Armstrong, 2008; Agard et al., 2011; Ballato et al., 2011; Verdel et al., 2011, McQuarrie and van Hinsberger, 2013). Early Oligocene high-K calc-alkaline to shoshonitic magmatism between ~38 and ~28 Ma produced gabbroic, gabbrodioritic, dioritic to monzonitic rocks, and late Oligocene to Miocene adakitic, high-K calc-alkaline magmatism between ~27 and ~21 Ma resulted in the emplacement of granite, granodiorite and quartz-monzonite (Moritz et al., in press; Rezeau et al., 2015).

The major ore deposits and prospects of the Zangezur-Ordubad region are porphyry Cu-Mo deposits (Table 1), and subsidiary epithermal prospects (Table 1) of lesser economic interest hosted by volcanic and plutonic rocks (Karamyan, 1978; Amiryan, 1984; Babazadeh et al., 1990; Moritz et al., in press). The Cenozoic porphyry deposits of the Zangezur-Ordubad region are significantly enriched in Mo with respect to the older late Jurassic-early Cretaceous porphyry deposits emplaced along the Somkheto-Karabagh magmatic arc at Teghout and in the Gedabek district (Karamyan, 1978; Babazadeh et al., 1990). Re-Os molybdenite dating (Table 2) reveals two main porphyry events (Moritz et al., in press). The first porphyry Cu-Mo event is associated with Eocene subduction-related magmatism, and includes the Agarak deposit (44.2 ± 0.2 Ma), and the Hankasar (43.07 ± 0.18 and 43.14 ± 0.17 Ma), Aygedzor (42.62 ± 0.17 and 43.19 ± 0.17 Ma) and Dastakert prospects (40.22 ± 0.16 to 39.97 ± 0.16 Ma; Table 2; Fig. 5). One skarn at a contact with an Eocene intrusion at Qefashen yielded a Re-Os molybdenite age of 44.70 ± 0.18 Ma (Table 2). The second event is late Oligocene in age, coeval with collision to post-collision magmatism, and includes the producing world-class Kadjaran deposit (27.2 ± 0.1 to 26.43 ± 0.11 Ma), and the past producing Paragachay deposit (26.78 ± 0.11 Ma; Fig. 5). According to K-Ar ages published by Bagdasaryan et al. (1969), epithermal mineralization is associated with both Eocene and Oligocene magmatic activity, at 37.5 ± 0.5 and 38.0 ± 2.5 Ma at the Tey-Lichkvaz gold prospect, and at 24 ± 1 Ma at the Atkis polymetallic prospect near Kadjaran (Fig. 5). One molybdenite from an aplite in the Kadjaran area yielded a Re-Os age of 22.87 ± 0.09 Ma (Table 2). Together with the K-Ar age at Atkis, it suggests the presence of a third mineralizing event at the Oligocene-Miocene transition, which is supported by the epithermal overprint observed at the Kadjaran deposit (Hovakimyan et al., 2015). Moritz et al. (in press) concluded that Oligo-Miocene collision to post-collision magmatism and porphyry ore deposit formation were linked to asthenospheric upwelling along translithospheric, transpressional regional faults between the Gondwana-derived South Armenian block and the Kapan block, resulting in decompression melting of lithospheric mantle, metasomatised during Eocene subduction.

The evolution and setting of the Zangezur-Ordubad region of the Lesser Caucasus is comparable to the Himalayan geodynamic environment along the Asian segment of the Tethyan belt, where protracted Mesozoic to Cenozoic magmatism also resulted in the emplacement of successive generations of subduction-related and collision to post-collision porphyry Cu-Mo deposits, with some of the later being associated with large-scale, regional strike-slip faults (Hou et al., 2003, 2011, 2015).

Zod/Sotk: An ophiolite-hosted low-sulfidation epithermal system

The Zod/Sotk gold deposit is hosted by the Jurassic-Cretaceous Sevan-Akera ophiolite complex (Fig. 2; Galoyan et al., 2009; Rolland et al., 2009b, 2010). The deposit is located at the intersection of the ophiolite belt with a ~N-oriented regional fault (Konstantinov and Grushin, 1970; Levitan, 2008), immediately to the NE of the Tsaghkunk-Zangezur (or Miskhan-Zangezur) tectonic zone (Kozerenko, 2004), which borders the easternmost part of the South Armenian block (Khain, 1975; Gamkrelidze, 1986; Saintot et al., 2006). The ophiolite complex is intruded by stocks and ~NS- and ~EW-oriented dikes of quartz diorite, syenite-diorite and porphyritic rhyolite (Konstantinov and Grushin, 1970; Kozerenko, 2004; Levitan, 2008; Konstantinov et al., 2010).

The gold mineralization is controlled by EW- and NW-oriented structures, along which gabbro intrusions are affected by quartz-talc-carbonate alteration, and by the contact with serpentinized peridotite. The main ore bodies are 30 steeply dipping, mainly EW-oriented subparallel zones, including quartz veins with sulfide lenses, veinlet zones in quartz porphyry dikes, and quartz vein networks with disseminated sulfides (Melikyan, 1976; Amiryan, 1984; Kozerenko, 2004; Levitan, 2008). The six largest ore bodies are 10 to 40 m thick and constitute ~80% of the resources (Levitan, 2008). A pre-mineralization carbonate-talc alteration with subsidiary quartz and disseminated pyrite is comparable to listwaenite alteration (Spiridonov, 1991). An overprinting ore-related alteration stage consists of intense silicification, and sericite and pyrite (Kozerenko, 2004; Levitan, 2008). The complex mineralogical composition of the deposit is the result of several subsequent stages, with pre-ore quartz-chalcedony-pyrite, followed by a quartz-pyrite-marcasite-arsenopyrite-sphalerite assemblage containing gold, tellurides, sulfosalts and sulfoarsenides (Table 1). Late and post-ore mineral assemblages include quartz, stibnite, marcasite, and carbonate (including rhodochrosite). Realgar and orpiment have also been reported by Amiryan (1984), Kozerenko (2004), Levitan (2008) and Konstantinov et al. (2010). The host rock, alteration, gangue and ore mineral characteristics of the Zod/Sotk deposit are comparable to the McLaughlin low sulfidation deposit located in the northern Coast Range of California, U.S.A. (Sherlock et al., 1995).

All authors agree that dikes and stocks were overprinted by hydrothermal alteration during mineralization. The felsic intrusions are variably interpreted as late Eocene (Konstantinov and Grushin, 1970), Oligocene to early Miocene (Kozerenko, 2004), or Miocene (Levitan, 2008). This explains why mineralization is broadly interpreted as Oligocene to Miocene in age. However, such Neogene ages are at variance with respect to the K-Ar whole rock alteration age of 43 ± 1.5 Ma reported by Bagdasaryan et al. (1969). This leaves the interpretation open whether the formation of the Zod/Sotk deposit coincides with Eocene magmatism or is a product of Neogene collision to post-collision tectonic and magmatic evolution along the Lesser Caucasus.

The Amulsar prospect: A major new gold discovery in the Lesser Caucasus

The precious metal Amulsar prospect (Fig. 2; Table 1) is hosted by late Eocene to early Oligocene volcano-sedimentary rocks in southern Armenia (Lydian International, 2016). The host rocks consist of multiple layers of volcanogenic conglomerate and breccia, fining upward into volcanogenic and marly mudstone, and local limestone. Andesitic and dacitic volcanic and volcaniclastic rocks are present in the lower stratigraphic units. Small plutons and subvolcanic intrusions are located to the west of the prospect, and contain sub-economic galena-chalcopyrite veins. There is both a marked lithological and a structural control on mineralization. Gold and silver mineralization is hosted by silicified volcanic-sedimentary rocks interlayered with porphyritic andesite, interpreted as sills affected by argillic alteration. Different structures were identified, which explain the final anatomy of the prospect. Several thrusts produced a large dissected fault-fold structure. The main ore-controlling structure consists of a highly, and multiply folded central zone, where precious metal mineralization is associated with small-scale and variably oriented accommodation faults and fractures. Late oblique normal faults have segmented the ore prospect (Lydian International, 2016).

The mineralization consists of gold and hematite with silica within fractures, and breccia zones. Early alteration includes silicification and argillic alteration with subsidiary alunite, and strong silica-hematite alteration is coeval with gold introduction. The Amulsar prospect has typical high- to intermediate-sulfidation epithermal characteristics (argillic alteration, presence of alunite). Local intrusions were dated at 33-34 Ma by K-Ar by Baghdasaryan and Ghukasian (1985), which suggests that the epithermal system may have formed during the Neogene, and may have been associated with the collision to post-collision evolution of the Lesser Caucasus.

The Meghradzor-Hanqavan ore cluster: An equivalent of the Meghri-Ordubad district?

This mining district occurs along the major NW-oriented and NE-dipping Marmarik fault, which belongs to the northern extension of the regional Tsaghkunk-Zangezur (or Miskhan-Zangezur) tectonic zone, and the dextral Pambak-Sevan-Sunik fault system (Fig. 2). Eocene to Holocene sedimentary and magmatic rocks outcrop in the eastern downthrown block along the Marmarik fault (Fig. 7), and the western uplifted block exposes the Jurassic intrusions, and basement rocks of the Tsaghkuniats massif (Shengelia et al., 2006; Hässig et al., 2015).

Meghradzor epithermal deposit: The Meghradzor deposit occurs within the vicinity of the major Eocene Pambak nepheline-bearing syenite (Fig. 7), and is hosted by middle Eocene andesite, tuff and tuff breccia intruded by post-late Eocene granite, granodiorite and alkaline syenite. The deposit was dated at 41.5 ± 1.0 Ma by K-Ar on sericite in altered host rocks (Bagdasaryan et al., 1969). It is a typical low-sulfidation epithermal system with various sulfides, tellurides and native gold in ~EW-oriented quartz-chalcedony-carbonate-sericite veins, and breccia zones (Table 1). The host rocks were silicified, and affected by sericite, pyrite and argillic alteration (Amiryan and Karapetyan, 1964).

Hanqavan Cu-Mo prospect: The Hanqavan prospect (Fig. 7) consists of a porphyry Cu-Mo stockwork hosted by a tonalite crosscut by quartz diorite and granodioritic dikes, which yielded a 33.3 ± 3 Ma age by whole rock K-Ar dating (Bagdasaryan et al., 1969). Re-Os molybdenite dating revealed an age of 29.34 ± 0.12 Ma for the porphyry Cu-Mo mineralization (Table 2). The mineralization contains various sulfides, tellurides and native gold, and is controlled by NE- and EW-oriented faults (Table 1).

The Eocene and Oligocene ages for the ore-forming events within this district are reminiscent of the different ore-forming pulses recognized in the Meghri-Ordubad mining district of the southernmost Lesser Caucasus (Fig. 2; Moritz et al., in press). It is likely, that the metal endowment of the Meghradzor-Hanqavan district is the result of repeated ore formation events controlled by the same major tectonic zone separating the Eurasian margin from the Gondwana-derived South Armenian block, extending from the southern to northern Lesser Caucasus, broadly coinciding with the Pambak-Sevan-Sunik fault zone (Fig. 2). Further studies should investigate whether a long-lived magmatic and tectonic evolution associated with translitospheric faults in a transpressional setting can explain pulsed ore formation in the Meghradzor-Hanqavan district.

The Adjara-Trialeti zone: Eocene subduction arc and back-arc setting or post-collisional setting?

Knowledge about the metallogenic setting of the Adjara-Trialeti belt in western Georgia is still fragmentary (Fig. 1; Khomeriki and Tuskia, 2005; Gugushvili, 2015). It consists of a Cretaceous volcanic arc related to northward subduction of Tethyan oceanic crust and is considered as a lateral extension of the Eastern Pontides (Fig. 1; Adamia et al., 1977, 2010; Yilmaz et al., 2001). Late Eocene shoshonitic magmatism of this belt is controversial (Yilmaz et al., 2001), as it has been interpreted in terms of mature arc magmatism (Lordkipanidze et al., 1984), back-arc rifting (Adamia et al., 1977; Lordkipanidze et al., 1979; Gugushvili, 1980), or a post-collision setting (Yilmaz and Boztuğ, 1996). The shoshonitic rocks are overlain by late Eocene calc-alkaline volcanic rocks, intruded by syenite, monzonite, diorite and granodiorite (Gugushvili, 1980, 2015). Porphyry Cu-Au and polymetallic (Pb-Zn-Au) prospects (Merisi, Uchamba, Lashe, Gudna, Goma) are associated with the late Eocene calc-alkaline rocks (Gugushvili, 2015). Hydrothermal alteration consists of silicification and sericite, alunite, dickite, diaspore, and pyrite (Table 1; Gugushvili, 1980, 2015). Gold-bearing fault zones and hydrothermal breccia veins, capped by a silicic zone, have been described adjacent to a quartz diorite overprinted by quartz-sericite alteration at the new Kela project (Lydian International, 2016). The late Eocene magmatic and ore belt extends to the east into the Artvin-Bolnisi zone (Fig. 1), where polymetallic and gold-bearing occurrences are associated with Eocene diorite and monzonite stocks at Moshevani and Bezaklo (Bezhanishvili, 1969; Gugushvili, 2015).

The geodynamic setting of the porphyry and epithermal prospects of the Adjara-Trialeti zone is open to question, because precise geochronological data are missing. The middle to late Eocene tectonic environment is generally interpreted as extensional and related to the opening of the eastern Black Sea, followed by compression and uplift at the end of the Eocene and the early Oligocene (Adamia et al., 2011). Gugushvili (2015) interprets the late Eocene calc-alkaline magmatism, and the porphyry and epithermal deposits and prospects within a subduction setting. However, the only subduction zone that may have been active during the late Eocene was located far to the south beneath the Bitlis massif (Fig. 3c), since collision of the Eastern Anatolian platform with the Eurasian margin occurred as early as the late Cretaceous along the Somkheto-Karabagh belt (Rolland et al., 2009 a, b; Meijers et al., 2015), and between the Paleocene and early Eocene in the adjacent Eastern Pontides (Okay and Şahintürk, 1997; Peccerillo and Taylor, 1976; Şengör and Yilmaz, 1981; Topuz et al., 2011; Robertson et al., 2013). Therefore, a post-collisional setting is an alternative scenario, which should be tested for the late Eocene geological and metallogenic evolution of the Adjara-Trialeti belt.

Relationship of the ore deposit districts of the Lesser Caucasus with adjoining tectonic provinces

Correlation of the Lesser Caucasus with the Eastern Pontides

During the Jurassic and Cretaceous evolution of the Eurasian active margin, the Eastern Pontides along the Black Sea constituted the lateral western extension of the Artvin-Bolnisi zone and the Somkheto-Karabagh belt into Turkey (Fig. 1; Adamia et al., 1977; 2011; Okay and Şahintürk, 1997; Yilmaz et al., 2000, 2001). Volcanogenic massive sulfide, porphyry and epithermal ore deposit districts of the Eastern Pontides (Yigit, 2009; Delibas et al., 2016), and deposits and prospects of the Georgian Artvin-Bolnisi and Adjara-Trialeti zones are typically grouped into the same metallogenic belt (Moon et al., 2001; Kekelia et al., 2004). Volcanogenic massive sulfide deposits of the Eastern Pontides are interpreted as late Cretaceous (Yigit, 2009; Eyuboglu et al., 2014), whereas ages for porphyry emplacement range between early to late Cretaceous (Delibas et al., 2016) and late Cretaceous to Eocene (Yigit, 2009), and epithermal deposits between late Cretaceous and Eocene (Yigit, 2009).

The late Cretaceous metallogenic event recognized in the Eastern Pontides and in the Artvin-Bolnisi zone can be attributed to final subduction and closure of the northern branch of the Neotethys along the Turkish-Georgian segment of the Eurasian margin (Fig. 3c). There is a general consensus that the early Cenozoic magmatic activity in the Eastern Pontides was related to post-collisional crustal thickening and delamination after Paleocene-early Eocene collision of the Tauride–Anatolide platform and the Eurasian plate (Okay and Şahintürk, 1997; Peccerillo and Taylor, 1976; Şengör and Yilmaz, 1981; Topuz et al., 2011; Robertson et al., 2013). During the middle to late Eocene, the geodynamic setting of the Eastern Pontides was extensional and was related to the opening of the eastern Black Sea, followed by compression and uplift at the end of the Eocene and beginning of the Oligocene (Yilmaz and Boztuğ, 1996; Okay, 2008; Topuz et al., 2011; Kaygusuz and Öztürk, 2015), although some authors suggest that extension went on until the late Miocene (Temizel et al., 2012). In brief, the Eocene porphyry-epithermal deposits/prospects of the Eastern Pontides are likely post-collisional, an interpretation, which should be tested for the adjacent Georgian Adjara-Trialeti metallogenic belt.

An intriguing controversy is the vergence of subduction along the Eastern Pontides and the Adjara-Trialeti zone during the Cretaceous and the early Cenozoic. Indeed, a majority of studies accept north-verging subduction during the Cretaceous until collision of the Tauride–Anatolide platform with Eurasia (e.g., Adamia et al., 1977; 2011; Yilmaz and Boztuğ, 1996; Okay and Şahintürk, 1997; Okay, 2008; Yilmaz et al., 2000, 2001; Delibas et al., 2016). However, some studies advocate a south-verging subduction from the Cretaceous until the Eocene, which extended from the Eastern Pontides along the entire Lesser Caucasus down to the Caspian Sea (Eyuboglu et al., 2011, 2012, 2014). The correct answer to this controversy certainly has fundamental implications for future metallogenic and geodynamic interpretations of the Lesser Caucasus and the Eastern Pontides.

Correlation of the Lesser Caucasus and the Iranian belts during the Mesozoic

Correlation of the Jurassic-Cretaceous Somkheto-Karabagh belt and Kapan zone with the Iranian belts to the south is open to question. The NE-oriented Araks strike-slip fault constitutes a major regional stratigraphic and structural limit between the Alborz and the Lesser Caucasus (Figs 1, 2 and 5; Sosson et al., 2010). Berberian (1983) interpreted the Transcaucasus–Talysh–western Alborz belt as a single Mesozoic Andean-type magmatic arc, and thus he concluded that the Alborz mountains were the eastern continuation of the Somkheto–Karabagh arc and the Kapan zone. However, in contrast to the Lesser Caucasus, no Jurassic and early Cretaceous arc-magmatism is reported in the Alborz, and basaltic magmatism did not begin before the Barremian in the central Alborz (Wensink and Varekamp, 1980) and late Cretaceous in the western Alborz (Salavati, 2008). Moreover, a thick sedimentary basin like the late Triassic to early Jurassic Shemshak Formation in Iran with an up to 4,000-m thick package of siliciclastic sedimentary rocks (e.g., Fürsich et al., 2005) is unknown in the Lesser Caucasus (Sosson et al., 2010). Finally, while the Greater Caucasus, the Alborz and other Iranian terranes were affected by the Triassic-Jurassic Cimmerian orogeny (Adamia et al., 1981, 2011; Saintot et al., 2006; Zanchi et al., 2006; Massodi et al., 2013), there is no evidence for such an orogenic phase along the Lesser Caucasus and the Eastern Pontides (Sosson et al, 2010; Topuz et al., 2013; Hässig et al., 2015). In brief, the Alborz and the Lesser Caucasus have contrasting Mesozoic tectonic, magmatic and sedimentary records, which also reflect different metallogenic evolutions, and explain the absence of ore districts with similar characteristics as Alaverdi, Kapan and Gedabek along the Alborz.

Correlation of the Lesser Caucasus and Cenozoic Iranian magmatic and metallogenic belts

Once the different Gondwana terranes (e.g., the South Armenian block) were accreted to the Eurasian margin by the Paleocene, middle Eocene magmatism and/or coeval deep-water clastic sedimentation took place across a vast area along the Tethyan belt, from southwest Turkey to Iran (Vincent et al., 2005). The Zangezur-Ordubad region of the southernmost Lesser Caucasus is the converging location of the major Cenozoic Iranian Urumieh-Dokhtar and Alborz magmatic and metallogenic belts (Fig. 1). The Alborz, the adjoining Talysh range, and the Lesser Caucasus underwent similar Cenozoic tectonic evolutions. The Talysh and the Alborz range represent back-arc systems during the Eocene, and underwent inversion, uplift and transpression during the late Eocene to early Oligocene (Brunet et al., 2003; Vincent et al., 2005; Ballato et al., 2010; Verdel et al., 2011; Asiabanha and Foden, 2012). In the Lesser Caucasus, Paleocene to late-middle Eocene thick molasse series were deposited in a foreland basin to the southwest of the Somkheto-Karabagh belt, and subsequently underwent late-middle Eocene to Miocene shortening (Sosson et al., 2010).

Magmas from the Iranian Urumieh-Dokhtar belt (Fig. 1) are characterized by predominantly normal arc and calc-alkaline compositions throughout the Cenozoic, except a few Miocene and Pliocene magmatic centers showing adakitic compositions attributed to slab melting or slab break-off following Arabia-Eurasia collision (Omrani et al., 2008; Shafiei et al., 2009; Yeganehfar et al., 2013). By contrast, the Alborz range and the southernmost Lesser Caucasus reveal broadly similar magmatic evolutions during the Cenozoic, evolving from dominantly normal arc, calc-alkaline compositions during the Eocene to adakitic and shoshonitic compositions sourced by a significant proportion of metasomatised lithospheric mantle during the Neogene (Moritz et al., in press). The Neogene shoshonitic and adakitic magmatism of the Alborz is attributed to decompression melting of metasomatised lithospheric mantle during extension and thinning of the crust (Aghazadeh et al., 2011; Castro et al., 2013). This contrasts with the transpressional geodynamic setting accompanied by crustal thickening during Neogene petrogenesis of shoshonitic and adakitic magmas as a consequence of decompressional melting of lower crust and lithospheric mantle in the southernmost Lesser Caucasus (Moritz et al., in press).

The ore deposit cluster of the Zangezur-Ordubad mining district of the southernmost Lesser Caucasus (Fig. 5) extends into the Iranian Cenozoic porphyry Cu-Mo Alborz/Arasbaran and Urumieh-

Dokhtar/Kerman belts (Fig. 1; Jamali et al., 2010; Aghazadeh et al., 2015; Simmonds and Moazzen, 2015). The Iranian porphyry deposits along these two belts are interpreted as post-collisional. The Iranian porphyry systems are Miocene in age, except two porphyry occurrences dated at 27-28 Ma (see Fig. 15 in Aghazadeh et al., 2015; Simmonds and Moazzen, 2015), which is comparable in age to the Oligocene Paragachay and Kadjaran deposits of the southernmost Lesser Caucasus (Fig. 5). In brief, while the Iranian and the Lesser Caucasian Cenozoic porphyry Cu-Mo metallogenic belts can be linked to each other, they reveal distinct differences based on recent interpretations. Although, all Neogene porphyry deposits are the product of collision to post-collision geodynamics, the main ones are Oligocene and related to transpressional tectonics in the southernmost Lesser Caucasus, whereas the Iranian porphyry deposits are predominantly Miocene (e.g. Sungun and Sar Cheshmeh; Aghazadeh et al., 2015; Hassanpour et al., 2015), and related to post-collisional extension and lithospheric mantle delamination (Shafiei et al., 2009; and see Fig. 16b in Aghazadeh et al., 2015). The north to south younging of the porphyry systems, from Eocene-Oligocene in the southernmost Lesser Caucasus to predominantly Miocene in Iran, coincides with the progressive north to south younging of Arabia-Eurasia collision (Agard et al., 2011).

Conclusions

The metallogenic setting of the Lesser Caucasus is the result of a long-lived geological evolution spanning from Jurassic nascent arc construction to Cenozoic post-collision. Our understanding about early ore formation during Jurassic arc construction along the Eurasian margin is certainly still fragmentary, especially because of poor geochronological constraints. The early magmatic evolution and its relationship with ore-forming events along the Somkheto-Karabagh belt and the Kapan zone need to be refined. The available data suggest that early metallogenic evolution was dominated by subaqueous magmatic-hydrothermal systems, VMS-style mineralization in a fore-arc environment or along the margins of a back-arc ocean located between the Eurasin margin and Gondwana-derived terranes. This metallogenic event apparently coincided broadly with a rearrangement of tectonic plates, resulting in steepening of the subducting plate during the middle to late Jurassic transition.

Late Jurassic and the early Cretaceous diachronous emplacement of typical porphyry Cu and high-sulfidation epithermal systems occurred along the Eurasian margin, once the arc was sufficiently thickened and sufficient fertile magmas were generated over time by MASH processes in the crust. Regional uplift and strong erosion is invoked to explain exhumation of the porphyry systems to surface; however it remains to be understood how the early Cretaceous epithermal systems were preserved despite such erosion processes. Low-sulfidation type epithermal deposits and transitional VMS-porphyry-epithermal systems were formed during migration of the magmatic arc into the hinterland, coinciding with progressive Late Cretaceous flattening of the subduction geometry, compression and uplift of the northern Lesser Caucasus belt in the Bolnisi-Artvin zone.

Collision of Gondwana-derived terranes with Eurasia resulted in closure of the northern branch of the Neotethys. This new plate geometry resulted in the rearrangement of subduction zones and set the stage for the next major metallogenic evolution of the Lesser Caucasus. Eocene porphyry Cu-Mo deposits and associated precious metal epithermal systems in the southernmost Lesser Caucasus were related to subduction-related magmatism. Final late Eocene-Oligocene accretion of Arabia with Eurasia resulted in Neogene collision to post-collision porphyry Cu-Mo deposit emplacement in the southernmost Lesser Caucasus, along major translithospheric faults. Further studies are required to constrain how other major low- and high-sulfidation epithermal deposits spatially associated with accretion and suture zones along the entire length of the Lesser Caucsus are either related to Eocene subduction-related magmatism or to Neogene collision/post-collision processes.

The northern geologic and metallogenic setting of the northern Lesser Caucasus is intimately linked to the Cretaceous and Cenozoic evolution of the Turkish Eastern Pontides. Therefore, further investigations should understand how Eocene ore systems of the Adjari-Trialeti belt are related to subduction or to post-collision processes. The Cenozoic magmatism and ore deposit belt of the southernmost Lesser Caucasus can be traced into the Cenozoic Iranian Urumieh-Dokhtar and Alborz belts. By contrast, the Alborz and the Eurasian margin exposed in the southernmost Lesser Caucasus record different Mesozoic tectonic, magmatic, sedimentary and metallogenic evolutions.

Acknowledgments

The research was supported by the Swiss National Science Foundation through the research grants 200020-121510, 200020-138130 and 200020-155928 and the SCOPES Joint Research Projects IB7620-118901 and IZ73Z0-128324. The authors would like to thank the staff of the Zangezur Copper-Molybdenum Combine, the Agarak Copper-Molybdenum Combine - GeoProMining for access to their mines, the Azerbaijan International Mining Company for logistical support, property access and sample handling in the Gedabek mining district and in Nakhitchevan, the Teghout mine and the Madneuli company. We thank the many students and colleagues from the University of Geneva, Switzerland (M. Calder, S. Gialli, P. Hemon, S. Hovakimyan, J. Lavoie, J. Mederer, H. Rezeau), and from Armenia, Azerbaijan and Georgia (Sh. Adamia, T. Beridze, S. Cleghorn, F. Hedjazi, Z. Kutelia, R. Migineishvili, M. Natsvlishvili, R. Overall, A. Rashad, M. Svanidze, A. Turner, A. Vardanyan, S. Zohrabyan), who participated since 2008 in field work and discussions, provided important pieces of information and logistical help, and helped in obtaining authorizations to have access to properties and mines described in this review. We would like to thank very much A.G. Tvalchrelidze, Y. Rolland and J. Richards for their critical reviews and comments.

References

Achikgiozyan, S.O., Zohrabyan, S.A., Karapetyan, A.I., Mirzoyan, H.G., Sargisyan, R.A., and Zaryan, R.N., 1987, The Kapan Mining District: Publishing House of the Academy of Sciences of the Armenian SSR, 198 p. (in Russian).

Adamia, Sh., and Gujabidze, G., 2004, Geological map of Georgia 1: 500,000 (on the basis of 1: 200,000 and 1:50,000 scale State Geological maps of Georgia), Department of Geology, Nodia Institute of Geophysics: http://www.ig-geophysics.ge/sakartvelo.html.

Adamia, Sh., Lordkipanidze, M., and Zakariadze, G., 1977, Evolution of an active margin as exemplified by the Alpine history of the Caucasus: Tectonophysics, v. 40, p. 183–199.

Adamia, Sh, A., Chkoutua, T., Kekelia, M., Lordkipanidze, M., Shavishvili, I., and Zakariadze, G., 1981, Tectonics of the Caucasus and adjoining regions: implications for the evolution of the Tethys ocean: Journal of Structural Geology, v. 3, p. 437-447.

Adamia, Sh., Alania, V., Chabukiani, A., Chichua, G., Enukidze, O., and Sadradze, N., 2010, Evolution of the late Cenozoic basins of Georgia (SW Caucasus): a review, in Sosson, M., Kaymakci, N., Stephenson, R.A., Bergerat, F., and Starostenko, V., eds, Sedimentary basin tectonics from the Black Sea and Caucasus to the Arabian platform: Geological Society of London Special Publication, v. 340, p. 239-259.

Adamia Sh., Zakariadze G., Chkhotua T., Sadradze N., Tsereteli N., Chabukiani A., and Gventsdze A., 2011, Geology of the Caucasus: A Review: Turkish Journal of Earth Sciences, v. 20, p. 489-544.

Agakishiev, A.M., Isaev, A.A., and& Shekinski, E.M., 1989, Report about results of exploration of the central part of Gizilbulag deposit during 1984-1989: Unpublished report, Territorial Geological Fund, Baku, Azerbaijan, 237 p. (in Russian).

Agard, P., Omrani, J., Jolivet, L., Whitechurch, H., Vrielynck, B., Spakman, W., Monié, P., Meyer, B., and Wortel, R., 2011, Zagros orogeny: a subduction-dominated process: Geological Magazine, v. 148, p. 692-725.

Aghazadeh, M., Castro, A., Badrzadeh, Z., and Vogt, K., 2011, Post-collisional polycyclic plutonism from the Zagros hinterland: the Shaivar Dagh plutonic complex, Alborz belt, Iran: Geological Magazine v. 148, p. 980-1008.

Aghazadeh, M., Hou, Z., Badrzadeh, Z., and Zhou, L., 2015, Temporal–spatial distribution and tectonic setting of porphyry copper deposits in Iran: Constraints from zircon U–Pb and molybdenite Re–Os geochronology: Ore Geology Reviews, v. 70, p. 385-406.

Alavi, M., 2007, Structures of the Zagros fold-thrust belt in Iran: American Journal of Sciences, v. 307, p. 1064-1095.

Akopyan, V.T., 1962, Stratigraphy of Jurassic and Cretaceous suites of South-Eastern Zangezur: Armenian Academy of Sciences SSR, 265 p. (in Russian).

Allen, M.B., and Armstrong, H.A., 2008, Arabia-Eurasia collision and the forcing of mid-Cenozoic global cooling: Palaeogeography, Palaeoclimatology, Palaeoecology, v. 265, p. 52-58.

Amiryan Sh.H., 1984, Gold ore formation of Armenian SSR: Yerevan, Publishing House of the Academy of Sciences Armenian SSR, 304 p. (in Russian).

Amiryan, Sh. H., and Karapetyan, A.I., 1964, Mineralogical-geochemical characteristics of the ores of the Mehgradzor gold deposit: Proceedings of the National Academy of Sciences of the Republic of Armenia, Earth Sciences, v. 17, p. 37-48 (in Russian).

Amiryan, Sh. H., Pidjyan G.H., and Faramazyan A.S., 1987, Mineralization stages and ore minerals of the Teghout ore deposit: Proceedings of the National Academy of Sciences of the Republic of Armenia, Earth Sciences, v. 40, p. 31-44 (in Russian with English abstract).

Amiryan, Sh. H., Azizbekyan, M.S., Altounyan, A.Z., and Faramazyan A.S., 1997, Mineralogical-geochemical and genetic specific features of the Toukhmanouk gold-polymetallic ore deposit: Proceedings of the National Academy of Sciences of the Republic of Armenia, Earth Sciences, v. 40, p. 34-40 (in Russian with English abstract).

Apkhazava M., 1988, Late Cretaceous volcanism and volcanic structures of Bolnisi volcano-tectonic depression: Unpublished Ph.D. thesis, Caucasian Institute of mineral resources, 1-269 p.

Asiabanha, A., and Foden, J., 2012, Post-collisional transition from an extensional volcano-sedimentary basin to a continental arc in the Alborz Ranges, N-Iran: Lithos, v. 148, p. 98–111.

Aslanyan, A.T., 1958, Regional geology of Armenia: Haypetrat Edition, Yerevan, Armenia, 430 p. (in Russian).

Azhgirey, A.G., and Berman, Y.S., 1984, Madneuli gold deposit, in Borodayevskaya, M.B., and Borodayevskyi, N.I., eds, Geology of the USSR gold deposits: Moscow, Central Scientific Research Geological Exploration Institute for Non-Ferrous and Noble Metals, v. 1, p. 245-257 (in Russian).

Azizi, H., and Moinevaziri, H., 2009, Review of the tectonic setting of Cretaceous to Quaternary volcanism in northwestern Iran: Journal of Geodynamics, v. 47, p. 167–179.

Babazadeh, V.M., Makhmudov, A.I., and Ramazanov, V.G., 1990, Porphyry-copper and molybdenum deposits: Azerbaijan Publication, Baku, 377 p. (in Russian with German and English abstracts).

Babazadeh, V.M., Musaev, S.D., Nasibov, T.N., and Ramazanov, V.G., 2003, Gold of Azerbaijan: Azerbaijanian National Encyclopaedia, 424 p. (in Russian).

Bagdasaryan, G.P., 1972, Radiological and geochronological, and geological-petrographic studies applied in formational analysis: Izvestia AN Arm. SSR, Nauki o Zemle, v. 5, p. 23-42 (in Russian).

Bagdasaryan, G.P., and Melkonyan, R.L., 1968, New data about petrography and geochronology of some volcanogenic and subvolcanic formations of the Alaverdi region: Proceedings of the National Academy of Sciences of the Republic of Armenia, Earth Sciences, v. 21, p. 93-101 (in Russian).

Bagdasaryan, G.P., Ghukasian, R.Kh., and Karamyan, K.A., 1969, Absolute dating of Armenian ore formations: International Geology Review, v. 11, p. 1166-1172.

Bagdasaryan, G.P., Ghukasian, R.K., and Kazaryan, K.B., 1978, Comparative study of the age of old metamorphic schists in the Hakhoum River Basin (Armenian SSR) by means of K–Ar and Rb–Sr techniques, in Geochronology of the Eastern-European Platform and Junction of the Caucasian–Carpathian System: Nauka publisher, p. 47–58 (in Russian).

Ballato, P., Uba, C.E., Landgraf, A., Strecker, M.R., Sudo, M., Stockli, D.F., Friedrich, A., and Tabatabaei, S.H., 2011, Arabia-Eurasia continental collision: Insights from late Tertiary foreland-basin evolution in the Alborz Mountains, northern Iran: Geological Society of America Bulletin, v. 123, p. 106-131.

Barrier, E., and Vrielynck, B., eds, 2008, Palaeotectonic Maps of the Middle East. CGMW.

Baskov, E.A., 2012, The fundamentals of paleohydrogeology of ore deposits: Springer-Verlag, 253 p.

Bazhenov, M.L., Burtman, V.S., and Levashova, N.L., 1996, Lower and middle Jurassic paleomagnetic results from the south Lesser Caucasus and the evolution of the Mesozoic Tethys ocean: Earth and Planetary Science Letters, v. 141, p. 79-89.

Behre Dolbear, 2005, Gold and copper projects, Azerbaijan, in Anglo Asian Mining PLC, Admission document, Part IV, p. 37-85.

Belov, A.A., 1968. On the history of tectonic development of the northern margin of the Iranian Elibaykal subplatform on Lesser Caucasus: Izvestia of the Academy of Sciences of SSSR, v. 10, p. 121-129 (in Russian).

Belov, A.A., 1969, Stratigraphy and structure of metamorphic volcanogenic and sedimentary stages of the Hanqavan-Zangezur fault in south-east Armenia: Bulletin MOIP, section geology, v. XIV, p. 65-77 (in Russian).

Belov, A.A., and Sokolov, S.D., 1973, Relics of Mesozoic oceanic crust among the crystalline complexes of the Miskhana massif of Armenia: Sovetskaya Geologia, v. 8, p. 26–41 (in Russian).

Berberian, M., 1983, The southern Caspian: a compressional depression floored by a trapped, modified oceanic crust: Canadian Journal of Earth Sciences, v. 20, p. 163–183.

Bezhanishvili, G., 1969, Geological and genetic peculiarities of the polymetallic occurrences of the Dambludi and Moshevani ore fields: Proceedings of the Geological Institute of the Georgian Academy of Sciences SSR, new series, Metsniereba publishsing house, Tbilisi, 130 p. (in Russian).

Brunet, M.-F., Korotaev, M.V., Ershov, A.V., and Nikishin, A.M., 2003, The South Caspian Basin: a review of its evolution from subsidence modelling: Sedimentary Geology, v. 156, p. 119–148

Burtman, V.S., 1994, Meso-Tethyan oceanic sutures and their deformation: Tectonophysics, v. 234, p. 305-327.

Butenko, I.P., 1947, Report about geological-exploration work on the Bitti-Bulak deposit for copper and arsenic: Unpublished report, Funds of the Azerbaijan Geological Department, 189 p. (in Russian).

Calder, M., 2014, Geological environment and genetic constraints of the Shamlugh ore deposit, Alaverdi district, Lesser Caucasus, Armenia: Unpublished MSc Thesis, University of Geneva, Switzerland, 107 p.

Chambefort, I., and Moritz, R., 2006, Late Cretaceous structural control and Alpine overprint of the high-sulfidation Cu–Au epithermal Chelopech deposit, Srednogorie belt, Bulgaria: Mineralium Deposita, v. 41, p. 259–280.

Chambefort, I., Moritz, R., and von Quadt, A., 2007, Petrology, geochemistry and U–Pb geochronology of magmatic rocks from the high-sulphidation epithermal Cu–Au Chelopech deposit, Srednogorie zone, Bulgaria: Mineralium Deposita, v. 42, p. 665–690.

Castro, A., Aghazadeh, M., Badrzadeh, Z., and Chichorro, M, 2013, Late Eocene–Oligocene post-collisional monzonitic intrusions from the Alborz magmatic belt, NW Iran. An example of monzonite magma generation from a metasomatized mantle source: Lithos, v. 180-181, p. 109-127.

Chiaradia, M., 2014, Copper enrichment in arc magmas controlled by overriding plate thickness, Nature Geoscience, v. 7, p. 43-46.

Cholahyan, L.S., A., S.M., and Sarkisyan, R.A., 1972, About the lithology of volcanoclastic rocks of the upper Bajocian of the left bank or the river Kavart: Proceedings of the National Academy of Sciences of the Republic of Armenia, Earth Sciences, v. 25, p. 36–41 (in Russian).

Çağatay, M.N., 1993, Hydrothermal alteration associated with volcanogenic massive sulfide deposits: Examples from Turkey: Economic Geology, v. 88, p. 606-621.

Cooke, D., Hollings, P., and Walshe, J. L, 2005, Giant porphyry deposits: Characteristics, distribution, and tectonic controls: Economic Geology, v. 100, p. 801-818.

Creaser, R.A., Papanastassiou, D.A., and Wasserburg, G.J., 1991, Negative thermal ion mass spectrometry of osmium, rhenium and iridium: Geochimica et Cosmochimica Acta, v. 55, p. 397–401.

Delibas, O., Moritz, R., Ulianov, A, Chiaradia, M., Saraç, C., Revan, K.M., and Göç, D., 2016, Cretaceous subduction-related magmatism and associated porphyry-type Cu-Mo ,mineralizations in the Eastern Pontides, Turkey: New constraints from geochronology and geochemistry: Lithos, v. 248-251, p. 119-137.

De Ronde, C., Hannington, M.D., Stoffers, P., Wright, I.C., Ditchburn, R.G., Reyes, A.G., Baker, E.T., Massoth, G.J., Lupton, J.E., Walker, S.L., Soong, C.W.R., Ishibashi, J., Lebon, G.T., Bray, C.J., and Resing, J.A., 2005, Evolution of a submarine magmatic-hydrothermal system: Brothers volcano, southern Kermadec arc, New Zealand: Economic Geology, v. 100, p. 1097-1133.

De Ronde, C. E. J., Massoth, G. J., Butterfield, D. A., Christenson, B. W., Ishibashi, J., Ditchburn, R. G., Hannington, M. D., Brathwaite, R. L., Lupton, J. E., Kamenetsky, V. S., Graham, I.J., Zellmer, G.F., Dziak, R.P., Embley, R.W., Dekov, V.M., Munnik, F., Lahr, J., Evans, L.J., and Takai, K., 2011, Submarine hydrothermal activity and gold-rich mineralization at Brothers Volcano, Kermadec Arc, New Zealand: Mineralium Deposita, v. 46, p. 541-584.

Dilek, Y., Imamverdiyev, N., and Altunkaynak, S., 2010, Geochemistry and tectonics of Cenozoic volcanism in the Lesser Caucasus (Azerbaijan) and the peri-Arabian region: collision-induced mantle dynamics and its magmatic fingerprint: International Geology Review, v. 52, p. 536-578.

Djrbashyan R.T., Guyumdjyan H.P., and Tayan R.N., 1976, Some features of the structure and formation of the Tertiary volcanic and sedimentary sequences of Zangezur (south-eastern part of Armenian SSR), in Volcanism and metallogeny of Armenian SSR: Publishing House of the Academy of Sciences of the Armemian SSR, Yerevan, v. 8, p. 60-77.

Djrbashyan R.T., Martirosyan Y.A., and Tayan R.N., 1977, Evidence for sediments from the Danish stage in the southeastern part of the Giratagh fault: Proceedings of the National Academy of Sciences of the Republic of Armenia, Earth Sciences, v. 30, p. 10-30. (in Russian).

Einaudi, M.T., Hedenquist, J.W., and Inan, E.E., 2003, Sulfidation state of fluids in active and extinct hydrothermal systems: Transition from porphyry to epithermal environments: Society of Economic Geologists Special Publication, v. 10, p. 285–313.

Eyuboglu, Y., Chung, S.-L., Santosh, M., Dudas, F.O., and Akaryali, E., 2011, Transition from shoshonitic to adakitic magmatism in the eastern Pontides, NE Turkey: Implications for slab window melting: Gondwana Research, v. 19, p. 413-429.

Eyuboglu, Y., Santosh, M., Yi, K., and Bektas, O., 2012, Discovery of Miocene adakitic dacite from the Eastern Pontides Belt (NE Turkey) and a revised geodynamic model for the late Cenozoic evolution of the Eastern Mediterranean region: Lithos, v. 146-147, p. 218-232.

Eyuboglu, Y., Santosh, M., Yi, K., Tuysuz, N., Korkmaz, S., Akaryali, E., Dudas, F.O., and Bektas, O., 2014, The Eastern Black Sea-type volcanogenic massive sulfide deposits: Geochemistry, zircon U–Pb geochronology and an overview of the geodynamics of ore genesis: Ore Geology Reviews, v. 59, p. 29-54.

Feresin, E., 2007, Fleece myth hints at golden age for Georgia: Nature, v. 448, p. 846.

Fürsich, F.T., Wilmsen, M., Seyed-Emami, K., Cecca, F., and Majidifard, R., 2005, The upper Shemshak Formation (Toarcian-Aalenian) of the Eastern Alborz (Iran): Biota and palaeoenvironments during a transgressive-regressive cycle: Facies, v. 51, p. 365-384.

Gabrielyan, A.A., Nazaretyan, S.N., and Ohannisyan, Sh.S., 1989, Deep faults of the territory of Armenia, in Nauka, M., ed., Geodynamics of the Caucasus, p. 36-45 (in Russian).

Galley, A.G., 1993, Semi-conformable alteration zones in volcanogenic massive sulphide districts: Journal of Geochemical Exploration, v. 48, p. 175-200.

Galley, A.G., 2003, Composite synvolcanic intrusions associated with Precambrian VMS- related hydrothermal systems: Mineralium Deposita, v. 38, p. 443-473.

Galley, A.G., Hannington, M.D., and Jonasson, I.R., 2007, Volcanogenic massive sulphide deposits. Mineral Deposits of Canada: A Synthesis of Major Deposit-Types, District Metallogeny, the Evolution of Geological Provinces, and Exploration Methods: Geological Association of Canada, Mineral Deposits Division Special Publication, v. 5, p. 141-161.

Galoyan, Gh., Rolland, Y., Sosson, M., Corsini, M., and Melkonyan, R., 2007, Evidence for superposed MORB, oceanic plateau and volcanic arc series in the Lesser Caucasus (Stepanavan, Armenia): Comptes Rendus Geosciences, v. 339, p. 482–492.

Galoyan, Gh., Rolland, Y., Sosson, M., Corsini, M., Billo, S., Verati, C., and Melkonyan, R., 2009, Geology, geochemistry and $^{40}Ar/^{39}Ar$ dating of Sevan ophiolites (Lesser Caucasus, Armenia): Evidence for Jurassic back-arc opening and hot spot event between the South Armenian Block and Eurasia: Journal of Asian Earth Sciences, v. 34, p. 135-153.

Galoyan, Gh.L., Melkonyan, R.L., Chung, S.-L., Khorenyan, R.H., Atayan, L.S., Hung, C.-H., and Amiraghyan, S.V., 2013, To the petrology and geochemistry of Jurassic island arc magmatic rocks of the Karabagh segment of the Somkheto-Karabagh terrain: Proceedings of the National Academy of Sciences of the Republic of Armenia, Earth Sciences, v. 64, 3-22 (in Russian).

Gambashidze, R., 1984, Geological development history of Georgia during the upper Cretaceous period. Metsniereba: Al. Janelidze Geological Institute of Georgian Academy of Science. Proceeding new series, v. 82, p. 1-111 (in Russian).

Gamkrelidze, I.P., 1986, Terranes of the Caucasus and adjacent areas: Tectonophysics, v. 127, p. 261-277.

Gamkrelidze, I.P., 1997, Geodynamic evolution of the Caucasus and adjacent areas in Alpine time: Bulletin of the Georgian National Academy of Sciences, v. 155, p. 391-394.

Gamkrelidze, I.P., and Shengelia, D.M., 1999, The new data about geological structure of the Dzirulla crystalline massif and the conditions of formation of magmatites: Proceedings of the Geological Institute of the Academy of Sciences Georgia, New Series, v. 114, p. 46–71.

Gamkrelidze, I.P., and Shengelia, D.M., 2007, Pre-Alpine geodynamics of the Caucasus, supasubduction regional metamorphism and granitoid magmatism: Bulletin of the Georgian National Academy of Sciences, v. 175, p. 57-65.

Geleishvili, V.I., 1989, Native gold of Southern Georgia: Bulletin of the Georgian Academy of Sciences SSR, v. 136, p. 605-608 (in Russian).

Gevorkyan, R., and Aslanyan, A., 1997, Armenia, in Moores, E.M., and Fairbridge, R.W., eds, Encyclopedia of European and Asian Regional Geology: Chapman and Hall, London, p. 26–34.

Ghazaryan, H.A., 1971, Main features of the magmatism of the Alaverdi ore district, in: Petrology of intrusive complexes of important ore districts of Armenian SSR : Publishing House of the Academy of Sciences of Armenian SSR, p. 7-116 (in Russian).

Gialli, S., 2013, The controversial polymetallic Madneuli deposit, Bolnisi district, Georgia: hydrothermal alteration and ore mineralogy: Unpublished M.Sc. thesis, University of Geneva, 143 p.

Gialli, S., Moritz, R., Popkhadze, N., Gugushvili, V., Migineishvili, R., and Spangenberg, J., 2012, The Madneuli polymetallic deposit, Lesser Caucasus, Georgia: Evidence for transitional to epithermal conditions, in SEG 2012 Conference, Lima, Peru, September 2012, abstract volume.

Golonka, J., 2004, Plate tectonic evolution of the southern margin of Eurasia in the Mesozoic and Cenozoic: Tectonophysics, v. 381, p. 235-273.

Guest, B., Stockli, D.F., Grove, M., Axen, G.J., Lam, P.S., and Hassanzadeh, J., 2006, Thermal histories from the central Alborz Mountains, northern Iran: implications for the spatial and temporal distribution of deformation in northern Iran: Geological Society of America Bulletin, v. 118, p. 1507-1521.

Gugushvili V., 1980, Hydrothermal process and mineralization in Mesozoic volcanic complexes of Southern Georgia: Proceeding of the Geological Institute of the Academy of Sciences GSSR, Tbilisi, 99 p. (in Russian).

Gugushvili, V., 2004, Two types of gold mineralization in the Bolnisi mining district related to Cretaceous volcanism: Proceedings of the Geological Institute of the Georgian Academy of Science new series, v. 119, p. 749-755.

Gugushvili, V., 2015, Precollision and postcollision metallogeny of gold.copper-base metal ores at the Phanerozoic evolution of the Tethys ocean: Published by Iv. Javakhishvili Tbilisi State University, A. Jalenidze Institute of Geology, 130 p.

Gugushvili, V., and Omiadze, K., 1988, Ignimbrite volcanism and ore formation: Geology of Ore Deposits, v 30, p. 105-109 (in Russian).

Gugushvili, V.I., Apkhazava, M.A., Engin, T., and Yilmaz, A., 2001, New type of sulphide ore deposits in subduction zones, in Yilmaz, A., Adamia, S., Engin, T., and Lazarshvili, T., Geological Studies of the area along Turkish-Georgian Border: MTA, Ankara, p. 251-271.

Gugushvili, V.I., Bukia, A.S., Goderdzishvili, N.N., Javakhidze, D.G., Zakaraia, D.P., Muladze, I.U., Shavishvili, I.D., Shubitidze, J.S., and Tchokhonelidze, M.J., 2014, Bolnisi ore district: geological development and structure, genesis of mineralization, economic potential and perspectives according to data for April 2014: Natsvlishvili M.P., ed., Caucasus Mining Group. Tbilisi. 55 p. (in Russian with English abstract).

Ghukasian, R.Kh., Tayan, R.N., and Haruntunyan, M.A., 2006, Rb-Sr investigations of magmatic rocks of Kadjaran ore field (Republic of Armenia), in Isotope dating of processes of ore mineralization, magmatism, sedimentation and metamorphism: Materials of III Russian conference on isotope geochronology, v. I, p. 213-216.

Hannington, M.D., 1997, The porphyry–epithermal–VMS transition: lessons from the Iskut River Area, British Columbia, and Modern Island Arcs : SEG Newsletter, v. 29, p. 12–13.

Hannington, M., 2011, Metallogeny of Western Pacific submarine volcanic vents, in Barra, F., Reich, M., Campos, E., and Tornos, F., eds, Let's talk ore deposits, Proceedings 11th biennial SGA meeting. Antofagasta, Chile, p. 13–15.

Hannington, M.D., de Ronde, C.E.J., and Petersen, S., 2005, Sea-floor tectonics and submarine hydrothermal systems: Economic Geology 100th Anniversary Volume, p. 111-141.

Hassanpour, S., Alirezaei, S., Selby, D., and Sergeev, S., 2015, SHRIMP zircon U–Pb and biotite and hornblende Ar–Ar geochronology of Sungun, Haftcheshmeh, Kighal, and Niaz porphyry Cu–Mo systems: evidence for an early Miocene porphyry-style mineralization in northwest Iran: International Journal of Earth Sciences, v. 104, p. 45-59.

Hauptmann, A., and Klein, S., 2009, Bronze age gold in Southern Georgia: ArcheoSciences, v. 33, p. 75-82.

Hässig, M., Rolland, Y., Sosson, M., Galoyan, G., Müller, C., Avagyan, A., and Sahakyan, L., 2013a, New structural and petrological data on the Amasia ophiolites (NW Sevan–Akera suture zone, Lesser Caucasus): Insights for a large-scale obduction in Armenia and NE Turkey: Tectonophysics, v. 588, p. 135–153.

Hässig, M., Rolland, Y., Sosson, M., Galoyan, G., Sahakyan, L., Topuz, G., Celik O.F., Avagyan, A., and Müller, C., 2013b, Linking the NE Anatolian and Lesser Caucasus ophiolites: evidence for large-scale obduction of oceanic crust and implications for the formation of the Lesser Caucasus-Pontides Arc: Geodinamica Acta, v. 26, p. 311-330.

Hässig, M., Rolland, Y., Sahakyan, L., Sosson, M., Galoyan, G., Avagyan, A., Bosch, D., and Müller, C., 2015, Multi-stage metamorphism in the South Armenian Block during the late Jurassic to early Cretaceous: Tectonics over south-dipping subduction of Northern branch of Neotethys: Journal of Asian Earth Sciences, v. 102, p. 4-23.

Hedenquist, J.W., Jr., Arribas, A., and Gonzalez-Urien, E., 2000, Exploration for epithermal gold deposits: Reviews in Economic Geology, v. 13, p. 245–277.

Hemon, P., 2013, The Gedabek uqartz-adularia-pyrite altered, Cu-Au-Ag epithermal deposit, Western Azerbaijan, Lesser Caucasus: Geology, alteration, mineralisation, fluid evolution and genetic model: Unpublished M.Sc. thesis, University of Geneva, 91 p.

Hemon, P., Moritz, R., Ramazanov, V., and Spangenberg, J., 2012, The Gedabek ore deposit: a lower Cretaceous epithermal system within the Lesser Caucasus of Western Azerbaijan, in SEG 2012 Conference, Lima, Peru, September 2012, abstract volume.

Herrington, R., Maslennikov, V., Zaykov, V., Seravkin, I., Kosarev, A., Buschmann, B., Orgeval, J., Holland, N., Tesalina, S., Nimis, P., and Armstrong, R., 2005a, Classification of VMS deposits: Lessons from the South Uralides: Ore Geology Reviews, v. 27, p. 203-237.

Herrington, R., Maslennikov, V., Zaykov, V., and Seravkin, I., 2005b, VMS Deposits of the South Urals, Russia: Ore Geology Reviews, v. 27, p. 238-239.

Hou, Z.Q., Ma, H.W., Zaw, K., Zhang, Y.Q., Wang, M.J., Wang, Z., Pan, G.T., and Tang, R.L., 2003, The Himalayan Yulong porphyry copper belt: product of large-scale strike–slip faulting in eastern Tibet: Economic Geology, v. 98, p. 125–145.

Hou, Z., Zhang, H., Pan, X., and Yang, Z., 2011, Porphyry Cu (–Mo–Au) deposits related to melting of thickened mafic lower crust: Examples from the eastern Tethyan metallogenic domain: Ore Geology Reviews, v. 39, p. 21-45.

Hou, Z., Yang, Z., Lu, Y., Kemp, A., Zheng, Y., Li, Q., Tang, J., Yang, Z., and Duan, L., 2015, A genetic linkage between subduction- and collision-related porphyry Cu deposits in continental collision zones: Geology, v. 43, p. 247-250.

Hovakimyan, S.E., 2008, Geological and structural peculiarities of formation of Lichk copper-molybdenum deposit (Southern Armenia): Proceedings of the National Academy of Sciences of the Republic of Armenia, Earth Sciences, v. 61, p. 21-24 (in Russian with English abstract).

Hovakimyan, S.E., 2010, Geological and structural conditions of formation Lichkvaz-Tey gold deposit (South Armenia): Proceedings of the National Academy of Sciences of the Republic of Armenia, Earth Sciences, v. 63, p. 22-29 (in Russian with English abstract).

Hovakimyan, S.E., and Tayan R.N., 2008, The Lichk-Ayguedzor ore field ruptures and mineralization location conditions: Proceedings of the National Academy of Sciences of the Republic of Armenia, Earth Sciences, v. 61, p. 3-12 (in Russian with English abstract).

Hovakimyan S., Moritz R., Tayan R., Harutyunyan M., and Rezeau H., 2015, The world-class Kadjaran Mo-Cu-porphyry deposit, Southern Armenia, Lesser Caucasus: structural controls, mineral paragenesis and fluid evolution, in André-Mayer, A.-S., Cathelineau, M., Muchez, P., Pirad, E., and Sindern S., eds, Mineral resources in a sustainable world, 13th SGA Biennial Meeting, 24-27 August 2015, France, Nancy, v. 1, p. 295-298.

Huston, D. L., Relvas, J. M. R. S., Gemmell, J. B., and Drieberg, S., 2011, The role of granites in volcanic-hosted massive sulphide ore-forming systems: an assessment of magmatic–hydrothermal contributions: Mineralium Deposita, v. 46, p. 473-507.

Ismet, A.R., Hassanov, R.K., Abdullaev, I.A., Bagirbekova, O.D., Jafarova, R.S., and Jafarov, S.A., 2003, Radiochronological study of geological formations of Azerbaijan: Nafta-Press, Baku, Azerbaijan, 191 p. (in Russian).

Ivanitsky T.V., Gvaramadze N. D., Mchedlishvili T. D., Shavishvili I. D., Nadareishvili D. G., and Machavariani M. Sh., 1969, Geochemistry and metallogenic specification of Adjara intrusives, Metsniereba publishsing house, Tbilisi, 120 p. (in Russian).

Jamali, H., Dilek, Y., Daliran, F., Yaghubpur, A., and Mehrabi, B., 2010, Metallogeny and tectonic evolution of the Cenozoic Ahar-Arasbaran volcanic belt, northern Iran: International Geology Review, v. 52, p. 608-630.

Jankovic, S. 1977, The copper deposits and geotectonic setting of the Tethyan Eurasian metallogenic belt: Mineralium Deposita, v. 12, p. 37-47.

Jankovic, S. 1997, The Carpatho-Balkanides and adjacent area: a sector of the Tethyan Eurasian metallogenic belt: Mineralium Deposita, V. 32, p. 426-433.

Kalvoda, J., and Bábek, O., 2010, The margins of Laurussia in central and southeast Europe and southwest Asia: Gondwana Research, v. 17, p. 526–545.

Karakaya, M.Ç., Karakaya, N., Küpeli, S., and Yavuz, F., 2012, Mineralogy and geochemical behavior of trace elements of hydrothermal alteration types in the volcanogenic massive sulfide deposits, NE Turkey: Ore Geology Reviews, v. 48, p. 197-224.

Karakhanian, A.S., Trifonov, V.G., Philip, H., Avagyan, A., Hessami, Kh., Jamali, F., Bayraktutan, M.S., Bagdassarian, H., Arakelian, S., Davtian, V., and Adilkhanyan, A., 2004, Active faulting and natural hazards in Armenia, eastern Turkey and northwestern Iran: Tectonophysics, v. 380, p. 189–219.

Karamyan, K.A., 1978, Geology, structure and condition of formation copper-molybdenum deposits of Zangezour ore region: Yerevan, Publishing House of the Academy of Sciences Armenian SSR, 179 p. (in Russian).

Karamyan K.A., Tayan R.N., and Guyumdjyan O.P., 1974, The main features of intrusion magmatism Zangezur region of the Armenian SSR: Proceedings of the National Academy of Sciences of the Republic of Armenia, v. 27, p. 54-65 (in Russian).

Karapetyan, A.I., Amiryan, S.H., Azizbekynam, S., Altunyan, A.Z., Melkonyan, R.L., Guyumjyan, O.P., Paronikyan, V.O., Nalbandyan, E.M., Kaplanyan, P.M., Galstyan, A.R., Grigotyan, L.A., and Zohrabyan, S.A., 1982, Predicting metallogenic map of the Alaverdi-Shamlugh-Akhtala ore junction: Unpublished report of National Academy of Sciences of Armenian SSR, Institute of Geological Sciences.

Karapetian, S.G., Jrbashian, R.T., and Mnatsakanian, A., Kh., 2001, Late collision rhyolitic volcanism in the north-eastern part of the Armenian highland: Journal of Volcanology and Geothermal Research, v. 112, p. 189-220.

Kashkai, M.A., 1965, Petrology and metallogeny of Dashkesan and other iron ore deposits in Azerbaijan: Nedra publishers, Moscow, 888 p. (in Russian with English abstract).

Kaygusuz, A., and Öztürk, M., 2015, Geochronology, geochemistry, and petrogenesis of the Eocene Bayburt intrusions, Eastern Pontides, NE Turkey: Evidence for lithospheric mantle and lower crustal sources in the high-K calc-alkaline magmatism: Journal of Asian Earth Sciences, v. 108, p. 97-116.

Kazmin, V.G., Sbortshikov, I.M., Ricou, L.-E., Zonenshain, L.P., Boulin, J., and Knipper, A.L., 1986, Volcanic belts as markers of the Mesozoic-Cenozoic active margin of Eurasia: Tectonophysics, v. 123, p. 123-152.

Kekelia, S., Kekelia, M., Otkhmezuri, Z., Özgür, N., Moon, C., 2004, Ore-forming systems in volcanogenic-sedimentary sequences by the example of base metal deposits of the Caucasus and East Pontic Metallotect: Bulletin of the Mineral Research and Exploration, v. 129, p. 1–16.

Kekelia, S. A., Kekelia, M. A., Kuloshvili, S. I., Sadradze, N. G., Gagnidze, N. E., Yaroshevich, V. Z., Asatiani G. G., Doebrich, J. L., Goldfarb, R. J., and Marsh, E. E., 2008, Gold deposits and occurrences of the Greater Caucasus, Georgia Republic: Their genesis and prospecting criteria : Ore Geology Reviews, v. 34, p. 369-389.

Kesler, S.E., Hall, C.M., Russell, N., Pinero, E., Sanchez, C.R., Perez, R.M., and Moreira, J., 2004, Age of the Camagüey gold–silver district, Cuba: Tectonic evolution and preservation of epithermal mineralization in volcanic arcs: Economic Geology, v. 99, p. 869–886.

Khachaturyan E.A., 1977, The mineralogy, geochemistry and genesis of ores of pyrite formations of Armenian SSR: Publishing House of the Academy of Sciences of Armenian SSR, Yerevan, 316 pp. (in Russian).

Khain, V.E., 1975, Structure and main stages in the tectono-magmatic development of the Caucasus: an attempt at geodynamic interpretation: American Journal of Science, v. 275-A, p. 131-156.

Khomeriki, G., and Tuskia, T., 2005, Geological structures and ore deposits of Adjara: Publisher Alioni, Batumi, Georgia, 111 p. (in Georgian).

Knipper, A.L., and Khain, E.V., 1980, Structural position of ophiolites of the Caucasus: Ofioliti, v. 2, p. 297-314.

Kontsantinov, M.M., and Grushin V.A., 1970, Geologic position of the Zod-Agduzdag gold-ore nodes in Transcaucasia: International Geology Review, v. 12, p. 1447-1453.

Konstantinov, M.M., Kryazhev, S.G., and Ustinov, V.I., 2010, Characteristics of the ore-forming system of the Zod gold-tellurium deposit (Armenia) according to isotopic data: Geochemistry International, v. 48, p. 946-949.

Kouzmanov, K., Moritz, R., von Quadt, A., Chiaradia, M., Peytcheva, I., Fontignie, D., Ramboz, C., and Bogdanov, K., 2009, Late Cretaceous porphyry Cu and epithermal Cu–Au association in the Southern Panagyurishte District, Bulgaria: the paired Vlaykov Vruh and Elshitsa deposits: Mineralium Deposita, v. 44, p. 611–646.

Kozerenko, S.V., 2004, Hydrothermal system of the Zod gold sulfide deposit, Armenia: Ore sources and formation conditions: Geochemistry International, v. 42, p. 188-190.

Kozlovsky, Y.A., ed., 1991, Mining Encyclopedia, v. 5, Nedra Press (in Russian).

Kusçu, I., Tosdal, R.M., Genclioglu-Kusçu, G., Friedman, R., and Ullrich, T.D., 2013, Late Cretaceous to middle Eocene magmatism and metallogeny of a Portion of the Southeastern Anatolian orogenic belt, East-Central Turkey: Economic Geology, v. 108, p. 641-666.

Large, R.R., McPhie, J., Gemmell, J.B., Herrmann, W., and Davidson, G.J., 2001, The spectrum of ore deposit types, volcanic environments, alteration halos, and related exploration vectors in submarine volcanic successions: some examples from Australia: Economic Geology, v. 96, p. 913–938.

Lavoie, J., 2015, Genetic constraints of the late-Cretaceous epithermal Beqtakari prospect, Bolnisi mining district, Lesser Caucasus, Georgia: Unpublished MSc Thesis, University of Geneva, Switzerland, 119 p.

Lavoie, J., Moritz, R., Popkhadze, N., and Spangenberg, J., 2015, The late Cretaceous epithermal Beqtakari prospect; Bolnisi mining district, Georgia, Lesser Caucasus, in André-Mayer, A.-S., Cathelineau, M., Muchez, P., Pirard, E., and Sindern, S., eds, Mineral resources in a sustainable world, 13th SGA Biennial Meeting, 12-15 August 2015, France, Nancy, v. 1, p. 313-316.

Lawley, C.J.M., and Selby, D., 2012, Re-Os geochronology of quartz-enclosed ultrafine molybdenite: Implications for ore geochronology: Economic Geology, v. 107, p. 1499–1505.

Lebedev, A.P., and Malkhasyan, E.G., 1965, Jurassic volcanism of Armenia : Publishing House Nauka, Moscow, 167 p. (in Russian).

Levitan, G., 2008, Gold deposits of the CIS: Xlibris corporation, Bloomington, Indiana, USA, 352 p.

Little, C.T.S., Magalashvili, A.G., and Banks, D.A., 2007, Neotethyan late Cretaceous volcanic arc hydrothermal vent fauna: Geology, v. 35, p. 835-838.

Lordkipanidze M., Zakariadze G., and Popolitov E., 1979, Volcanic evolution of marginal and inter-arc basins: Tectonophysics, v. 57, p. 71-83.

Lordkipanidze, M., Meliksetian, B., and Djarbashian, R., 1989, Mesozoic-Cenozoic magmatic evolution of the Pontian-Crimean-Caucasus region: Mémoire de la Société Géologique de France, v. 154, p. 103-124.

Lydian International, 2016, www.lydianinternational.co.uk.

Mamedov, A.O., 1983, Report about results of detailed exploration of copper-porphyry ores within Kedabek-Bittibulakh ore-bearing zone during 1979-1982: Unpublished report, Funds of the Azerbaijan Geological Department, 144 p. (in Russian).

Markey, R., Stein, H.J., Hannah, J.L., Zimmerman, A., Selby, D., and Creaser, R.A., 2007, Standardizing Re-Os geochronology: A new molybdenite reference material (Henderson, USA) and the stoichiometry of Os salts: Chemical Geology, v. 244, p. 74–87.

Markus, M.A., 2002, The formation of massive sulfide ores in black shales of the Eastern Caucasus: Evidence from the Kızıl Dere Orefield : Lithology and Mineral Resources, v. 37, p. 157-161.

Masterman, G.J., White, N., C., Wilson, C.J.L., and Pape, D., 2002, High-sulfidation gold deposits in ancient volcanic terranes: insights from the Mid-Paleozoic Peak Hill deposit, NSW: Society of Economic Geology Newsletter, v. 51, p. 10–16.

Matveev, A., Spiridonov, E., Grigoryan, S., Tabatabaei, S., and Filimonov, S., 2006, Mineralogical and geochemical characteristics and predicted reserves of gold-base metal ore mineralization in southern Armenia and northwestern Iran. Geochemistry International, v. 44, p. 814–824.

Mayringer, F., Treloar, P.J., Gerdes, A., Finger, F., and Shengelia, D., 2011, New age data from the Dzirula Massif, Georgia: Implications for the evolution of the Caucasian Variscides: American Journal of Science, v. 311, p. 404-441.

McQuarrie, N., and van Hinsbergen, D.J.J., 2013, Retrodeforming the Arabia-Eurasia collision zone: Age of collision versus magnitude of continental subduction: Geology, v. 41, p. 315-318.

McQuarrie, N., Stock, J.M., Verdel, C., and Wernicke, B.P., 2003, Cenozoic evolution of the Neotethys and implications for the causes of plate motions: Geophysical Research Letters, v. 30, p. 1-6.

Mederer, J., 2013. Regional setting, geological context and genetic aspects of polymetallic hydrothermal ore deposits from the Kapan ore district, southern Armenia: a contribution to the Mesozoic island arc metallogeny of the Lesser Caucasus: Ph.D. thesis, University of Geneva, Switzerland, Terre et Environnement, 161.

Mederer, J., Moritz, R., Ulianov, A., and Chiaradia, M., 2013, Middle Jurassic to Cenozoic evolution of arc magmatism during Neotethys subduction and arc-continent collision in the Kapan Zone, southern Armenia: Lithos, v. 177, p. 61–78.

Mederer. J., Moritz, R., Zohrabyan, S., Vardanyan, A., and Melkonyan, R., 2014, Base and precious metal mineralization in the Jurassic-Cretaceous arc of the Lesser Caucasus - a comparison of the contrasting Drmbon, Alaverdi and Kapan mining districts: Ore Geology Reviews, v. 58, p. 185-207.

Meijers, M.J.M., Smith, B., Kirscher, U., Mensink, M., Sosson, M., Rolland, Y., Grigoryan, A., Sahakyan, L., Avagyan, A., Langereis, C., and Müller, C., 2015, A paleolatitude reconstruction of the South Armenian Block (Lesser Caucasus) for the late Cretaceous: constraints on the Tethyan realm: Tectonophysics, v. 644–645, p. 197–219.

Melikyan, L.S., 1976, Geological-structural control of the Sotk ore field: Proceedings of the National Academy of Sciences of the Republic of Armenia, Earth Sciences, v. 29, p. 3-12 (in Russian).

Melkonyan, R.L., 1965. About the problem of the genesis of plagiogranite and trondhjemite (based on the example of the Alaverdi ore district): Proceedings of the National Academy of Sciences of the Republic of Armenia, Earth Sciences, v. 18, p. 32-41 (in Russian).

Melkonyan, R.L., 1976, Petrology, mineralogy and geochemistry of intrusive complexes of Alaverdi ore region, in Meliksetyan B.M., and Melkonyan R.L., eds, Petrology and geochemistry of intrusive complexes of some ore regions of Armenian SSR: Publishing House of the Academy of Sciences of Armenia SSR, p. 137-281 (in Russian).

Melkonyan, R.L., Khorenian, R.A., and Chiboukhchian, Z.H., 2000, On the issue of the Mesozoic magmatism in the Tsahkounk-Zanghezour zone of the Lesser Caucasus: Proceedings of the National Academy of Sciences of the Republic of Armenia, Earth Sciences, v. 53, p. 17–29 (in Russian with English abstract).

Melkonyan, R.L., and Ghukasian, R.Kh., 2004, About the issue of the age of Koghb-Shnokh intrusive complex: Proceedings of the National Academy of Sciences of the Republic of Armenia, Earth Sciences, v. 57, p. 29-35 (in Russian with English abstract).

Melkonyan, R.L., Ghukasian, R.Kh., Tayan, R.N., and Haruntunyan, M.A., 2008, Geochronometry of the Meghri pluton monzonites (Armenia) – results and consequences: Proceedings of the National Academy of Sciences of the Republic of Armenia, v. 61, p. 3-9 (in Russian with English abstract).

Melkonyan, R.L., Ghukasian, R.Kh., Tayan, R.N., Khorenyan, R.A., and Hovakimyan, S.E., 2010, The stages of copper-molybdenum ore formation in Southern Armenia (by the results of Rb-Sr isotope age estimations): Proceedings of the National Academy of Sciences of the Republic of Armenia, v. 63, p. 21-32 (in Russian with English abstract).

Migineishvili, R., 2002, A possible model for formation for the Madneuli copper-gold deposit: Georgian Academy of Sciences, A. Janelidze Geological Institute Proceeding new series, v. 117, p. 473-480.

Migineishvili, R., 2005, Hybrid nature of the Madneuli Cu-Au deposit, Georgia: Geochemistry, Mineralogy and Petrology (Journal of the Bulgarian Academy of Sciences, v. 43, p. 128-132.

Migineishvili, R., and Gavtadze, T., 2010, Age of the Madneuli Cu-Au deposit, Georgia: Evidence from new nannoplankton data: Bulletin of the Georgian National Academy of Sciences, v. 4, p. 85-91.

Mkrtchyan S.S, Karamyan K.A., and Arevshatyan T.A., 1969, Kadjaran copper-molybdenum deposit: Publishing House of the Academy of Armenian Sciences SSR, 330 p. (in Russian).

Mohajjel M., and Fergusson, C.L., 2000, Dextral transpression in late Cretaceous continental collision, Sanandaj-Sirjan zone, western Iran: Journal of Structural Geology, v. 22, p. 1125-1139.

Moon, C.J., Gotsiridze, G., Gugushvili, V., Kekelia, M., Kekelia, S., Migineishvili, R., Otkhmezuri, Z., and Özgür, N., 2001, Comparison of mineral deposits between Georgian and Turkish sectors of the Tethyan metallogenic belt, in Piestrzynski, A., et al., eds, Mineral Deposits at the Beginning of the 21st Century, Proceedings 6th Biennial SGA Meeting, Krakow, Poland, p. 309–312.

Moritz, R., Kouzmanov, K., Petrunov, R., 2004, Late Cretaceous Cu–Au epithermal deposits of the Panagyurishte district, Srednogorie zone, Bulgaria: Swiss Bulletin of Mineralogy and Petrology, v. 84, p. 79-99.

Moritz, R., Selby, D., Ovtcharova, M., Mederer, J., Melkonyan, R., Hovamkimyan, S., Tayan, R., Popkhadze, N., Gugushvili, V., and Ramazanov V., 2012, Diversity of geodynamic settings during Cu, Au and Mo ore formation in the Lesser Caucasus: new age constraints. European Mineralogical Conference, Frankfurt, Germany, 2-6 September 2012, Abstract volume.

Moritz, R., Rezeau, H., Ovtcharova, M., Tayan, R., Melkonyan, R., Hovamkimyan, S., Ramazanov V., Selby, D., Ulianov, A., Chiaradia, M., and Putlitz, B., in press, Long-lived, stationary magmatism and pulsed porphyry systems during Tethyan subduction to post-collision evolution in the southernmost Lesser Caucasus, Armenia and Nakhitchevan: Gondwana Research, doi: 10.1016/j.gr.2015.10.009.

Musaev, S.D., and Shirinov, A., 2002, Report about the results of explorative-estimation studies on gold in the NW part of Dashkesan ore region during 2000-2002: Unpublished report, Territorial Geological Fund, Baku, Azerbaijan, 195 p. (in Russian).

Nalbandyan, E.M., 1968, Characteristics of hydrothermal metamorphism related to the polyphase development of middle Jurassic volcanism in the Alaverdi ore region: Proceedings of the National Academy of Sciences of the Republic of Armenia, Earth Sciences, v. 21, p. 16-22 (in Russian).

Nalbandyan, E.M., and Paronikyan, V.O., 1966, About ore-bearing rocks of the Alaverdi deposit: Proceedings of the National Academy of Sciences of the Republic of Armenia, Earth Sciences, v. 19, p. 90-94 (in Russian).

Neill, I., Meliksetian, K., Allen, M.B., Navasardyan, G., and Kuiper, K., 2015, Petrogenesis of mafic collision zone magmatism: The Armenian sector of the Turkish–Iranian plateau: Chemical Geology, v. 403, p. 4–41.

Okay, A.I., 2008, Geology of Turkey: A synopsis: Anschnitt, v. 21, p. 19-42.

Okay, A.I., and Sahintürk, Ö., 1997, Geology of the Eastern Pontides, in Robinson, A.G., ed., Regional and Petroleum Geology of the Black Sea and Surrounding Region: American Association of Petroleum Geologists Memoir, v. 68, p. 291–311.

Okay, A.I., Zattin, M., and Cavazza, W., 2010, Apatite fission-track data for the Miocene Arabia-Eurasia collision: Geology, v. 38, p. 35-38.

Omrani, J., Agard, P., Whitechurch, H., Benoit, M., Prouteau, G., and Jolivet, L., 2008, Arc magmatism and subduction history beneath the Zagros Mountains, Iran: a new report of adakites and geodynamic consequences: Lithos, v. 106, p. 380–398.

Okrostsvaridze, A., Akimidze, K., Gagnidze, N., Akimidze, A., and Abuashvili, D., 2015, Ore Occurences in the Georgian Segment of the Eastern Greater Caucasus: New Research Results : Bulletin of the Georgian National Academy of Sciences, v. 9, p. 102-110.

Paronikyan V.O., 1962, On the mineralogy of ore of the Akhtala polymetalic deposit: Izvestia of Sciences of Armenian SSR, Geologic and Geographic Sciences, v. 6, p. 3-12 (in Russian).

Paronikyan, V.H., and Ghukasian, R.Kh., 1974, About absolute age of muscovite from Teghout ore manifestation: Proceedings of the National Academy of Sciences of the Republic of Armenia, Earth Sciences, v. 27, p. 57-58 (in Russian).

Peccerillo, A., and Taylor, S.R., 1976, Geochemistry of upper Cretaceous volcanic rocks from the Pontic chain, Northern Turkey: Bulletin of Volcanology, v. 39, p. 557–569.

Philip, H., Cisternus, A., Gvishiani, A., and Gorshkov, A., 1989, The Caucasus: an actual example of the initial stages of a continental collision: Tectonophysics, v. 161, p. 1-21.

Philip, H., Avagyan, A., Karakhanian, A., Ritz, J.-F., and Rebai, S., 2001, Estimating slip rates and recurrence intervals for strong earthquakes along an intracontinental fault; example of the Pambak–Sevan–Sunik Fault (Armenia) : Tectonophysics, v. 343, p. 205–232.

Pijyan, G.O., 1975, Copper-molybdenum formation of Armenian SSR: Publishing House of the Academy of Armenian Sciences SSR, 309 p. (in Russian).

Popkhadze, N., Moritz, R., and Gugushvili, V., 2014, Architecture of upper Cretaceous rhyodacitic hyaloclastite at the polymetallic Madneuli deposit, Lesser Caucasus, Georgia: Central European Journal of Geoscience, v. 6, p. 308–329.

Ramazanov, V.G., and Kerimli, U.I., 2012, The formation of gold-quartz-sulphide veins of Pyazbashi deposit and some patterns of their distribution: Baku University Publications, v. 2, p. 124-144 (in Russian with English abstract).

Rezeau, H., Moritz, R., Wotzlaw, J.-F., Hovakimyan, S., Tayan, R., and Selby, D., 2015, Pulsed porphyry Cu-Mo formation during protracted pluton emplacement in southern Armenia, Lesser Caucasus: the potential role of crustal melting for ore recycling, in André-Mayer, A.-S., Cathelineau, M., Muchez, P., Pirard, E., and Sindern, S., eds, Mineral resources in a sustainable world, 13^{th} SGA Biennial Meeting, 12-15 August 2015, France, Nancy, v. 1, p. 343- 346.

Richards, J.P., 2003, Tectono-magmatic precursors for porphyry Cu-(Mo-Au) deposit formation: Economic Geology, v. 98, p. 1515–1533.

Richards, J.P. 2015. Tectonic, magmatic, and metallogenic evolution of the Tethyan orogen: From subduction to collision. Ore Geology Reviews 70, 323–345.

Robertson, A.H.F., Parlak, O., and Ustaömer, T., 2013, Late Palaeozoic–early Cenozoic tectonic development of Southern Turkey and the easternmost Mediterranean region: evidence from the inter-relations of continental and oceanic units, in Robertson, A.H.F., Parlak, O., and Ülügenç, U.C., eds, Geological development of Anatolia and the easternmost Mediterranean region: Geological Society of London Special publication, v. 372, p. 9-48.

Rolland, Y., Billo, S., Corsini, M., Sosson, M., and Galoyan, G., 2009a, Blueschists of the Amassia–Stepanavan Suture Zone (Armenia): linking Tethys subduction history from E-Turkey to W-Iran: International Journal of Earth Sciences, v. 98, p. 533–550.

Rolland, Y., Galoyan, G., Bosch, D., Sosson, M., Corsini, M., Fornari, M., and Vérati, C., 2009b, Jurassic Back-arc and hot-spot related series in the Armenian ophiolites – implications for the obduction process: Lithos, v. 112, p. 163–187.

Rolland, Y., Galoyan, G., Sosson, M., Melkonyan, R., and Avagyan, A., 2010, The Armenian ophiolite: insights for Jurassic back-arc formation, lower Cretaceous hot spot magmatism and upper Cretaceous obduction over the South Armenian Block, in Sosson, M., Kaymakci, N., Stephenson, R.A., Bergerat, F., and Starostenko, V., eds, Sedimentary basin tectonics from the Black Sea and Caucasus to the Arabian platform: Geological Society of London Special publication, v. 340, p. 353-382.

Rolland, Y., Sosson, M., Adamia, Sh., and Sadradze, N., 2011, Prolonged Variscan to Alpine history of an active Eurasian margin (Georgia, Armenia) revealed by $^{40}Ar/^{39}Ar$ dating: Gondwana Research, v. 20, p. 798-815.

Rolland, Y., Perincek, D., Kaymakci, N., Sosson, M., Barrier, E., and Avagyan, A., 2012, Evidence for ~80-75 Ma subduction jump during Anatolide-Tauride-Armenian block accretion and ~48 Ma Arabia-Eurasia collision in Lesser Caucasus-east Anatolia: Journal of Geodynamics, v. 56-57, p. 76-85.

Rubinstein, M.M., Adamia, S.A., Bagdasaryan, G.P., and Gugushvili, V.I., 1983, About the genetic relation of the copper pyritic-baritic-base metal deposits of the Bolnisi region with upper Cretaceous volcanism: Bulletin of the Academy of Sciences of the Georgian SSR, v. 109, p. 570-576 (in Russian with English abstract).

Rye, R.O., 2005, A review of the stable-isotope geochemistry of sulfate minerals in selected igneous environments and related hydrothermal systems: Chemical Geology, v. 215, p. 5–36.

Rye, R.O., Bethke, P.M., and Wasserman, M.D., 1992, The stable isotope geochemistry of acid sulfate alteration: Economic Geology, v. 87, p. 225–262.

Saintot, A., Brunet, M.-F., Yakovlev, F., Sébrier, M., Stephenson, R., Ershov, A., Chalot-Prat, F., and McCann, T., 2006, The Mesozoic-Cenozoic tectonic evolution of the Greater Caucasus, in Gee, D.G., and Stephenson, R.A., eds, European Lithosphere Dynamics: Geological Society of London Memoirs, v. 32, p. 277-289.

Salavati, M., 2008, Petrology, geochemistry and mineral chemistry of extrusive alkalic rocks of the Southern Caspian Sea Ophiolite, Northern Alborz, Iran: evidence of alkaline magmatism in Southern Eurasia: Journal of Applied Sciences, v. 8, p. 2202–2216.

Sander, M.V., and Einaudi, M.T., 1990, Epithermal deposition of gold during transition from propylitic to potassic alteration at Round Mountain, Neveada: Economic Geology, v.85, p. 285-311.

Sarkisyan, R.A., 1970, About the presence of different age subvolcanic dacite quartz porphyries in Kapan ore field: Proceedings of the National Academy of Sciences of the Republic of Armenia, Earth Sciences, v. 23, p. 13–17 (in Russian).

Selby, D., and Creaser, R.A., 2001a, Late and mid-Cretaceous mineralization in the northern Canadian Cordillera: Constraints from Re-Os molybdenite dates: Economic Geology, v. 96, p. 1461–1467.

Selby, D., and Creaser, R.A., 2001b, Re-Os Geochronology and systematics in molybdenite from the Endako porphyry molybdenum deposit, British Columbia, Canada: Economic Geology, v. 96, p. 197–204.

Sevunts, A.G., 1972, About regularities of sulfur isotope distribution in the ores of the Alaverdi group of deposits: Proceedings of the National Academy of Sciences of the Republic of Armenia, Earth Sciences, v. 25, p. 29-36 (in Russian).

Shafiei, B., Haschke, M., and Shahabpour, J. 2009, Recycling of orogenic arc crust triggers porphyry Cu mineralization in Kerman Cenozoic arc rocks, southeastern Iran: Mineralium Deposita, v. 44, p. 265–283.

Shengelia, D.M., Tsutsunava, T.N., and Shubitidze, L.G., 2006, New data on structure, composition, and regional metamorphism of the Tsakhkunyats and Akhum-Asrikchai massifs, the Lesser Caucasus: Doklady Earth Sciences, v. 409A, p. 900-904.

Sherlock, R.L., Tosdal, R.M., Lehrman, N.J., Graney, J.R., Losh, S., Jowett, E.C., and Kesler, S.E., 1995, Origin of the McLaughlin mine sheeted vein complex: Metal zoning, fluid inclusion, and isotopic evidence: Economic Geology, v. 90, p. 2156-2181.

Sillitoe, R.H., 2010, Porphyry copper systems: Economic Geology, v. 105, p. 3–41.

Simmonds, V., and Moazzen, M., 2015, Re–Os dating of molybdenites from Oligocene Cu–Mo–Au mineralized veins in the Qarachilar area, Qaradagh batholith (northwest Iran): implications for understanding Cenozoic mineralization in South Armenia, Nakhchivan, and Iran: International Geology Review, v. 57, p. 290-304.

Simmons, S.F., White, N.C., and John, D.A., 2005, Geological characteristics of epithermal precious and base metal deposits: Economic Geology 100th Anniversary Volume, p. 485-522.

Smoliar, M.I., Walker, R.J., and Morgan, J.W., 1996, Re-Os ages of group IIA, IIIA, IVA, and IVB iron meteorites: Science, v. 271, p. 1099–1102.

Sopko, P.F., 1961, Geology of Pyrite Deposits in the Alaverdi Ore District: Publishing House of the Academy of Sciences of the Armenian SSR, Yerevan, 170 p. (in Russian).

Sosson, M., Rolland, Y., Müller, C., Danelian, T., Melkonyan, R., Kekelia, S., Adamia, S., Babzadeh, V., Kangarli, T., Avagyan, A., Galoyan, G., and Mosar, J., 2010, Subductions, obduction and collision in the Lesser Caucasus (Armenia, Azerbaijan, Georgia), new insights, in Sosson, M., Kaymakci, N., Stephenson, R.A., Bergerat, F., and Starostenko, V., eds, Sedimentary basin tectonics from the Black Sea and Caucasus to the Arabian platform: Geological Society of London Special Publication, v. 340, p. 329-352.

Spiridonov, E.M., 1991, Listvenites and zodites: International Geology Review, v. 33, p. 397-407.

Stöllner, T., Craddock, B., Gambaschidze, I., Gogotchuri, G., Hauptmann, A., Hornschuch, A., Klein, F., Löffler, I., Mindiashwili, G., Murwanidze, B., Senczek, S., Schaich, M., Steffens, G., Tamasashvili, K., Timberlake, S., Jansen, M., and Courcier, A., 2014, Gold in the Caucasus: New research on gold extraction in the Kura-Araxes culture of the 4th millennium BC and earl 3rd millennium BC: Tagungen des Landesmuseums für Vorgeschichte Halle, v. 11, p. 71-109.

Şengör, A.M.C., and Yilmaz, Y., 1981, Tethyan evolution of Turkey; A plate tectonic approach: Tectonophysics, v. 75, p. 181-241.

Tayan, R.N., 1984, The feature evolution of fractures of Kadjaran ore field: Proceedings of the National Academy of Sciences of the Republic of Armenia, v. 37, p. 21-29 (in Russian with English abstract).

Tayan, R.N., Plotnikov, E.P., and Abdurakhmanov, R.U., 1976, Some features of emplacement of geological structure of the Zangezour-Nakhichevan region of Lesser Caucasus: Proceedings of the National Academy of Sciences of the Republic of Armenia, v. 29, p. 12-20 (in Russian).

Tayan, R.N., Harutunyan, M.A., and Hovhannisyan, A.E., 2005, To the problem of dislocation of copper-molybdenum and gold-polymetallic formations in southern Zangezour and opportunities for small ore deposits identification through elements-admixtures in pyrites: Proceedings of the National Academy of Sciences of the Republic of Armenia, v. 58, p. 17-24 (in Russian with English abstract).

Tayan, R.N., Sarkissyan, S.P., and Oganesyan, A.E., 2007, Geological and structural conditions for the formation of the Agarak copper-molybdenum deposit (Southern Armenia) : Proceedings of the National Academy of Sciences of the Republic of Armenia, v. 60, p. 28–34 (in Russian).

Temizel, I., Arslan, M., Ruffet, G., and Peucat, J.-J., 2012, Petrochemistry, geochronology and Sr–Nd isotopic systematics of the Tertiary collisional and post-collisional volcanic rocks from the Ulubey (Ordu) area, Eastern Pontide, NE Turkey: Implications for extension-related origin and mantle source characteristics: Lithos, v. 128, p. 126-147.

Topuz, G., Alther, R., Schwarz, W.H., Siebel, W., Satır, M., and Dokuz, A., 2005, Postcollisional plutonism with adakite-like signatures: the Eocene Saraycık granodiorite (Eastern Pontides, Turkey) : Contributions to Mineralogy and Petrology, p. 150, v. 441–455.

Topuz, G., Okay, A. I., Altherr, R., Schwarz, W. H., Siebel, W., Zack, T., Satır, M., and Şen, C., 2011, Post-collisional adakite-like magmatism in the Ağvanis Massif and implications for the evolution of the Eocene magmatism in the Eastern Pontides (NE Turkey): Lithos, v. 125, p. 131–150.

Topuz, G., Göçmengil, G., Rolland, Y., Çelik, Ö.F., Zack, T., and Schmitt, A.K., 2013, Jurassic accretionary complex and ophiolite from northeast Turkey: no evidence for the Cimmerian continent: Geology, v. 41, p. 255–258.

Torró, L., Proenza, J.A., Melgarejo, J.C., Alfonso, P., Farré de Pablo, J., Colomer, J.M., García-Casco, A., Gubern, A., Gallardo, E., Cazañas, X., Chávez, C., Del Carpio, R., León, P., Nelson, C.E., Lewis, J.F., 2016, Mineralogy, geochemistry and sulfur isotope characterization of Cerro de Maimón (Dominican Republic), San Fernando and Antonio (Cuba) lower Cretaceous VMS deposits: Formation during subduction initiation of the proto-Caribbean lithosphere within a fore-arc: Ore Geology Reviews, v. 72, p. 794-817.

Tumanyan, G.A., 1992, Peculiarities of structure and position of Kapan anticlinorium: Proceedings of the National Academy of Sciences of the Republic of Armenia, Earth Sciences, v. 45, p. 3–11 (in Russian).

Tvalchrelidze, G.A., 1980, Copper metallogeny of the Caucasus, in Jankovic, S. and Sillitoe, R.H., eds, European Copper Deposits: proceedings of an International Symposium held at Bor, Yugoslavia 18-22 September 1979: Society for Geology Applied to Mineral Deposits, Belgrade University, p. 191-196.

Tvalchrelidze, G.A., 1984, Main features of metallogeny of the Caucasus, in Janelidze, T.V. and Tvalchrelidze, A.G., eds, Proceedings of the Sixth Quadrennial IAGOD Symposium: E. Schweizerbat'sche Verlagsbuchhandlung, Stuttgart, vol. 1, p. 1-5.

Vardanyan, A.V., 2008, Geological structure of Drmbon gold-copperpyrite depoit and peculiarities of its structure: Proceedings of the National Academy of Sciences of the Republic of Armenia, Earth Sciences, v. 61, p. 3-13 (in Russian with English abstract).

Vardanyan, A.V., and Zohrabyan, S.A., 2008, Explosive-injective breccia-conglomerates of the Drmbon gold–copper pyrite deposit: Proceedings of the National Academy of Sciences of the Republic of Armenia, Earth Sciences, v. 61, p. 14–20 (in Russian with English abstract).

Verdel, C., Wernicke, B.P., Hassanzadeh, J., and Guest B., 2011, A Paleogene extensional arc flare-up in Iran: Tectonics, v. 30, TC3008.

Vincent, S.J., Allen, M.B., Ismail-Zadeh, A.D., Flecker, R., Foland, K.A., and Simmons, M.D., 2005, Insights from the Talysh of Azerbaijan into the Paleogene evolution of the South Caspian region: Geological Society of America Bulletin, v. 117, p. 1513-1533.

Völkening, J., Walczyk, T., and Heumann, K.G., 1991, Osmium isotope ratio determinations by negative thermal ionization mass spectrometry: International Journal of Mass Spectrometry and Ion Processes, v. 105, p. 147–159.

Von Quadt, A., Moritz, R., Peytcheva, I., and Heinrich, C., 2005, Geochronology and geodynamics of upper Cretaceous magmatism and Cu–Au mineralization in the Panagyurishte region of the Apuseni–Banat–Timok–Srednogorie belt (Bulgaria): Ore Geology Reviews, v. 27, p. 95–126.

Wensink, H., and Varekamp, J., 1980, Paleomagnetism of basalts from Alborz: Iran part of Asia in the Cretaceous: Tectonophysics, v. 68, p. 113–129.

Wheatley, C.J.V., and Acheson, D., 2011, Independent technical report of Toukhmanuk mine project and Getik prospect, Armenia, in conformance with NI 43-101 guidelines: Behre Dolbear International Limited, United Kingdom, 84 p.

Wolfe, B., and Gossage, B., 2009, Technical report for the Kapan project, Kapan, Armenia: Unpublished report, Perth, Australia, Coffey Mining Pty Ltd on behalf of Deno Gold Mining Company CJSC, 270 p.

Yeganehfar, H., Reza Ghorbani, M., Shinjo, R., and Ghaderi, M., 2013, Magmatic and geodynamic evolution of Urumieh–Dokhtar basic volcanism, Central Iran: major, trace element, isotopic, and geochronologic implications: International Geological Review, v. 55, p. 767-786.

Yigit, O. 2009, Mineral deposits of Turkey in relation to Tethyan metallogeny: Implications for future mineral exploration: Economic Geology, v. 104, p. 19-51.

Yilmaz, S., and Boztuğ, D., 1996, Space and time relations of three plutonic phases in the Eastern Pontides, Turkey: International Geology Reviews, v. 38, p. 935–956.

Yilmaz, A., Adamia, Sh., Chabukiani, A., Chkhotua, T., Erdogan, K., Tuzcu, S., and Karabilykoglu, M., 2000, Structural correlation of the southern Transcaucasus (Georgia)-eastern Pontides (Turkey), in Bozkurt, E., Winchester, J.A. and Piper, J.D.A., eds, Tectonics and magmatism in Turkey and the surrounding area: Geological Society of London Special Publication, v. 173, p. 171-182.

Yilmaz, A., Engİn, T., Adamia, Sh., and Lazarashvili, T., eds, 2001, Geological Studies of the Area Along Turkish-Georgian Border: Mineral Research and Exploration Institute (MTA) of Turkey, Report, 388 p.

Zakariadze, G.S., Magakyan, R.G., Tsameryan, O.P., Sobolev, A.V., and Kolesov, G.M., 1987, Problems of early Alpine evolution of the Lesser Caucasus as raised by geochemical data of volcanic series of the island arc type: in The structure of seismic focal zones: Publishing House Nauka, Moscow, p. 150-167 (in Russian).

Zakariadze, G.S., Dilek, Y., Adamia, S.A., Oberhänsli, R.E., Karpenko, S.F., Bazylev, B.A., and Solov'eva, N., 2007, Geochemistry and geochronology of the Neoproterozoic Pan-African Transcaucasian Massif (Republic of Georgia) and implications for island arc evolution of the late Precambrian Arabian-Nubian shield: Gondwana Research, v. 11, p. 92-108.

Zamani, G. B., and Masson, F., 2014, Recent tectonics of East (Iranian) Azerbaijan from stress state reconstructions: Tectonophysics, v. 611, p. 61–82.

Zanchi, A., Berra, F., Mattei, M., Ghassemi, M.R., and Sabouri, J., 2006, Inversion tectonics in central Alborz, Iran: Journal of Structural Geology, v. 28, p. 2023–2037.

Zohrabyan, S.A., 2007, About the problem of the genesis of pyrite deposits in Armenia: Proceedings of the National Academy of Sciences of the Republic of Armenia, Earth Sciences, v. 60, p. 32-36 (in Russian with English abstract).

Zohrabyan, S.A., and Melkonyan, R.L., 1999, Role of structural factors on the location of mineralization in iron-pyrite deposits of the Alaverdi-Kapan zone: Proceedings of the National Academy of Sciences of the Republic of Armenia, Earth Sciences, v. 52, p. 31-40 (in Russian with English abstract).

Zohrabyan, S.A., Mirzoyan, G.G., and Sarkisyan, N.A., 2003, Bartsravan ore field - geology, structure, ore mineralization: Proceedings of the National Academy of Sciences of the Republic of Armenia, Earth Sciences, v. 56, p. 30–38 (in Russian).

Zonenshain, L.P., and Le Pichon, X., 1986, Deep basins of the Black Sea and Caspian Sea as remnants of Mesozoic back-arc basins: Tectonophysics, v. 123, p. 181-211.

Figure captions

Figure 1. Geological map from eastern Turkey to Iran highlighting the Lesser Caucasus area from Mederer et al. (2014), with additional information from Azizi and Moinevaziri (2009), Hässig et al. (2013a, b) and Zamani and Masson (2014). The Lesser Caucasus consists of the Somkheto-Karabagh belt along the Eurasian margin, the ophiolites of the Sevan-Akera suture zone and the South Armenian block. The South Armenian block and the Eastern Anatolian platform are of Gondwanian origin. Abbreviations of tectonic zones and faults: ABV - Artvin-Bolnisi volcanic-arc; ATB – Adjara-Trialeti belt; IAES – Izmir-Ankara-Erzinkan suture; KGF – Khustup-Giratagh fault.

Figure 2. Simplified geological map of the Lesser Caucasus (after Mederer et al., 2014), and major regional faults (from Philip et al., 2001; Karakhanian et al., 2004). Legend of the geological background same as in Figure 1. The location of the maps of the major ore districts discussed in this review include from north to south: the Bolnisi district (Fig. 8), the Alaverdi district (Fig. 4), the Toukhmanouk-Meghradzor-Hanqavan ore cluster (Fig. 7), the Gedabek district (Fig. 6a), and the Kapan and Zangezur-Ordubad districts (Fig. 5). Other deposits and prospects discussed in the review are indicated by the small yellow boxes. Abbreviations of the ore deposits and prospects (yellow boxes): A – Amulsar, C – Chovdar, G – Gosha, M – Mehmana, and Z – Zod/Sotk. Abbreviations of the regional faults and major Cenozoic plutons: AF – Akerin fault, AkhF – Akhourian fault, BP – Bargushat pluton, DP – Dalidag pluton, GF – Garni fault, GSF – Geltareshka-Sarjkhamich fault, KGF – Khustup-Giratagh fault, MOP – Meghri-Ordubad pluton, PP – Pambak pluton, PSSF – Pambak-Sevan-Sunik fault system, SSF? - sublatudinal strike-slip fault (as suggested by Kazmin et al., 1986, Gabriyelyan et al., 1989, and Hässig et al., 2013a), TF – Tabriz fault.

Figure 3. Geodynamic reconstruction of the Tethyan belt centred on the Lesser Caucasus (LCR) for Callovian (a), Campanian (b), Lutetian (c), and Rupelian (d) times (modified from Barrier and Vrielynck, 2008). Additional information for the Callovian time (a) are from Hässig et al. (2013a) for the position of the northern spreading center, the intra-oceanic subduction zone, and from Melkonyan et al. (2000) and Hässig et al. (2015) for the interpretation of a south-verging subduction zone beneath SAB. The main ore-forming events are shown for the geodynamic stage that is the closest in age. Abbreviations: ABV - Artvin-Bolnisi volcanic-arc; AR – Alborz range; ATB – Adjara-Trialeti basin; BFB – Balkan fold-belt; BPM – Bitlis-Pütürge massif; EAP – Eastern Anatolian platform; GCB –

Greater Caucasus basin; GKF – Great Kevir fault; KOM – Khoy ophiolite massif; LCR – Lesser Caucasus range; LCV – Lesser Caucasus volcanic arc; MZT – Main Zagros thrust; PAM – Peri-Arabian massif; PoR – Pontides range; PoV – Pontides volcanic arc; SAB – South Armenian block; SAM – Sevan-Akera ophiolitic massif; SCB – South-Caspian basin; SkB – Sakarya block; SSB – Sanandaj-Sirjan block; TaP - Taurus platform; UDV – Urumieh-Dokhtar volcanic-arc; ZDF – Zagros deformation front (most abbreviations and domain names from Barrier and Vrielynck, 2008).

Figure 4. Simplified geology of the Alaverdi mining district (modified from Karapetyan et al., 1982; Mederer et al., 2014; Calder, 2104).

Figure 5. Simplified geological map of the Kapan and the Zangezur-Ordubad region, which includes the Kapan and the Meghri-Ordubad mining districts (after Karmyan et al., 1974; Tayan et al., 1976, 2005; Achikgiozyan et al., 1987; Babazadeh et al., 1990; Mederer et al., 2014). The Meghri-Ordubad district is hosted by the composite Meghri-Ordubad and Bargushat plutons included in the Gondwana-derived South Armenian block. The Kapan block with its mining district and the Shikahogh and Bartsravan prospects belongs to the Eurasian margin. The Khustup-Giratagh fault (KGF) is the major tectonic break between the Kapan block and the Zangezur-Ordubad region (South Armenian block).

Figure 6. a – Simplified geological map of the Gedabek mining district. **b** – Simplified geological map of the Chovdar mining district. **c** – Simplified geological map of the Gosha prospect (after Behre Dolbear, 2005).

Figure 7. Simplified geological map of the Toukhmanouk-Hanqavan-Meghradzor ore cluster.

Figure 8. Simplified geological map of the Bolnisi mining district (geology from Adamia and Gujabidze, 2004).

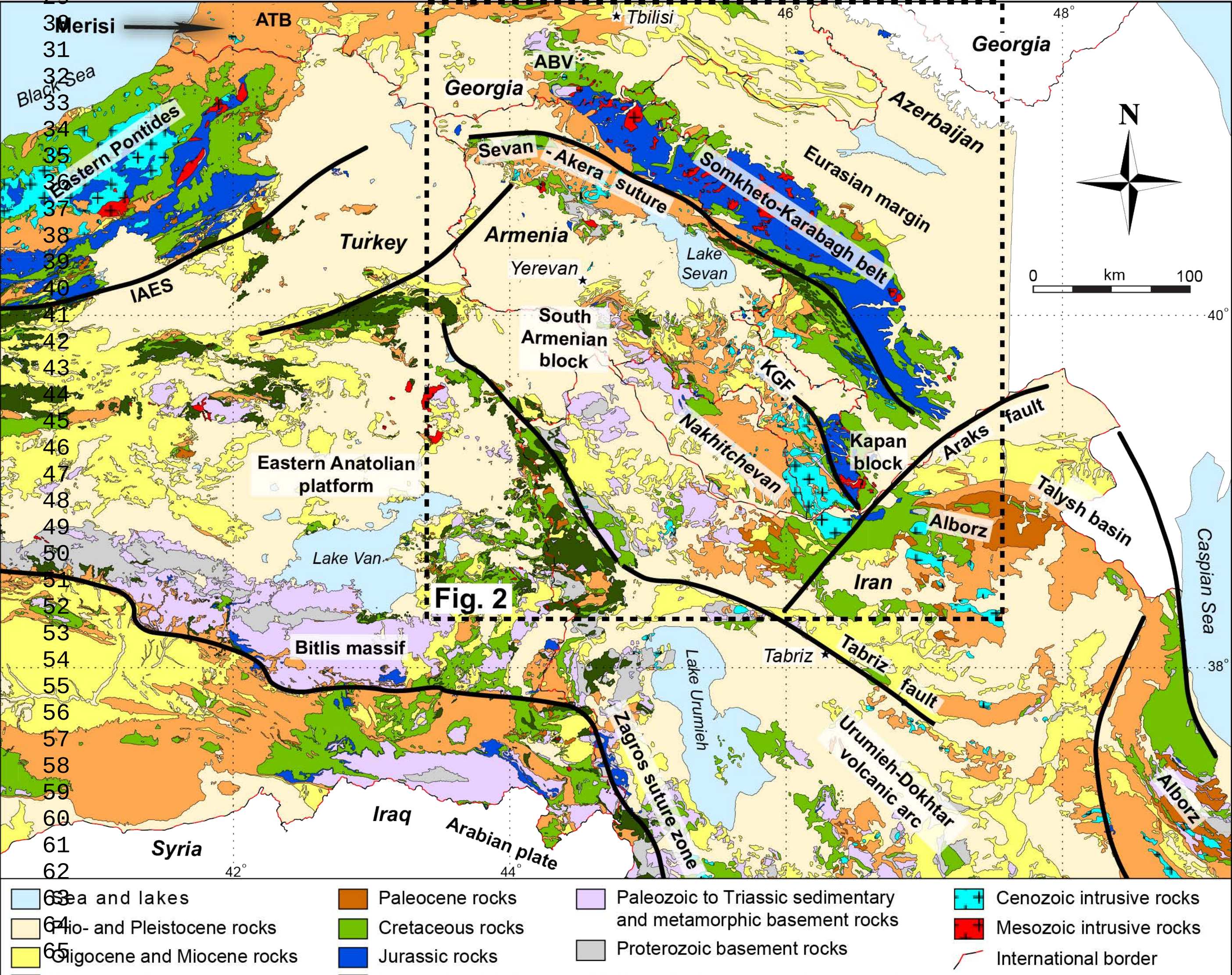
Merisi
ATB
Tbilisi
46°
48°
Georgia
Black Sea
ABV
Georgia
Azerbaijan
Eastern Pontides
Sevan - Akera suture
Somkheto-Karabagh belt
Eurasian margin
N
Turkey
Armenia
Lake Sevan
Yerevan
0 km 100
IAES
40°
South Armenian block
KGF
Nakhitchevan
Kapan block
Araks fault
Eastern Anatolian platform
Talysh basin
Alborz
Lake Van
Iran
Caspian Sea
Fig. 2
Bitlis massif
Tabriz
Tabriz fault
38°
Lake Urumieh
Zagros suture zone
Urumieh-Dokhtar volcanic arc
Alborz
Iraq
Arabian plate
Syria
42°
44°
Sea and lakes
Plio- and Pleistocene rocks
Oligocene and Miocene rocks
Eocene rocks
Paleocene rocks
Cretaceous rocks
Jurassic rocks
Mesozoic ophiolites
Paleozoic to Triassic sedimentary and metamorphic basement rocks
Proterozoic basement rocks
Major faults and tectonic boundaries
Cenozoic intrusive rocks
Mesozoic intrusive rocks
International border

Fig. 1

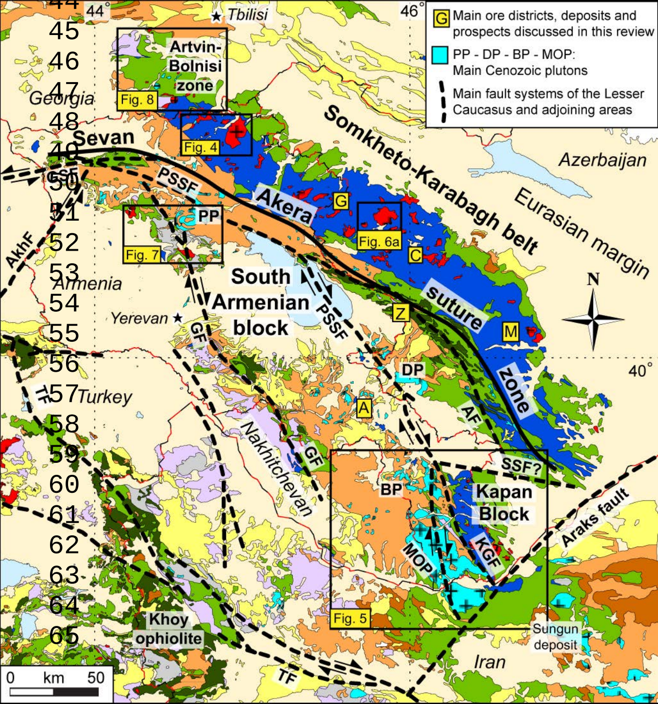

44°
Tbilisi
46°
Main ore districts, deposits and prospects discussed in this review
PP - DP - BP - MOP: Main Cenozoic plutons
Main fault systems of the Lesser Caucasus and adjoining areas
Artvin-Bolnisi zone
Fig. 8
Georgia
Fig. 4
Sevan
Somkheto-Karabagh belt
Azerbaijan
Eurasian margin
PSSF
Akera
G
Fig. 6a
C
PP
Fig. 7
AkhF
South Armenian block
Armenia
PSSF
suture
Z
M
N
Yerevan
GF
DP
40°
Zone
Turkey
TF
A
AF
Nakhitchevan
GF
SSF?
BP
Kapan Block
Araks fault
MOP
KGF
Fig. 5
Sungun deposit
Khoy ophiolite
Iran
TF
0 km 50

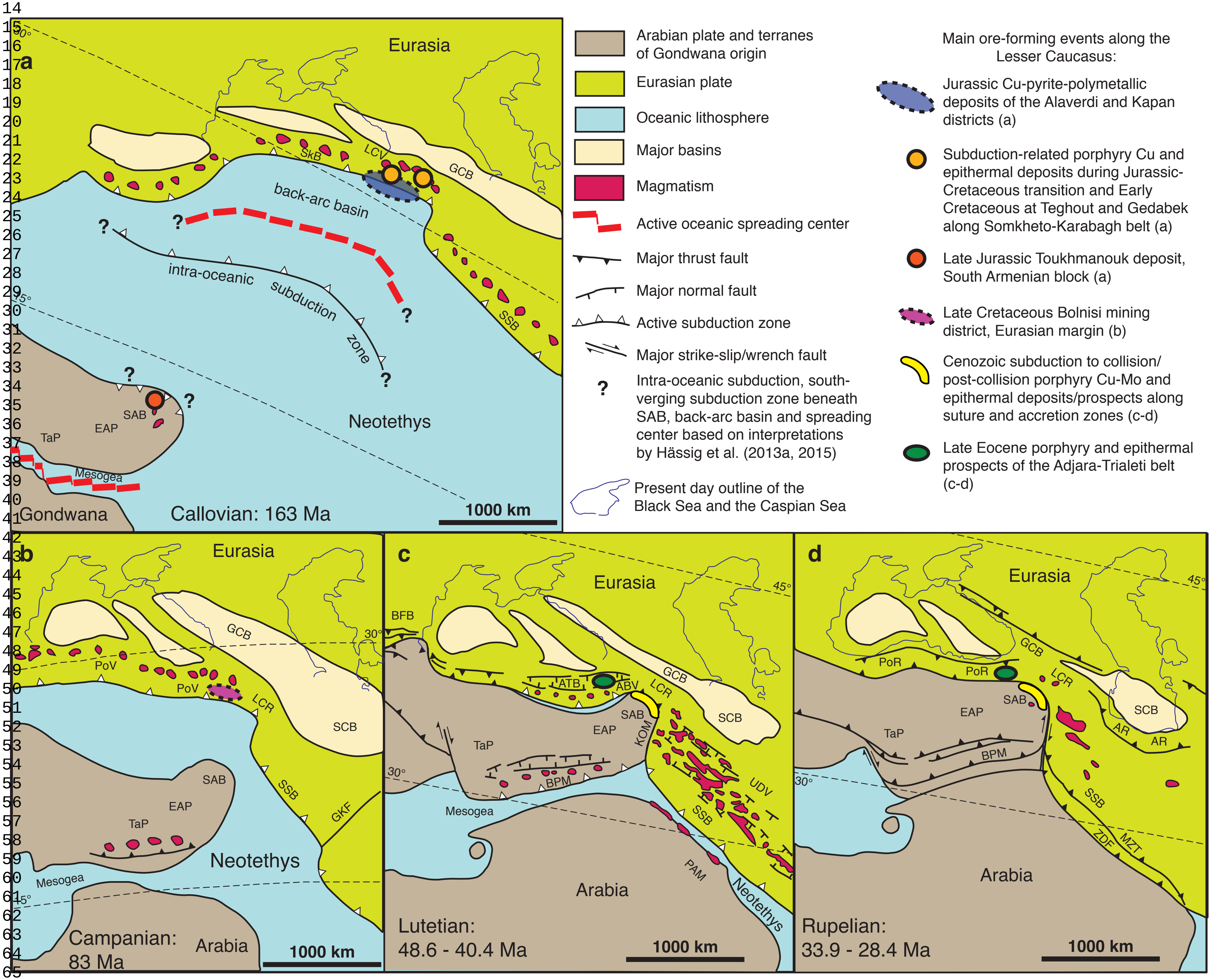
a
Eurasia
30°
15°
SkB
LCV
GCB
back-arc basin
intra-oceanic
subduction
zone
?
SSB
SAB
EAP
TaP
Mesogea
Neotethys
Gondwana
Callovian: 163 Ma
1000 km
Arabian plate and terranes of Gondwana origin
Eurasian plate
Oceanic lithosphere
Major basins
Magmatism
Active oceanic spreading center
Major thrust fault
Major normal fault
Active subduction zone
Major strike-slip/wrench fault
Intra-oceanic subduction, south-verging subduction zone beneath SAB, back-arc basin and spreading center based on interpretations by Hässig et al. (2013a, 2015)
Present day outline of the Black Sea and the Caspian Sea
Main ore-forming events along the Lesser Caucasus:
Jurassic Cu-pyrite-polymetallic deposits of the Alaverdi and Kapan districts (a)
Subduction-related porphyry Cu and epithermal deposits during Jurassic-Cretaceous transition and Early Cretaceous at Teghout and Gedabek along Somkheto-Karabagh belt (a)
Late Jurassic Toukhmanouk deposit, South Armenian block (a)
Late Cretaceous Bolnisi mining district, Eurasian margin (b)
Cenozoic subduction to collision/post-collision porphyry Cu-Mo and epithermal deposits/prospects along suture and accretion zones (c-d)
Late Eocene porphyry and epithermal prospects of the Adjara-Trialeti belt (c-d)
b
Eurasia
PoV
GCB
30°
LCR
SCB
SSB
GKF
SAB
EAP
TaP
Neotethys
Mesogea
15°
Campanian: 83 Ma
Arabia
1000 km
c
Eurasia
45°
BFB
ATB
ABV
GCB
LCR
SAB
EAP
KOM
SCB
TaP
UDV
BPM
SSB
30°
Mesogea
PAM
Arabia
Neotethys
Lutetian: 48.6 - 40.4 Ma
1000 km
d
Eurasia
45°
GCB
PoR
LCR
SAB
EAP
SCB
TaP
AR
BPM
30°
SSB
ZDF
MZT
Arabia
Rupelian: 33.9 - 28.4 Ma
1000 km

Fig. 3

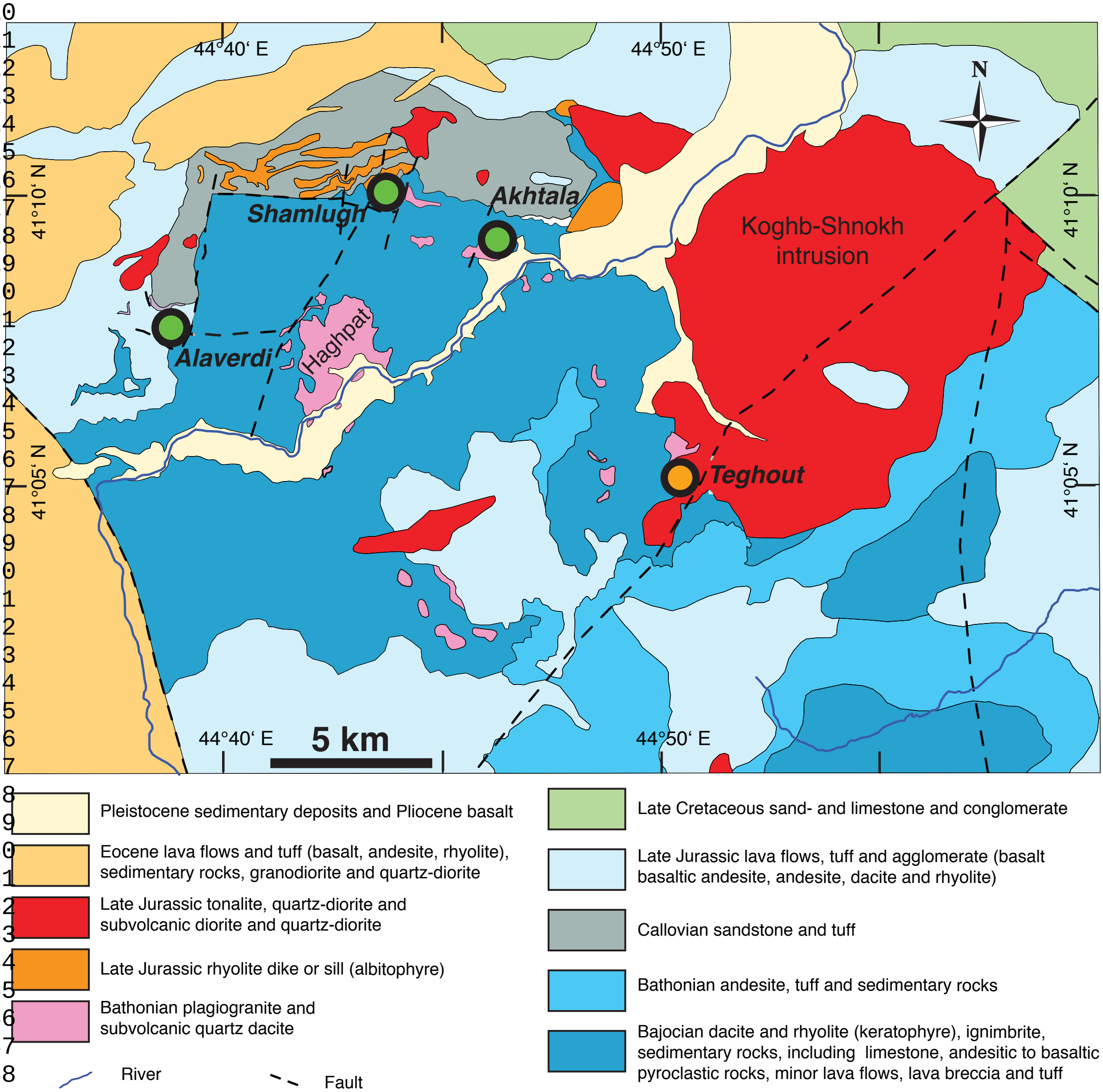
44°40‘ E
44°50‘ E
N
41°10‘ N
41°05‘ N
Shamlugh
Akhtala
Koghb-Shnokh
intrusion
Alaverdi
Haghpat
Teghout
44°40‘ E
5 km
44°50‘ E
Pleistocene sedimentary deposits and Pliocene basalt
Eocene lava flows and tuff (basalt, andesite, rhyolite), sedimentary rocks, granodiorite and quartz-diorite
Late Jurassic tonalite, quartz-diorite and subvolcanic diorite and quartz-diorite
Late Jurassic rhyolite dike or sill (albitophyre)
Bathonian plagiogranite and subvolcanic quartz dacite
River
Fault
Late Cretaceous sand- and limestone and conglomerate
Late Jurassic lava flows, tuff and agglomerate (basalt basaltic andesite, andesite, dacite and rhyolite)
Callovian sandstone and tuff
Bathonian andesite, tuff and sedimentary rocks
Bajocian dacite and rhyolite (keratophyre), ignimbrite, sedimentary rocks, including limestone, andesitic to basaltic pyroclastic rocks, minor lava flows, lava breccia and tuff

Fig. 4

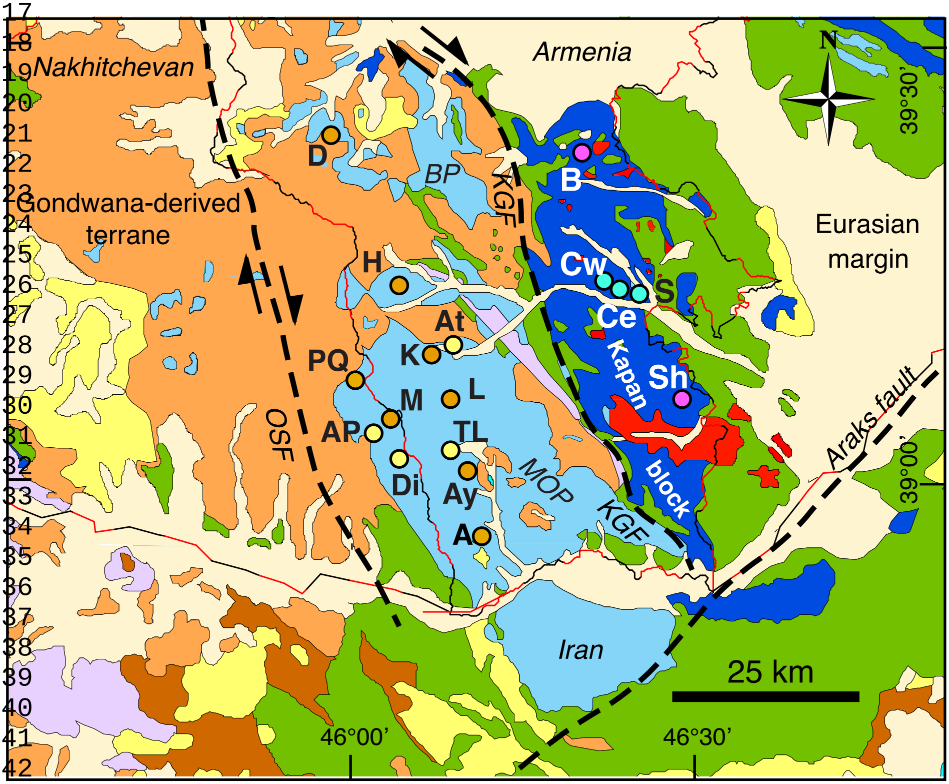

Plio-Pleistocene sedimentary and volcanic rocks

Oligo-Miocene sedimentary and volcanic rocks

Composite Eocene to Miocene pluton

Eocene sedimentary and volcanic rocks

Paleocene sedimentary rocks

Early Cretaceous gabbro, diorite, quartz-diorite

Cretaceous basaltic, andesitic, dacitic, rhyodacitic lava

Jurassic andesitic, dacitic, rhyolitic lava, breccia lava, tuff and hyaloclastite

Proterozoic basement rocks

Regional fault

Cu, Cu-Au and polymetallic veins and stockwork-type deposits of Kapan district

Porphyry-type/associated prospect

Porphyry Cu-Mo deposit/prospect

Gold-base metal epithermal prospect

Deposits and prospects:
A: Agarak (*MOP*)
AP: Aygurt and Piyazbashi (*MOP*)
At.Aitkis (*MOP*)
Ay: Aygedzor (*MOP*)
B: Bartsravan (*Kapan*)
Ce: Centralni East (*Kapan*)
Cw: Centralni West (*Kapan*)
D: Dastakert (*BP*)
Di: Diakhchay (*MOP*)
H: Hankasar (*MOP*)
K: Kadjaran (*MOP*)
L: Lichk (*MOP*)
M: Misdag (*MOP*)
PG: Paragachay and Qapujuk (*MOP*)
S: Shahumyan (*Kapan*)
Sh: Shikahogh (*Kapan*)
TL: Tey-Lichkvaz (*MOP*)

BP: Bargushat pluton
KGF: Khustup-Giratagh fault
MOP: Meghri-Ordubad pluton
OSF: Ordubad-Salvard fault

Fig. 5

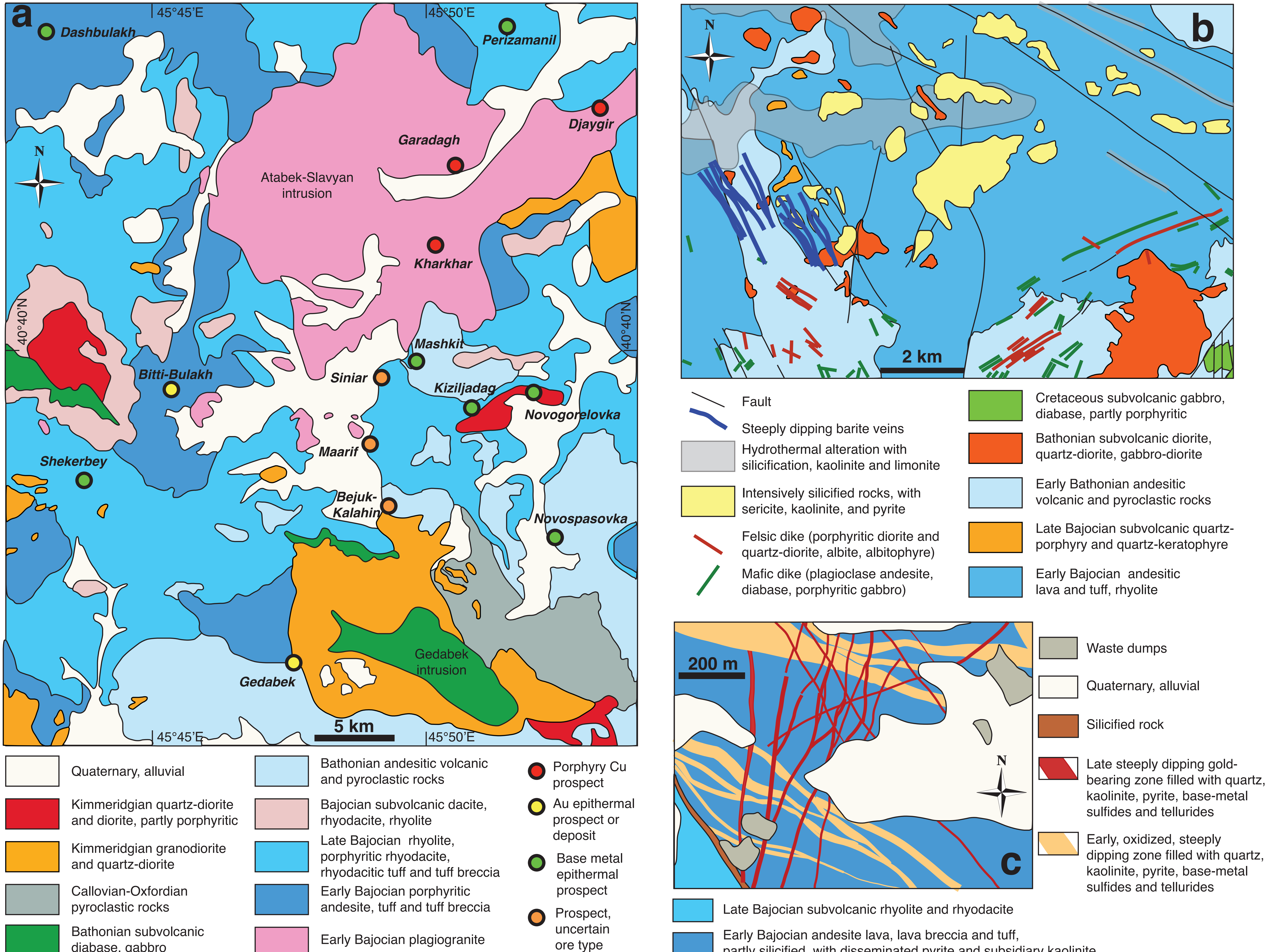
a
45°45'E
45°50'E
40°40'N
N
Dashbulakh
Perizamanil
Djaygir
Garadagh
Atabek-Slavyan
intrusion
Kharkhar
Mashkit
Siniar
Bitti-Bulakh
Kiziljadag
Novogorelovka
Maarif
Shekerbey
Bejuk-
Kalahin
Novospasovka
Gedabek
intrusion
Gedabek
5 km
Quaternary, alluvial
Kimmeridgian quartz-diorite and diorite, partly porphyritic
Kimmeridgian granodiorite and quartz-diorite
Callovian-Oxfordian pyroclastic rocks
Bathonian subvolcanic diabase, gabbro
Bathonian andesitic volcanic and pyroclastic rocks
Bajocian subvolcanic dacite, rhyodacite, rhyolite
Late Bajocian rhyolite, porphyritic rhyodacite, rhyodacitic tuff and tuff breccia
Early Bajocian porphyritic andesite, tuff and tuff breccia
Early Bajocian plagiogranite
Porphyry Cu prospect
Au epithermal prospect or deposit
Base metal epithermal prospect
Prospect, uncertain ore type
b
N
2 km
Fault
Steeply dipping barite veins
Hydrothermal alteration with silicification, kaolinite and limonite
Intensively silicified rocks, with sericite, kaolinite, and pyrite
Felsic dike (porphyritic diorite and quartz-diorite, albite, albitophyre)
Mafic dike (plagioclase andesite, diabase, porphyritic gabbro)
Cretaceous subvolcanic gabbro, diabase, partly porphyritic
Bathonian subvolcanic diorite, quartz-diorite, gabbro-diorite
Early Bathonian andesitic volcanic and pyroclastic rocks
Late Bajocian subvolcanic quartz-porphyry and quartz-keratophyre
Early Bajocian andesitic lava and tuff, rhyolite
c
200 m
N
Waste dumps
Quaternary, alluvial
Silicified rock
Late steeply dipping gold-bearing zone filled with quartz, kaolinite, pyrite, base-metal sulfides and tellurides
Early, oxidized, steeply dipping zone filled with quartz, kaolinite, pyrite, base-metal sulfides and tellurides
Late Bajocian subvolcanic rhyolite and rhyodacite
Early Bajocian andesite lava, lava breccia and tuff, partly silicified, with disseminated pyrite and subsidiary kaolinite

Fig. 6

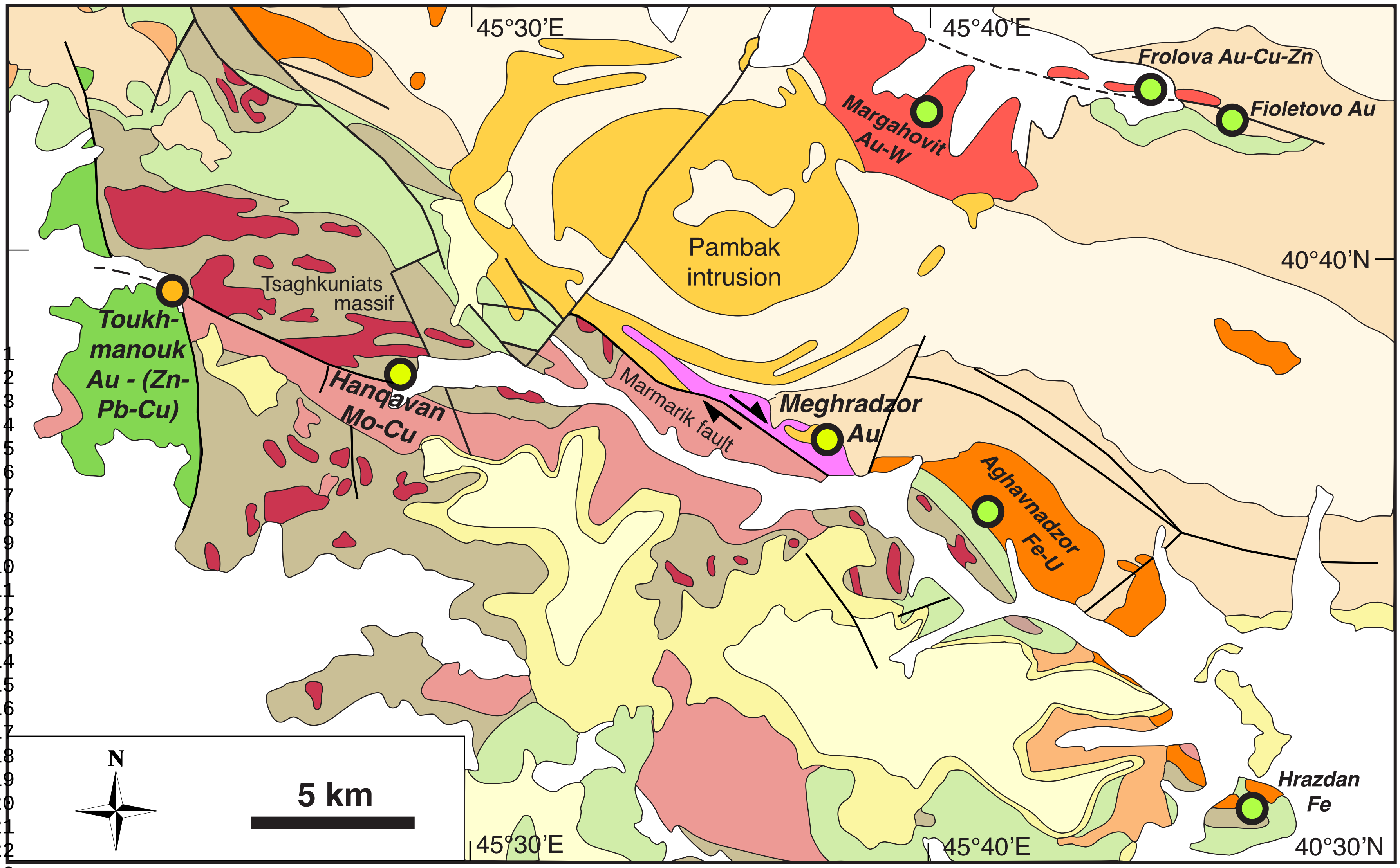

- Pleistocene-Holocene trachybasalt, trachyandesite, andesite,tuff and sedimentary deposits
- Late Pliocene-Pleistocene basaltic andesite, andesite, and volcanogenic sedimentary rocks
- Late Miocene-Early Pliocene andesitic tuff, rhyolite, perlite, obsidian, pumice sandstone, argillic rocks
- Post-late Eocene granite and granodiorite
- Post-late Eocene alkaline syenite, pseudo-leucite syenite and nepheline syenite
- Post-late Eocene poryphyritic granite and syenogranite
- Late Eocene diorite, quartz diorite, quartz syenite, monzonite, syenogranite, gabbro, diorite, tonalite, granodiorite and granite
- Late Eocene basalt, basaltic andesite, andesite, trachyandesite, trachyte, tephrite, rhyolite and pyroclastic rocks (Pambak suite)
- Middle Eocene basaltic andesite, andesite, dacite and rhyolite and tuff breccia and sandstone (Basum and Shirak suites)
- Early Eocene basaltic andesite, andesite, dacite, lava breccia, and sedimentary rocks
- Late Cretaceous limestone, marl, sandstone and conglomerate
- Early Cretaceous diabase, basalt, basaltic andesite, pyroclastic rocks, siltstone, mudstone
- Late Jurassic diorite, gabbro-diorite, granodiorite, quartz diorite, tonalite, leucogranite
- Neo-Proterozoic trondhjemite, plagiogranite, albitite, granite, gneiss, serpentinite, gabbro
- Neo-Proterozoic metamorphic basement rocks (Arzakan and Hanqvan suites)
- Fault

Fig. 7

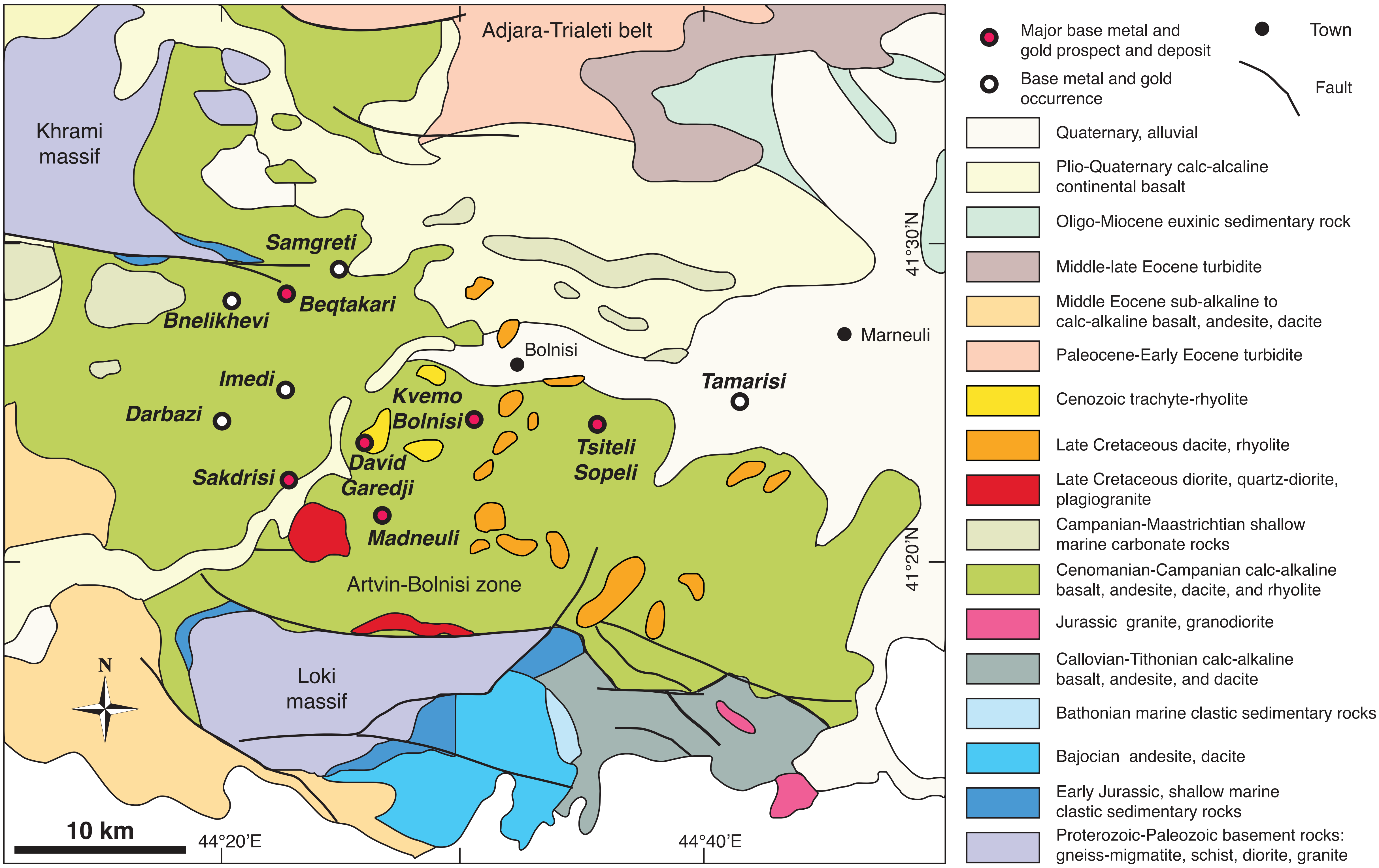
Adjara-Trialeti belt
Khrami
massif
Samgreti
Beqtakari
Bnelikhevi
Imedi
Darbazi
Sakdrisi
Kvemo
Bolnisi
David
Garedji
Madneuli
Tsiteli
Sopeli
Bolnisi
Tamarisi
Marneuli
Artvin-Bolnisi zone
Loki
massif
N
10 km
44°20'E
44°40'E
41°30'N
41°20'N
Major base metal and
gold prospect and deposit
Base metal and gold
occurrence
Town
Fault
Quaternary, alluvial
Plio-Quaternary calc-alcaline
continental basalt
Oligo-Miocene euxinic sedimentary rock
Middle-late Eocene turbidite
Middle Eocene sub-alkaline to
calc-alkaline basalt, andesite, dacite
Paleocene-Early Eocene turbidite
Cenozoic trachyte-rhyolite
Late Cretaceous dacite, rhyolite
Late Cretaceous diorite, quartz-diorite,
plagiogranite
Campanian-Maastrichtian shallow
marine carbonate rocks
Cenomanian-Campanian calc-alkaline
basalt, andesite, dacite, and rhyolite
Jurassic granite, granodiorite
Callovian-Tithonian calc-alkaline
basalt, andesite, and dacite
Bathonian marine clastic sedimentary rocks
Bajocian andesite, dacite
Early Jurassic, shallow marine
clastic sedimentary rocks
Proterozoic-Paleozoic basement rocks:
gneiss-migmatite, schist, diorite, granite

Fig. 8

Table 1 - Main ore deposits and prospects of the Lesser Caucasus. Based on similar tables published by Mederer et al. (2014) and Moritz et al. (in press).

Deposit name	Deposit type	Reserves-ore grade	Status	Age	Host rock geology	Main mineralogy	Alteration	Ore body geometry	References
Somkheto-Karabagh belt (Eurasian margin) - Alaverdi mining district (see Figure 4)									
Alaverdi	Cu-pyrite bodies and polymetallic veins	1.2Mt @ 5.6% Cu, 0.12 g/t Au, 5.8 g/t Ag (indicated-inferred resources)	Closed	135 ± 6Ma, 142 ± 6Ma (K-Ar sericite age of altered host rock)	Bajocian dacitic tuff and andesitic agglomerate	Chalcopyrite, pyrite, sphalerite, bornite, chalcocite, and subsidiary galena, tennantite, stannite, emplectite, argentite, native gold and silver, electrum, arsenopyrite. Quartz, sericite, chlorite, anhydrite, gypsum, calcite, dolomite.	Silicification, sericite, chlorite, carbonate, pyrite	Structurally-controlled by NNW- and NNE-oriented faults, and lithological contacts. Subvertical veins in deeper part; stockwork and subhorizontal, stratiform lenses in shallower part.	Nalbandyan (1968), Khatchaturyan (1977), and Zohrabyan and Melkonyan (1999). Ages by Bagdasaryan et al. (1969)
Shamlugh	Cu-pyrite bodies and polymetallic veins	4 Mt @ 3.53% Cu - 1.70% Pb - 4.96% Zn - 1.03 g/t Au - 8.1 g/t Ag (Proven-probable reserves and indicated resources)	Open pit and underground mining	Maximum age: 155 ± 1 Ma (U-Pb zircon age of altered rhyolite sill). 142 ± 6 Ma and 161 ± 4 Ma (K-Ar whole rock and sericite ages of altered host rock)	Bajocian basaltic andesitic, andesitic and dacitic tuff and lava breccia, overlain by a rhyolite sill (named albitophyre)	Chalcopyrite, pyrite, sphalerite, bornite, chalcocite, and subsidiary galena, tennantite, stannite, emplectite, argentite, native gold and silver, electrum, marcasite. Quartz, sericite, chlorite, barite, calcite, gypsum.	Silicification, sericite, chlorite, carbonate, pyrite, hematite	Structurally-controlled by NNW- and NNE-oriented faults, and lithological contacts. Subvertical veins in deeper part; stockwork and subhorizontal, stratiform lenses in shallower part.	Nalbandyan (1968), Khatchaturyan (1977), and Zohrabyan and Melkonyan (1999). Ages by Bagdasaryan et al. (1969) and Calder (2014)
Akhtala	Polymetallic lenses and veins	1.2 Mt @ 0.58% Cu - 1.67% Pb - 4.48% Zn - 1.3 g/t Au - 104 g/t Ag (Proven-probable reserves and indicated resources)	Closed	141 ± 5 Ma and 150 ± 5.5 Ma (K-Ar whole rock age of altered host rock)	Bajocian subvolcanic quartz-dacite, andesite and basalt	Galena, sphalerite, chalcopyrite, tennantite, tetrahedrite, and subsidiary bornite, chalcocite, marcasite, cassiterite, argentite, electrum, native gold and silver. Barite, quartz, sericite, chlorite, calcite, gypsum.	Silicification, sericite, chlorite, carbonate, pyrite, pyrophyllite, dickite	Stockwork and subhorizontal, stratiform lenses. Intersection of dikes and NE-oriented fractures with NS-oriented faults. EW-oriented veins	Paronikyan (1962), Nalbandyan (1968), and Zohrabyan and Melkonyan (1999). Ages by Bagdasaryan et al. (1969)
Teghout	Porphyry Cu-(Mo)	460 Mt @ 0.34% Cu - 0.01% Mo - 0.01 g/t Au	Open pit mining since 2015	145.5 ± 0.5 Ma and 149 ± 3 Ma (K-Ar sericite age) and 145.85 ± 0.59 Ma (Re-Os molybdenite age)	Middle-late Jurassic polyphase intrusion, including quartz-diorite, biotite-hornblende tonalite and leucogranite	Chalcopyrite, pyrite, molybdenite; subsidiary sphalerite, galena, bornite, tetrahedrite, magnetite, chalcocite, covellite, and rare enargite, luzonite and native gold. Quartz, anhydrite, carbonates, sericite	Quartz, sericite, pyrite, subsidiary kaolinite	Stockwork, disseminated	Amiryan et al. (1987), and Melkonyan and Ghukasian (2004). Ages: Paronikyan and Ghukasian (1974) and this study (Table 2)
Kapan zone (Eurasian margin) - Kapan mining district (see Figure 5)									
Shahumyan	Polymetallic veins	2006–2011: 1.8 Mt @ 1.53 ppm Au, 29.8 ppm Ag, 0.24% Cu and 1.52% Zn; Open pit potential: 36.3 Mt @ 3.13 g/t AuEq or 335 Mt @ 1.19 g/t AuEq	Underground mining	156.14 ± 0.79 Ma (Ar/Ar alunite). 140 ± 3 Ma and 149 ± 1 Ma (K-Ar whole rock age of altered host rock)	Middle Jurassic subvolcanic quartz-dacite, andesite and injection breccia	Pyrite, chalcopyrite, sphalerite, galena, fahlore, tellurides, enargite, digenite, bornite, chalcocite, native gold and silver. Gangue: quartz, carbonate, anhydrite, sericite and kaolinite.	Phyllic alteration, and advanced argillic (alunite), and hematite in uppermost part	Subvertical EW-oriented veins	Maatvev et al. (2006), Mederer (2013), Mederer et al. (2014)., and Achikgiozyan et al. (1987). Ages from Bagdasaryan et al. (1969) and Mederer et al. (2014)
Centralni West	Cu sulfide-quartz veins and stockwork	Estimated 30.000 t mined since 1843 @ 1.16% Cu (both Centralni deposits together)	Underground operation closed 2008	161.78 ± 0.79 Ma (Ar/Ar sericite)	Middle Jurassic breccia lava, hyalo-clastite, lava flows	Chalcopyrite, pyrite, and minor galena and fahlore. Gangue: quartz and carbonates	Chlorite, quartz, epidote and carbonate alteration. Sericite close to ore	EW-oriented veins	Mederer (2013), Mederer et al. (2014), Achikgiozyan et al. (1987). Age from Mederer et al. (2014)
Centralni East	Cu-Au, sulfide stockwork	see above	Underground and open pit abandoned in 2004	144.7 ± 4.2 Ma (Re-Os pyrite isochron)	Middle Jurassic lava flows and tuff	Chalcopyrite, colusite, fahlore, and minor luzonite, galena, enargite, covellite, tellurides	Argillic alteration and silicification, diaspore, dickite	Stockwork	Mederer (2013), Mederer et al. (2014), Achikgiozyan et al. (1987). Age from Mederer et al. (2014)

Table 1 - continued

Deposit name	Deposit type	Reserves-ore grade	Status	Age	Host rock geology	Main mineralogy	Alteration	Ore body geometry	References
Somkheto-Karabagh belt (Eurasian margin) - Gedabek mining district, Gosha prospect and Chovdar deposit (Figure 6)									
Gosha	High-sulfidation epithermal	7.4 Mt @ 4.7 g/t Au - 6.33 g/t Ag (Proven-probable reserves and indicated-inferred resources)	Prospect	Uncertain, possibly late Jurassic or early Cretaceous	Bajocian andesite intruded by rhyodacitic subvolcanic intrusion	Gold with pyrite and tellurides, lesser amounts of chalcopyrite, arsenopyrite, base-metal sulphides and sulphosalts	Silicification, disseminated pyrite, kaolinite	Orthogonal system of NS and EW subvertical kaolinite-pyrite-quartz veins. Better ore grades in crosscutting areas of both structures	Babazadeh et al. (2003). Behre Dolbearr (2005)
Djaygir	Porphyry Cu	117 Mt @ 0.354% Cu (Indicated to inferred resources)	Prospect	Early Cretaceous	Late Jurassic quartz-diorite intruded in Bajocian tonalite, andesitic to rhyodacitic tuff and tuff-sandstone	Pyrite, chalcopyrite, and subsidiary miolybdenite	Quartz, sericite, pyrite, kaolinite, chlorite	Disseminated and stockwork	
Kharkhar	Porphyry Cu	22.6 Mt @ 0.367% Cu - 0.003 % Mo - 0.2 g/t Au - 2-4 g/t Ag (Indicated to inferred resources)	Prospect	133.3 ± 0.5 Ma (Re-Os molybdenite age)	Late Jurassic quartz-diorite intruded in Bajocian tonalite	Pyrite, chalcopyrite, bornite, covellite, chalcocite, molybdenite	Quartz, sericite, pyrite, kaolinite	Disseminated and stockwork	Babazadeh et al. (1990). Age from this study (Table 2)
Garadagh	Porphyry Cu	41.5 Mt @ 0.43% Cu - 0.002% Mo (Indicated to inferred resources)	Prospect	Early Cretaceous	Late Jurassic quartz-diorite intruded in Bajocian tonalite	Pyrite, chalcopyrite, bornite, covellite, chalcocite, molybdenite	Quartz, sericite, pyrite, kaolinite	Disseminated and stockwork	Babazadeh et al. (1990)
Bitti-Bulakh	High-sulfidation epithermal	Past production: 16,000 t @ 2% Cu. Unknown reserves and resources: 0.53 g/t Au - 0.5 g/t Ag - 1.07% Cu	Closed	Early Cretaceous	Bajocian andesite and tuff, intruded by plagiogranite	Pyrite, enargite, barite, chalcopyrite, famatinite, subsidiary fahlore, sphalerite, galena, covellite	Silicification, sericite, argillic alteration (kaolinite)	Disseminated and lenses	Butenko (1947).
Novogorelovka	Epithermal polymetallic	Unknown reserves and resources: 0.53 g/t Au- 0.5 g/t Ag - 1.07% Cu	Prospect	Early Cretaceous	Early Bajocian andesite and late Jurassic subvolcanic quartz-dacite intrusion	Fe-rich sphalerite, chalcopyrite, pyrite	Silicification, sericite, argillic alteration (kaolinite)	Lens-shaped orebody	Mamedov (1983)
Maarif		32 Mt @ 0.51-0.72 % Cu - 0.01% Mo - 0.5-2 g/t Au (Probable reserves)	Prospect	Early Cretaceous	Bajocian andesitic porphyry intruded by subvolcanic rhyodacite	Pyrite-chalcopyrite-molybdenite	Sliicification, sericite, disseminated pyrite, chlorite	Stockwork	
Gedabek	Low- to intermediate/ high-sulfidation epithermal	20.3 Mt @ 1.145 g/t Au - 0.29% Cu - 9.46 g/t Ag (Proven and probable reserves, and indicated resources)	In production	Early Cretaceous	Highly altered quartz porphyry (dacite?) intruding Jurassic andesitic volcanic and volcaniclastic rocks	Pyrite, chalcopyrite, sphalerite, stephanite, barite, native gold, bornite, chalcoite, covvelite	Silicification, sericite, pyrite, argillic alteration	Disseminated, vein-type and semi-massive to massive pyrite lenses	Mamedov (1983), Behre Dolbear (2005), Hemon et al. (2012) and Hemon (2013)
Chovdar	High-sulfidation epithermal	18.08 Mt @ 2.19 g/t Au - 16.72 g/t Ag (Probable reserves and indicated-inferred resources)	In production	Uncertain, possibly late Jurassic or early Cretaceous	Bajocian tuff, andesite, dacite and rhyolite	Pyrite, gold, enargite, tennantite-tetrahedrite, barite	Silicification. Vuggy quartz. Argillic alteration (kaolinite)		Musaev and Shirinov (2002)
Somkheto-Karabagh belt (Eurasian margin) - Mehmana mining district (see location in Figure 2)									
Gizilbulak/ Drmbon	Cu-Au, epithermal?	3.3 Mt @ 3.9 g/t Au - 5.1g/t Ag - 1.3%Cu (indicated-inferred resources)	Closed since 2014	Post-Oxfordian	Bajocian basaltic andesite to dacite	Pyrite, chalcopyrite, native gold, hematite, and subsidiary sphalerite, galena, bornite and tennantite-tetrahedrite	Silicification, sericite, carbonate, chlorite, hematite	Lens-shaped, stockwork and disseminated	Agakishiev et al. (1989), Khachanov (1993), Vardanyan (2008) and Mederer et al. (2014)

Table 1 - continued

Deposit name	Deposit type	Reserves-ore grade	Status	Age	Host rock geology	Main mineralogy	Alteration	Ore body geometry	References
Artvin-Bolnisi zone (Eurasian margin) - Bolnisi mining district (Figure 8) and Dagkasaman area									
Madneuli	Transitional VMS-porphyry-epithermal	Cu-polymetallic ore: 30 Mt @ 0.35% Cu - 0.4 g/t Au. Epithermal ore: 8 Mt @ 0.55 g/t Au (Proven and probable reserves)	Open pit mining	Late Cretaceous	Late Cretaceous tuff, and volcanic and sedimentary rocks. U-Pb zircon ages of dikes crosscutting Mashevera unit: 86.6-87.1 Ma.	Pyrite, chalcopyrite, sphalerite, barite, galena, tennantite, tetrahedrite, hematite, tellurides, sulfobismuthites, native gold and silver, subsidiary enargite, chalcosite, covellite and bornite	Silicification, sericite, chlorite,	Stockwork, stratiform massive sulphide lenses, breccia pipes, veins	Gugushvili et al. (2001), Migineishvili (2002, 2005), Gialli et al. (2012) Gialli (2013), Popkhadze et al. (2014), Gugushvili (2015). U-Pb ages from Moritz et al. (2012).
Sakdrisi	Low-sulfidation epithermal	Cu-Au ore: 4 Mt @ 0.59% Cu, 1.06 g/t Au; Epithermal: 8.6 Mt @ 1.77 g/t Au (Proven and probable reserves)	Open pit mining	Late Cretaceous	Late Cretaceous tuff, and volcanic and volcanoclastic rocks	Base metal sulfides, pyrite, native gold, barite, quartz, chalcedony, hematite	Silicification, argillic alteration (illite, montmorillonite, kaolinite)	Disseminated, breccia pipes and stockwork	Gugushvili (2004, 2015), and Gugushvili et al. (2014)
Beqtakari	Low-sulfidation epithermal	9.4 Mt @ 2.93 g/t Au - 33 g/t Ag - 1.5% Zn -0.75% Pb	In development	Late Cretaceous	Campanian felsic to intermediate calc-alkaline andesitic-rhyodacitic volcanic rocks	Sphalerite, chalcopyrite, galena, pyrite, tennantite, tetrahedrite, marcasite	Silicification, argillic alteration (illite, montnorillonite)	Disseminated precious metal zone in silificied rocks and breccia, with host rocks clasts cemented by ore minerals	Lavoie (2015) and Lavoie et al. (2015)
Dagkasaman	Precious metal vein-type	0.7 Mt @ 4.38 g/t Au - 18.64 g/t Ag (Probable reserves)	Prospect	Cretaceous?	Late Cretaceous tuff and volcanic rocks	Gold, sphalerite, and other base metal sulfides	Silicification, albitization	Veins and stokwork	
Miskhan/Tsaghqunk-Zangezur-Ordubad zone: Meghri-Ordubad mining district (Figure 5)									
Dastakert	Porphyry Cu-Mo	9.6 Mt @ 0.95% Cu - 0.043% Mo	In development	40.22 ± 0.16 Ma to 39.97 ± 0.16 Ma (Molybdenite Re-Os age)	Eocene granodiorite and andesite-basalte	Molybdenite, chalcopyrite, pyrite, bornite, chalcocite, covellite, emplectite, enargite, luzonite, magnetite, gold, pyrrhotite, sphalerite, tetrahedrite / tennantite, alabandite.	Silicification, sericite, argillic alteration (kaolinite), carbonates	NW-oriented fracture zone. Stockwork and breccia (ore minerals in matrix of breccia)	Karamyan (1978), Pijyan (1975). Ages from this study (Table 2)
Hankasar	Porphyry Cu-Mo	10.4 Mt @ 0.45% Cu - 0.038% Mo	In development	43.14 ± 0.17 Ma (Molybdenite Re-Os age)	Late Eocene granodiorite and quartz-diorite	Molybdenite, chalcopyrite, pyrite, galena, sphalerite. Gangue: quartz, sericite, chlorite, carbonates, K-feldspar, biotite.	Silicification, sericite, carbonates	Veins	Karamyan (1978). Ages from this study (Table 2)
Paragachay	Porphyry Cu-Mo	Past production: 460 tons of Mo. Ore grades: 0.01-2.50 % Mo - 0.1-21.5% Cu - 1 g/t Au	Closed	26.78 ± 0.11 Ma (Molybdenite Re-Os age)	Quartz-diorite, quartz syenodiorite	Chalcopyrite, pyrite, molybdenite, magnetite	Silicification, sericite, K-feldspar, argillic alteration (kaolinite)	Vein, stockwork	Babazadeh et al. (1990). Ages from this study (Table 2)
Qapujuk	Porphyry Cu-Mo	0.95 Mt @ 1.14% Cu - 0.17% Mo - 0.3 g/t Au - 4.0 g/t Ag	Prospect	Eocene-Oligocene	Gabbrodiorite, diorite, quartz syenodiorite	Molybdenite, chalcopyrite,	Silicification, sericite, K-feldspar, argillic alteration (kaolinite)		Babazadeh et al. (1990)
Kadjaran	Porphyry Cu-Mo	2244 Mt @ 0.18% Cu - 0.021% Mo - 0.02 g/t Au (Proven and probable reserves, and indicated resources)	In production	27.2 ± 0.1 Ma to 26.43 ± 0.11 Ma (Molybdenite Re-Os age)	Oligocene monzonite, quartz-monzonite, monzodiorite	Pyrite, molybdenite, chalcopyrite, magnetite, sphalerite, galena, subsidiary covellite, enargite, luzonite, bornite,chalcocite, gold, tellurides, tetrahedrite / tennantite.	Sericite, quartz, disseminated pyrite, argillic alteration (kaolinite), carbonate	Stockwork	Mkrtchyan et al. (1969), Karamyan (1978), Tayan (1984). Ages from this study (Table 2)

Table 1 - continued

Deposit name	Deposit type	Reserves-ore grade	Status	Age	Host rock geology	Main mineralogy	Alteration	Ore body geometry	References
Miskhan/Tsaghqunk-Zangezur-Ordubad zone: Meghri-Ordubad mining district - continuation (Figure 5)									
Atkis	Epithermal, polymetallic	1.71 g/t Au - 29.4 g/t Ag - 0.79% Cu. No reported tonnage.	Prospect	24 ± 1 Ma (K-Ar age of sericite from altered host rock)	Monzonite-hornfels contact	Chalcopyrite, pyrite, sphalerite, galena, molybdenite. Gangue: quartz, calcite	Silicification, sericite, pyrite, kaolinite, chlorite, carbonate	Veins	Mkrtchyan et al. (1969). Age from Bagdasaryan et al. (1969)
Misdag	Porphyry Cu-Mo	350 Mt @ 0.43% Cu (Inferred resources)	Prospect	Likely Oligocene	Granodiorite, quartz-syenodiorite, quarz-monzonite	Chalcopyrite, pyrite, molybdenite, magnetite, quartz	Silicification, sericite, K-feldspar, argillic alteration (kaolinite)	Vein, stockwork	Babazadeh et al. (1990)
Agyurt	Epithermal	1.13 Mt @ 1.28% Cu - 6.39 g/t Au - 23.4 g/t Ag (Probable reserves to inferred resources)	Prospect	Eocene-Oligocene	Granodiorite, diorite, quartz syenodiorite	Native gold and silver, sulphosalts,pyrite, chalcopyrite, molybdenite, galena, sphalerite, magnetite, quartz		NS-oriented veins dipping steeply to the W	Babazadeh et al. (1990)
Piyazbashi	Epithermal	1.7 Mt @8.6 g/t Au - 3.4 g/t Ag (Prove- probable reserves, and inferred-indicated resources)	Prospect	Eocene-Oligocene	Andesitic tuff and flow	Native gold, various sulfides, quartz	Silicification, argillic alteration (kaolinite)	Veins	Ramazanov and Kerimli (2012)
Lichk	Porphyry Cu-Mo	34 Mt @ 0.63% Cu - 0.033% Mo - 0.05 g/t Au (Proven and probable reserves)	Prospect	Oligocene-Miocene?	Early Miocene porphyritic granodiorite	Chalcopyrite, bornite, pyrite, molybdenite, hematite, magnetite. Gangue: quartz, sericite, carbonates	Silicification, sericite, argillic alteration (kaolinite), carbonates	Stockwork	Pijyan (1975), Karamyan (1978), and Hovakimyan (2008)
Diakhchay	Porphyry Cu-Mo	14.4 Mt @0.44% Cu - 0.015% Mo	Prospect	Eocene-Oligocene	Quartz-diorite	Chalcopyrite, pyrite, molybdenite, magnetite, quartz	Silicification, sericite, K-feldspar, argillic alteration (kaolinite)	Vein, stockwork, along main Ordubad fault	Babazadeh et al. (1990)
Tey-Lichkvaz	Epithermal, polymetallic	3.5 Mt @ 0.44% Cu - 5.93 g/t Au - 35.12 g/t Ag (Proven and probable reserves).	Prospect	37.5 ± 0.5 Ma and 38 ± 2.5 Ma (K-Ar age of sericite from altered host rock)	Eocene granodiorite and syenodiorite and Middle Eocene basalt and andesite	Native gold, chalcopyrite, arsenopyrite, tellurides, pyrite	Silicification, sericite, carbonates	Stockwork and vein	Amiryan (1984), Hovakimyan (2010), Hovakimyan and Tayan (2008). Ages by Bagdasaryan et al. (1969)
Terterasar	Epithermal, polymetallic	0.5 Mt @ 11 g/t Au - 74.8 g/t Ag - 0.45% Cu (Proven and probable reserves)	Prospect	Late Eocene?	Eocene granodiorite and syenodiorite and Middle Eocene basalt and andesite	Native gold, base metal sulphides, pyrite chalcopyrite, arsenopyrite, tellurides. Gangue: quartz, carbonates	Sericite, carbonates, argillic alteration (kaolinite), carbonates silicification	Veins and veinlets	Amiryan (1984), Hovakimyan and Tayan (2008)
Aygedzor	Porphyry Cu-Mo	51.6 Mt @ 0.172% Cu - 0.042% Mo (Proven and probable reserves and indicated resources)	Prospect	42.62 ± 0.17 Ma (Molybdenite Re-Os age)	Eocene granodiorite, syenogranite	Molybdenite, chalcopyrite, galena, sphalerite, pyrite, enargite, quartz	Silicification, sericite, argillic alteration (kaolinite), carbonates	Stockwork and vein	Pijyan (1975), Karamyan (1978), and Hovakimyan and Tayan (2008). Age from this study (Table 2)
Agarak	Porphyry Cu-Mo	45 Mt @ 0.5% Cu - 0.029% Mo- 0.025 g/t Au - 1.19 g/t Ag (Proven and probable reserves)	In production	44.2 ± 0.2 Ma (Molybdenite Re-Os age)	Eocene porphyritic leucocratic granodiorite, syenogranite	Pyrite, molybdenite, chalcopyrite, bornite, magnetite, sphalerite, galena, covellite, subsidiary covellite, enargite. Gangue: quartz, sericite, chlorite, carbonates, K-feldspar, biotite	Sericite, quartz, disseminated pyrite, argillic alteration (kaolinite), carbonate, albite, chlorite, biotite	Stockwork	Pijyan (1975), Karamyan (1978), and Tayan et al. (2007). Age from this study (Table 2)

Deposit name	Deposit type	Reserves-ore grade	Status	Age	Host rock geology	Main mineralogy	Alteration	Ore body geometry	References
Sevan-Akera suture zone (see location in Figure 2)									
Zod - Sotk	Low-sulfidation epithermal	23 Mt @ 7.0 g/t Au - 8.5 g/t Ag (Proven-probable reserves to indicated resources)	In production	43 ± 1.5 Ma (K-Ar whole rock alteration age), but interpreted as Oligocene to Miocene (Kozerenko, 2004; Levitan, 2008)	Late Jurassic gabbro, peridotite, amphibolite, serpentinite (ophiolite assemblage)	Pyrite, sphalerite, native gold, tellurides, sulfosalts, stibnite, realgar, orpiment. Gangue: quartz, chalcedony, calcite, rhodochrosite, siderite, breunnerite	Carbonate (listwaenite), quartz, talc, sericite, montmorillonite, dickite, beidellite	Mostly EW-oriented, deeply steeping quartz veins	Amiryan (1984), Melikyan (1976), Spiridonov (1991), Kozerenko (2004) and Levitan (2008). Age from Bagdasaryan et al. (1969)
Miskhan/Tsaghqunk-Zangezur zone: Amulsar and Meghradzor-Hanqavan ore cluster (Figure 7)									
Amulsar	High-sulfidation epithermal	122.4 Mt @ 0.77 g/t Au - 3.5 g/t Ag (Measured and indicated reserves)	In development	Unknown, Oligocene-Miocene?	Eocene-Oligocene andesite, subvolcanic porphyritic andesite,andesitic-dacitic tuff, volcanic breccia. Monzonite-granosyenite dated at 33-34 Ma by K-Ar.	Base metal sulfides, gold, hematite	Silicification, vuggy silica, alunite, hematite	NE- and NW-oriented fault control on subvertical ore bodies	Intrusion age from Bagdasaryan and Ghukasian (1985). Lydian International (2016)
Meghradzor	Epithermal	0.38 Mt @ 12.4 g/t Au (Proven-probable reserves)	In production	41.5 ± 1.0 Ma (K-Ar age of sericite from altered wall rock)	Late Eocene monzonite, monzodiorite, quartz-syenite, syenogranite, andesite, dacite, tuff; late Jurassic-early Cretaceous tonalitie, quartz-diorite; Precambrian schist	Pyrite, native gold,sphalerite, chalcopyrite, galena, tellurides, molybdenite, pyrrhotite. Gangue: quartz, carbonates, sericite	Silicification, sericite, disseminated pyrite, argillic alteration (kaolinite)	Pinch-swell quartz veins along detachment zones	Amiryan and Karapetyan (1964). Age from Bagdasaryan et al. (1969)
Hanqavan	Porphyry/ stockwork Cu-Mo	109 Mt @ 0.044% Mo and 2.2 Mt oxidized ore @ 0.6% Cu (indicated-inferred resources)	Reserve and resource estimation	29.34 ± 0.12 Ma (Molybdenite Re-Os age)	Tonalite crosscut by granodioritic dikes	Pyrite, chalcopyrite, molybdenite, galena, magnetite, scheelite, sphalerite, covellite, tellurides, native gold. Gangue: quartz, calcite, ankerite, siderite.	Silicification, sericite, carbonates	Structurally controlled by NE- and EW-oriented faults	Age from this study (Table 2)
Tsaghkuniat massif - South Armenian block (Figure 7)									
Toukhmanouk	Precious metal-sulfide vein-type/stockwork	21.92 Mt @ 1.62 g/t Au - 4.88 g/t Ag (Proven-probable reserves and indicated resources)	Reserve and resource estimation	146.1 ± 0.6 Ma (Molybdenite Re-Os age)	Late Jurassic mafic volcanic rocks and Proterozoic trondhjemite	Sphalerite, galena, arsenopyrite, pyrite, chalcopyrite, gold, tellurides, arsenopyrite. Gangue: quartz and subsidiary carbonate	Argillic alteration, sericite, pyrite	NE-oriented 150-200m wide alteration and mineralized zone, containing subvertical quartz veins, typically rimmed by sulphides	Amiryan et al. (1997), and Wheatley and Acheson (2011). Age from this study (Table 2)
Adjara-Trialeti belt (see location in Figure 1)									
Merisi	Porphyry-Cu, polymetallic, epithermal	2.9 Mt @ 0.38% Cu and 0.75 g/t Au (Proven and probable reserves)	Closed	Late Eocene	Middle Eocene mafic volcanic rocks and tuff breccia. Late Eocene shoshonitic rocks. Late Eocene calc-alkaline andesite, diorite, granodiorite, syenite-diorite, syenite.	Chalcopyrite, galena, sphalerite, and subordinate marcasite, hematite, native gold and silver, sulfosalts, barite	Silicification, sericite, disseminated pyrite, argillic alteration (kaolinite)	Subvertical, EW- to NW-oriented veins	Gugushvili (1980, 2015). Khomeriki and Tuskia (2005)

Table 2 - Re-Os Data for Molybdenite from ore deposits and prospects of the Lesser Caucasus

Sample number	Location	Deposit type	Description	Wt (g)	Re (ppm)	±	^{187}Re (ppm)	±	^{187}Os (ppb)	±	Re-Os age (Ma)	±[a]	±[b]
Somkheto-Karabagh belt (Eurasian margin): Alaverdi and Gedabek districts (Figs 4 and 6a, respectively)													
RO404-3_XX-11-02C	Kharkhar, Gedabek district (Fig. 6a)	Porphyry Cu	Quartz-molybdenite vein in porphyry intrusion	0.022	766.8	2.8	482.0	1.8	1071.3	3.3	133.27	0.53	0.68
RO812-8_Teghout-N7/83	Teghout, Alaverdi district (Fig. 4)	Porphyry Cu	Quartz–molybdenite vein, thickness ~0.5 cm, in tonalite-porphyry, Alteration: silicification and sericite (elevation ~900m)	0.011	506.9	2.5	318.6	1.5	775.1	3.4	145.85	0.59	0.74
Tsaghkuniat massif - South Armenian block (Fig. 7)													
RO812-5_Toukhmanouk	Toukhmanouk	Intrusion-hosted gold and base metal stockwork	Disseminated molybdenite in tonalite-granodiorite (Mirac intrusion)	0.024	117.8	0.4	74.0	0.3	180.5	0.5	146.14	0.59	0.74
Miskhan/Tsaghqunk-Zangezur zone: Zangezur-Ordubad mining district (Fig. 5)													
RO280-2_N2	Agarak	Porphyry Cu-Mo	Quartz–molybdenite-chalcopyrite vein, thickness ~3 cm, alteration: K- feldspar, sericite, argillic, silicification (elevation ~1070m)	0.024	538.8	1.9	338.7	1.2	249.6	0.7	44.2	0.18	0.22
RO812-7_Aygedzor_NRM-0560	Aygedzor	Porphyry Cu-Mo	Quartz-molybdenite stockwork, vein thickness ~1.6m, in granodiorite, alteration: sericitization and argillic (elevation 1100m)	0.011	1141.0	5.5	717.2	3.5	509.5	2.3	42.62	0.17	0.22
RO404-8_R32	Aygedzor	Porphyry Cu-Mo	Quartz–molybdenite vein, thickness ~5 cm, in granodiorite (Rb-Sr isochrone age: 41.8 Ma; Melkonyan et al., 2010)	0.035	727.5	2.4	457.3	1.5	329.2	0.9	43.19	0.17	0.22
RO812-2_Dastaker_NRM-0547	Dastakert	Breccia-hosted Cu-Mo	Molybdenite from matrix of breccia, in granodiorite and volcanic rocks, alteration: silicification, sericitization (elevation ~2300m)	0.023	212.1	0.8	133.3	0.5	89.4	0.3	40.22	0.16	0.20
RO812-4_Dastakert_N98m/75	Dastakert	Breccia-hosted Cu-Mo	Quartz–molybdenite–chalcopyrite matrix of breccia with clasts of volcanic rocks	0.020	235.6	0.9	148.1	0.6	98.7	0.3	39.99	0.16	0.20
RO391-4_R13	Dastakert	Breccia-hosted Cu-Mo	Quartz–molybdenite–chalcopyrite matrix of breccia with clasts of volcanic rocks	0.028	315.8	1.1	198.5	0.7	132.3	0.4	39.99	0.16	0.20
RO391-5_98M/75	Dastakert	Breccia-hosted Cu-Mo	Quartz–molybdenite–chalcopyrite matrix of breccia with clasts of volcanic rocks (elevation ~2200m)	0.052	207.9	0.7	130.7	0.4	87.0	0.2	39.97	0.16	0.20
RO812-3_Ankaser_N72p	Hanqasar	Porphyry Cu-Mo	Quartz-molybdenite stockwork in porphyry intrusion, veinlet zone, thickness ~5 cm, in granodiorite, alteration: silification, weak sericitization (elevation 2000m)	0.022	76.3	0.3	47.9	0.2	34.5	0.1	43.14	0.17	0.22
RO404-7_R16	Hanqasar	Porphyry Cu-Mo	Quartz–molybdenite–chalcopyrite vein, thickness ~30 cm, adit N4, in granodiorite of Gekhi intrusion (K-Ar whole rock age: 38.6 Ma, and biotite age: 42 Ma; Melkonyan et al., 2008, 2010) (elevation ~2200m)	0.045	45.1	0.2	28.3	0.1	20.3	0.1	43.07	0.18	0.22
RO812-1_Kajaran_N160m/75	Kadjaran	Porphyry Cu-Mo	Quartz-chalcopyrite-molybdenite stockwork and veins in porphyry intrusion, vein, thickness 10-12 cm, in monzonite, alteration: weak silification, sericite, argillic, carbonates (elevation ~1950m)	0.022	322.4	1.2	202.6	0.7	90.5	0.3	26.80	0.11	0.14
RO391-1_KJ-10-11D	Kadjaran	Porphyry Cu-Mo	Quartz-chalcopyrite-molybdenite vein, thickness 6-8 cm, host rock-monzonite; alteration: weak silification, sericite, argillic, carbonates (elevation ~1935m)	0.050	222.6	0.7	139.9	0.5	63.0	0.2	27.02	0.11	0.14
RO391-2_KJ-10-13A	Kadjaran	Porphyry Cu-Mo	Quartz-chalcopyrite-molybdenite vein, thickness 8-10 cm, inmonzonite; alteration: weak silification, sericite, argillic, carbonates (elevation ~1935m)	0.050	160.4	0.5	100.8	0.3	44.4	0.1	26.43	0.11	0.13
RO391-3_KJ-10-01C	Kadjaran	Porphyry Cu-Mo	Quartz-chalcopyrite-molybdenite vein, thickness 6-8 cm, host rock -monzonite; alteration: weak silification, sericite, argillic, carbonates (elevation ~1920m)	0.051	104.3	0.3	65.6	0.2	29.2	0.1	26.70	0.11	0.14
RO280-1_NI	Kadjaran	Porphyry Cu-Mo	Quartz–molybdenite vein, thickness ~12 cm, in monzonite, alteration: K-feldspar, sericite, argillic, carbonates (elevation ~2100m)	0.042	368.3	1.2	231.5	0.8	104.9	0.3	27.2	0.11	0.14
RO404-9_R15	Kadjaran, middle stream Iry	Porphyry Cu-Mo	Molybdenite disseminated in aplitic granite crosscutting porphyry granodiorite (U-Pb zircon age: 22.22 ± 0.02 Ma; Moritz et al., in press) (elevation ~2000m)	0.045	197.9	0.7	124.4	0.4	47.4	0.1	22.87	0.09	0.12
RO812-6_Kaler_NRM-0574	Kaler	Pegmatite	Pegmatitic vein, thickness 1.2m, in monzonite, alteration: weak silification, argillic (elevation 2050)	0.010	1085.2	5.5	682.1	3.5	352.4	1.6	31.00	0.12	0.16
RO404-5_119999	Paragachay	Porphyry Cu-Mo	Quartz-molybdenite stockwork in porphyry intrusion	0.030	258.6	0.9	162.5	0.6	72.5	0.2	26.78	0.11	0.14
RO404-6_M14	Qefashen, Gekhi intrusion	Garnet skarn	Skarn in contact with the Gekhi intrusion, thickness ~0.5cm (elevation ~2100m)	0.021	108.1	0.4	67.9	0.3	50.6	0.2	44.70	0.18	0.22
Miskhan/Tsaghqunk-Zangezur zone: Meghradzor-Hanqavan ore cluster (Fig. 7)													
RO404-4_HAN-11-01	Hankavan	Porphyry Cu-(Mo)	Quartz–molybdenite vein and stockwork, in tonalite cut by pre-ore granodiorite and porphyry granite dykes (age: 31.7 ± 32.9 Ma, whole-rock K-Ar dating; Bagdasaryan, 1972), alteration: chlorite, sericite, carbonates (elevation ~2050m)	0.021	173.4	0.6	109.0	0.4	53.3	0.2	29.34	0.12	0.16

[a] age uncertainty includes all analytical sources of uncertainty
[b] age uncertainty includes all analytical sources of uncertainty and the uncertainty in the ^{187}Re decay constant